Investigating Biogenic Sources of Enantiomers and the Effect of Drought on the Emissions of Chiral Compounds

Dissertation

Zur Erlangung des Grades

“Doktor rerum naturalium (Dr. rer. nat.)”

Im Promotionsfach Chemie

Am Fachbereich Chemie, Pharmazie und Geowissenschaften

Der Johannes Gutenberg-Universität Mainz

Max Planck Graduate Center

Joseph Christopher Byron

geb. in Birmingham, Vereinigtes Königreich

Mainz, Oktober 2021

MAX PLANCK INSTITUTE FOR CHEMISTRY

JOHANNES GUTENBERG UNIVERSITÄT MAINZ

Max Planck Graduate Center mit der Johannes Gutenberg-Universität

1. Berichterstatter:
2. Berichterstatter:

Tag der mündlichen Prüfung:

I hereby declare that I wrote the dissertation submitted without any unauthorized external assistance and used only sources acknowledged in the work. All textual passages which are appropriated verbatim or paraphrased from published and unpublished texts as well as all information obtained from oral sources are duly indicated and listed in accordance with bibliographical rules. In carrying out this research, I complied with the rules of standard scientific practice as formulated in the statutes of Johannes Gutenberg University Mainz to insure standard scientific practice.

Mainz, 6th October 2021, Joseph Byron

In loving memory of my brave, strong, and wonderful mother.

I love you and miss you so much.

1966-2020

Contents

x

Abstract

Chirality is the name given to explain structures that exist in mirror-image forms. In chemistry, it occurs when a compound contains an asymmetric carbon centre, giving rise to two configurations known as enantiomers ((-) and (+)) which are chemically the same but cannot be superimposed onto one another. Traditionally, studies on the analysis of biogenic volatile organic compounds (BVOCs) in the atmosphere have commonly failed to separate enantiomers since enantiomers share many of the same properties, such as boiling point and reaction rates with atmospheric oxidants. Yet biological systems are known to be enantioselective, resulting in imbalances of enantiomers seen throughout plants. At present, the reason why different species of plants have evolved to emit a certain ratio of enantiomers still largely remains a mystery. This thesis addresses the following four topics:

1. Determining the enantiomeric signatures of monoterpene emissions from branches and stems of pine trees (*Pinus pinaster Ait*.), and the soil in a Mediterranean maritime pine tree plantation. The enantiomeric signatures of a tree were previously thought to be uniform across the whole of the tree's structure. In this study, branch emissions contained a higher percentage of (+)-pinene enantiomers to the sum of total enantiomers than the emissions from the stem and the soil. Hitherto neglected sources of volatile organic compounds (VOCs), soil and stems, contributed significantly to the overall VOC flux, most notably under high moisture conditions. Hence, these results suggest that the enantiomeric signatures of different sources can be used to identify shifts in the contributions of emission sources.

2. Analysis of the effect of drought on the abundance of chiral monoterpenes and isoprene to an extended drought and rewetting experiment inside a tropical rainforest mesocosm. Tropical rainforests contribute a significant portion of BVOCs to the atmosphere. Thus, it is important to investigate how drought manipulates those emissions since droughts are expected to become more common throughout the 21st century. In this investigation, drought increased the abundance of monoterpenes in the atmosphere, with a larger increase measured for (-)-enantiomers than for (+)-enantiomers). Labelling the atmosphere with $^{13}CO_2$ revealed that (-)-α-pinene was mainly a *de novo* emission, whereas (+)-α-pinene was only emitted from storage pools. Severe drought increased the monoterpene emission from storage pools, which has the potential to cause a negative feedback effect on the climate by enhancing cloud formation. These results demonstrate how enantiomers should be considered as separate compounds, instead of the common practice of measuring and modelling them together as a single compound.

3. Analysis of the chiral terpenoid emissions from two different tropical plant species, *Clitoria fairchildiana,* and *Piper* sp., during a 9.5 week extended drought and rewetting experiment inside an indoor tropical rainforest mesocosm. Different studies have found that drought increases, decreases or has no effect on monoterpene emissions. Therefore, a complete understanding of how drought affects monoterpene emissions does not yet exist. Many past drought experiments have focused on the effect of drought on Mediterranean and boreal plant species, but few studies exist which focus on tropical plant species. In this study, monoterpene emissions were generally found to increase and decrease at specific points during the drought. Furthermore, the monoterpene enantiomer emissions were found to respond differently from *C. fairchildiana*, but responded in the same manner from *Piper* sp.

4. The abundance of chiral monoterpenes emitted from a pine tree, *Pinus heldreichii*, was measured before and after mechanical wounding using sorbent cartridges in combination with offline gas chromatography-time of flight-mass spectrometry (GC-ToF-MS), and cavity-enhanced chiral polarimetry (CCP). Both instruments showed differences between the dynamics of the total monoterpene concentration and chiral signal of the plant emissions, which became more negative in response to mechanical wounding. This study of the mechanical stress response of chiral monoterpene emissions highlights the importance of real-time in situ measurements of chiral VOCs emitted from vegetation. Additionally, for the first time, CCP was directly connected to GC for the separation and detection of chiral compounds. The first chromatogram to be obtained with a CCP detector is shown here.

Zusammenfassung

Chiralität ist die Bezeichnung für Strukturen, die in spiegelbildlicher Form vorliegen. In der Chemie tritt dies auf, wenn eine Verbindung ein asymmetrisches Kohlenstoffzentrum enthält, wodurch zwei Konfigurationen entstehen, die als Enantiomere ((-) und (+)) bezeichnet werden, die chemisch gleich sind, sich aber nicht übereinander legen lassen. In der Vergangenheit ist es bei Studien zur Analyse biogener flüchtiger organischer Verbindungen in der Atmosphäre in der Regel nicht gelungen, die Enantiomere zu trennen, da viele ihrer Eigenschaften wie Siedepunkt und Reaktionsgeschwindigkeit mit atmosphärischen Oxidationsmitteln gleich sind. Es ist jedoch bekannt, dass biologische Systeme enantioselektiv sind, was zu einem Ungleichgewicht der Enantiomere in Pflanzen führt. Der Grund, warum sich verschiedene Pflanzenarten so entwickelt haben, dass sie ein bestimmtes Verhältnis von Enantiomeren emittieren, bleibt derzeit noch weitgehend ein Rätsel. Die vorliegende Arbeit befasst sich mit den folgenden vier Themen:

1. Bestimmung der enantiomeren Signaturen von Monoterpenemissionen aus Zweigen und Stämmen von Kiefern (*Pinus pinaster Ait.*) und aus dem Boden in einer mediterranen Seekiefernplantage. Bisher war man davon ausgegangen, dass die enantiomeren Signaturen eines Baumes über die gesamte Baumstruktur hinweg einheitlich sind. In dieser Studie enthielten die Emissionen aus den Zweigen einen höheren Anteil an (+)-Pinen-Enantiomeren an der Summe der Enantiomere als die Emissionen aus dem Stamm und dem Boden. Die bisher vernachlässigten VOC-Quellen Boden und Stängel trugen erheblich zum gesamten VOC-Fluss bei, vor allembei hoher Feuchtigkeit. Diese Ergebnisse deuten darauf hin, dass die enantiomeren Signaturen verschiedener Quellen genutzt werden können, um Verschiebungen in den Beiträgen der Emissionsquellen zu erkennen.

2. Analyse der Auswirkung von Trockenheit auf die Häufigkeit von chiralen Monoterpenen und Isopren in einem ausgedehnten Trockenheits- und Wiederbefeuchtungsexperiment in einem tropischen Regenwald-Mesokosmos. Dürren stellen ein besonderes Risiko für tropische Regenwälder dar, da sie mehr BVOCs in die Atmosphäre abgeben als alle anderen Waldökosysteme. Die Trockenheit erhöhte die Häufigkeit von Monoterpenen in der Atmosphäre, wobei ein größerer Anstieg für (-)-Enantiomere als für (+)-Enantiomere gemessen wurde.) Die Markierung der Atmosphäre mit $^{13}CO_2$ zeigte, dass (-)-α-Pinen hauptsächlich de novo emittiert wurde, während (+)-α-Pinen nur aus Speicherpools freigesetzt wurde. Schwere Trockenheit erhöhte die Emission von Monoterpenen aus Speicherpools, was möglicherweise einen negativen Rückkopplungseffekt auf das Klima hat, indem es die Wolkenbildung verstärkt. Diese Ergebnisse zeigen, dass Enantiomere als getrennte Verbindungen betrachtet werden sollten, anstatt sie wie üblich zusammen als eine einzige Verbindung zu messen und zu modellieren.

3. Analyse der chiralen Terpenoidemissionen von zwei verschiedenen tropischen Pflanzenarten, *Clitoria fairchildiana* und *Piper* sp., während eines 9,5-wöchigen Experiments mit längerer Trockenheit und Wiederbefeuchtung in einem tropischen Regenwald-Mesokosmos. In verschiedenen Studien wurde festgestellt, dass Trockenheit die Emission von Monoterpenen erhöht, vermindert oder nicht beeinflusst. Daher ist noch nicht vollständig geklärt, wie Trockenheit die Monoterpenemissionen beeinflusst. Viele frühere Dürreexperimente konzentrierten sich auf die Auswirkungen von Trockenheit auf mediterrane und boreale

Pflanzenarten, aber es gibt nur wenige Studien, die sich auf tropische Pflanzenarten konzentrieren. In dieser Studie wurde festgestellt, dass die Monoterpenemissionen im Allgemeinen zu bestimmten Zeitpunkten während der Dürre zu- und abnehmen. Darüber hinaus wurde festgestellt, dass die Emissionen der Monoterpen-Enantiomere bei *C. fairchildiana* unterschiedlich, bei *Piper* sp. jedoch in gleicher Weise reagierten.

4. Die Menge an chiralen Monoterpenen, die von einer Kiefer (Pinus heldreichii) emittiert werden, wurde vor und nach einer mechanischen Verwundung mit Hilfe von Sorptionsmittelkartuschen in Kombination mit Offline-Gaschromatographie-Flugzeit-Massenspektrometrie (GC-ToF-MS) und cavity-verstärkter chiraler Polarimetrie gemessen. Beide Instrumente zeigten Unterschiede in der Dynamik der Gesamtmonoterpenkonzentration und des chiralen Signals der Pflanzenemissionen, die als Reaktion auf die mechanische Verwundung negativer wurden. Diese Studie über die Reaktion der chiralen Monoterpenemissionen auf mechanische Beanspruchung unterstreicht die Bedeutung von Echtzeit-In-situ-Messungen chiraler VOC-Emissionen aus der Vegetation. Außerdem wurde CCP zum ersten Mal direkt an die GC angeschlossen, um chirale Verbindungen zu trennen und nachzuweisen. Das erste Chromatogramm, das mit einem CCP-Detektor erhalten wurde, ist hier abgebildet.

Chapter 1: Introduction

1.1. Chirality

In 1848, Louis Pasteur separated an equal (racemic) mixture of sodium ammonium paratartrate crystals by hand into two sets of optically active isomers (enantiomers). In doing so, he achieved the first documented enantiomeric separation. He recognized that the crystals had a fundamental 'handedness', possessing different orientations in space, yet were chemically identical (Pasteur 1848). Since then, chirality has appeared as an important phenomenon in other fields of scientific research; one such field is molecular biology. Since amino acids contain an asymmetric carbon centre, they exist in mirror-image forms denoted by L and D. This gives rise to chiral enzymes, receptors, and carrier proteins. Moreover, enzymes that are made from L-amino acids will discriminate between the enantiomers of sugars, preferentially interacting with D-sugars (Wolfrom, Lemieux, and Olin 1949, Melcher 1974). This results in biological systems commonly consisting of L-amino acids and D-sugars as opposed to L-amino acids and L-sugars or D-amino acids and D-sugars. This interaction is analogous to a left hand feeling more comfortable holding a right hand instead of another left hand. Interestingly, if an enzyme consisting of L-amino acids were to incorporate even one D-amino acid into its structure instead, disastrous consequences can occur involving the enzyme becoming misshapen and inactive. Cases of that happening have been implicated in various diseases (Ulbricht 1981, Bastings et al. 2019). To prevent that from happening, the human body produces specific enzymes that eliminate D-amino acids.

For massless particles, namely photons, chirality is defined as the projection of a particle's spin in the direction of its momentum and is equivalent to the particle's helicity. An interesting phenomenon occurs when plane-polarized light is incident on a chiral structure; the light will become either right or left circularly polarized. Strikingly, this phenomenon manifests itself in nature, as sunlight is 0.1% circularly polarized due to the scattering of photons caused by aerosols in the atmosphere (Lough and Wainer 2002). At sunrise, there is an excess of right circularly polarized light whereas at sunset there is an excess of left circularly polarized light. The interaction of plane polarized light with chiral molecules can be exploited to gain information about the chiral molecule. When plane-polarized radiation is incident on a chiral molecule, the light will be rotated by an angle, α, dependent on the wavelength of light. However, if this experiment is performed with a constant wavelength on a range of chiral compounds, each compound will possess a characteristic angle of rotation. Furthermore, the left and right components of circularly polarized light can be differentially absorbed, known as circular dichroism (Lough and Wainer 2002).

Despite the importance of enantiomeric selectivity in other fields of research, little attention has been given to enantiomers in atmospheric chemistry as enantiomers are commonly measured and modelled together (Jardine et al. 2017, Yáñez-Serrano et al. 2018, Guenther et al. 2012). Differentiating enantiomers is often overlooked since they have identical chemical properties such as boiling point, vapour pressure, and reactivity with oxidants (Zannoni et al. 2020). The few studies that resolved enantiomers have shown that there is a wealth of knowledge to be gained from studying chirality in biosphere-atmosphere interactions (Zannoni et al. 2020, Williams et al. 2007, Song et al. 2014). Past research has revealed that there are unexplained variations in the chiral composition of the atmosphere over various forests and during different seasons. During April 2005, it was found that the air in a boreal forest in Hyytiälä, Finland, contained an excess of (+)-enantiomers of the predominant monoterpene α-pinene. Contrastingly, in October 2005 as part of the same study, the atmosphere over a tropical rainforest in South America (Suriname, Guyana and French Guyana) found that the air contained an excess of (-)-enantiomers (Williams et al. 2007). Furthermore, the enantiomeric composition of the air at a measurement station situated on the Iberian peninsula,

Spain, was revealed to be seasonally dependent (Song et al. 2011). During the summer, there was a strong excess of the (-)-enantiomer (94%), whereas during the winter there was a slight excess of the (+)-enantiomer (51%). More recently, a surprising difference in chirality was measured between the top and bottom of a 325 m measurement tower in the amazon rainforest, in addition to changes in chirality seen with changes in season and time (Zannoni et al. 2020). It was suggested that this phenomenon was caused by insect emissions local to the measurement site. The lack of confirmed explanations as to why such differences in chirality are seen in field studies suggests that there is more to be learned about biogenic chiral emissions. The following paragraphs will explain the role that BVOCs play in the atmosphere, specifically isoprenoids.

1.2. Biogenic volatile organic compounds (BVOCs)

The term volatile organic compounds (VOCs) refers to almost all carbon-containing compounds whose vapour pressure is approximately greater than or equal to 0.01 kPa, thereby allowing them to vaporise under ambient conditions. Excluded from this group are carbon monoxide (CO), carbon dioxide (CO_2), and methane (CH_4). Despite contributing a small fraction to the total composition of the atmosphere, it is estimated that many VOCs are present in the atmosphere in the sub-parts per billion (ppb) range. The estimated number of VOCs in the atmosphere that has so far been measured is thought to be somewhere in the range of 10^4-10^5 and incredibly, this is thought to be only a small percentage of the VOCs that are actually present (Goldstein and Galbally 2007). Depending on the source, VOCs are commonly labelled as either anthropogenic or biogenic. Biogenic sources account for the greatest amount of VOC emissions with an average of 860-1100 Tg (VOC) yr^{-1} (Sindelarova et al. 2014). Whereas emissions from anthropogenic sources are ca. a factor of 6 lower than biogenic sources, accounting for an average of 150-160 Tg (VOC) yr^{-1} (Hoesly et al. 2018). Furthermore, biogenic and anthropogenic emissions are not uniformly distributed around the globe. The tropics contribute the greatest amount of BVOCs to the atmosphere, most notably, the Amazon rainforest, South America, which emits ca. 40% of all BVOCs (Guenther et al. 2012).

1.2.1. Oxidative capacity of BVOCs

Once emitted, BVOCs become a part of a dynamic atmosphere where they can undergo a range of processes such as photolysis, mixing, advection, dry/wet deposition, and oxidation (Seinfeld and Pandis 2012). BVOCs are mostly oxidised by the hydroxyl radical, ozone , or the nitrate radical. Upon consecutive oxidation processes, BVOCs will grow in size and form secondary organic aerosol (SOA) but these carbon chains can also fragment leading to the formation of lower molecular weight compounds. Thus, given time, all gas-phase oxidation processes of VOCs would ultimately lead to the production of CO_2, if not physically removed by wet or dry deposition (Hallquist et al. 2009). The primary oxidant of VOCs in the troposphere during the daytime is the hydroxyl radical because its formation is dependent on the photolysis of ozone at wavelengths less than 310 nm. The resulting excited oxygen atom (O^1D) reacts with a water molecule to form OH. VOCs react more rapidly with OH than methane and by suppressing OH in certain regions can prolong the lifetime of methane in the local atmosphere and influence the atmosphere's ability to clean itself (Peñuelas and Staudt 2010). Since methane is classed as a greenhouse gas, increases in BVOC can have an indirect influence on the Earth's radiative balance.

1.2.2. Isoprenoids

Isoprenoids is the collective name given to an extensive family of diverse VOCs, which are formed from units comprising of five carbons. Based upon the number of C5 units that the compounds contain, they are subdivided into hemiterpenes (C5), monoterpenes (C10), sesquiterpenes (C15), diterpenes (C20), triterpenes (C30), tetraterpenes (C40), and polyterpenes (>C45). The biggest contribution to the atmosphere out of all BVOCs is isoprene (69.2%) (Sindelarova et al. 2014). Monoterpenes are a large subclass of biogenic hydrocarbons that can have linear or cyclic structures (**Fig. 1**). Whereas isoprene is known to be emitted directly following synthesis within the leaf, known as *de novo* emission, monoterpenes can be emitted *de novo* or emitted from specialised or non-specialised storage pools. Specialised storage pools refer to the pools located inside structures such as resin duct, whereas, non-specialised storage pools refers to lipid or aqueous phase storage within a plant leaf, mostly common in tropical species (Niinemets and Reichstein 2002).

Some monoterpenes contain an asymmetric carbon (or chiral) centre and therefore exist as an enantiomeric pair (**Fig. 2**). The emission ratio of the enantiomers is often not equal (non-racemic) as one of the enantiomers in the air will dominate over the other enantiomer. Little is known about the benefits of emitting particular ratios of enantiomers to the plant, however past studies have revealed that insects react differently to each enantiomer and enantiomers act as signalling compounds to some species of insects (Erbilgin and Raffa 2000, Renwick, Hughes, and Krull 1976).

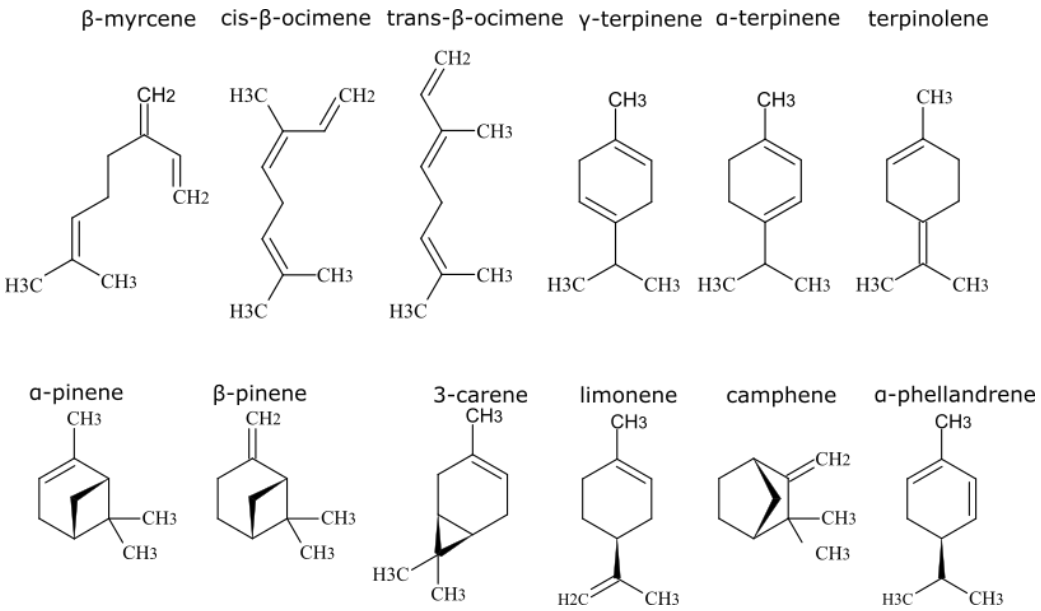

Figure 1. Structures of the most important monoterpenes that were investigated within this thesis.

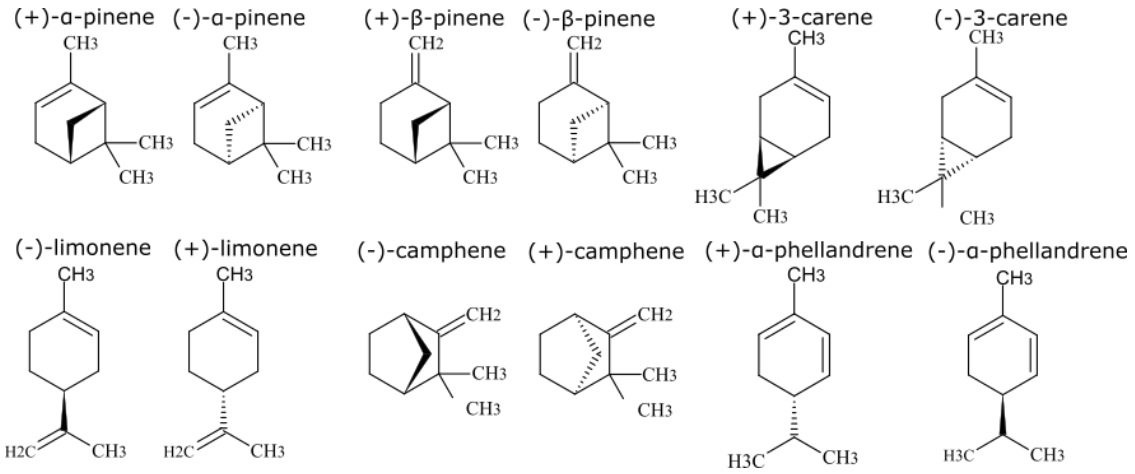

Figure 2. Structures of a selection of chiral monoterpenes that were investigated within this thesis.

1.2.3. Biosynthesis of isoprenoids

Isoprenoids are produced by two different pathways: in the chloroplasts via 2-C-methyl-D-erythitol 4-phosphate (MEP) pathway or in the cytoplasm via the mevalonate pathway (MVA) (Sharkey, Wiberley, and Donohue 2007). The MEP pathway is directly linked to the Calvin cycle, where assimilated carbon from uptaken CO_2, is fixed into glyceraldehyde 3-phosphate (G3P). The MEP pathway involves a series of enzymatically driven reactions, beginning with the reaction of G3P with pyruvate and ending with the formation of the precursor to all isoprenoids, dimethylallyl diphosphate (DMAPP), and its isomer, isopentanyl diphosphate (IPP). Isoprene can be formed by isoprene synthase acting on DMAPP. Through the combination of DMAPP and IPP, Geranyl Diphosphate (GPP) is formed, the precursor to all monoterpenes (Kesselmeier and Staudt 1999). A family of enzymes known as terpene synthases are then able to convert GPP into an array of monoterpenes, but one monoterpene will characteristically be produced most commonly (Degenhardt, Köllner, and Gershenzon 2009b). Terpene synthases are enantiomerically specific. Meaning that if one produced monoterpene is orientated in the (-) configuration, then any other chiral products will also be (-) (Phillips, Savage, and Croteau 1999, Degenhardt, Köllner, and Gershenzon 2009b). Further combination of GPP with an increasing number of DMAPP units leads to the formation of larger substrates which can be used to form their corresponding isoprenoid e.g. Farnesyl diphosphate (C_{15}) and geranylgeranyl diphosphate (C_{20}) are the common acyclic precursors for sesquiterpenes and diterpenes respectively etc. (Lichtenthaler, Rohmer, and Schwender 1997, Croteau 1987, Kesselmeier and Staudt 1999).

Once isoprenoids have been synthesized, they can either be emitted directly from the leaf to the surrounding environment, termed *de novo* emission, or they can be sent to specific or non-specific storage pools (Niinemets and Reichstein 2002, Ghirardo et al. 2010, Staudt et al. 2017). Specific (or specialised) storage pools refer to plant organs such as resin ducts, typically found in boreal trees, which contain a highly concentrated amount of isoprenoids and be used for purposes such as healing when the plant is wounded by various stressors. Non-specific storage refers to aqueous phase or lipid phase storage pools contained within the leaves and is typical of tropical plant species (Niinemets and Reichstein 2002). Since monoterpenes are relatively hydrophobic (possessing low Henry's constants) and are lipophilic (possessing large octanol/water coefficients) they are a lot more likely to be stored in the lipid phase (Copolovici and Niinemets 2005, Noe et al. 2006). Isoprene is not stored in the plant at all and is always emitted *de novo* (Sharkey, Wiberley, and Donohue 2007). Monoterpenes can be

emitted *de novo* and be emitted from storage pools (Staudt et al. 2017, Ghirardo et al. 2010, Kuhn et al. 2004, Staudt and Seufert 1995). Since the mixture of emitted monoterpenes varies between plant species and chemotype, it is likely that the ratio of *de novo* emission to storage emission also varies (Ghirardo et al. 2010). Moreover, it is also the case that *de novo* and storage emissions will exhibit different dependencies on factors such as light and temperature (Staudt et al. 2017). This is because *de novo* emissions are directly coupled with photosynthesis. Since they are emitted from the leaf directly following biosynthesis, the temperature response of a purely *de novo* emission (e.g. isoprene) resembles the temperature dependence of an enzyme catalysed reaction, exponentially increasing up to an optimum temperature (~40°C) and then rapidly decreasing. However, storage emissions of compounds such monoterpenes are uncoupled from biosynthesis and so the temperature response is modelled on an exponential curve and is driven by temperature affecting vitalization and diffusion processes (Staudt et al. 2017).

It is generally accepted that sesquiterpenes are synthesized by the MVA pathway (Kesselmeier and Staudt 1999). Nevertheless, it has also been reported that the MEP pathway, taking place in the plastids, can contribute IPP to the cytosol for the formation of sesquiterpenes (Bartram et al. 2006). Despite their relatively short atmospheric lifetimes (~mins.), sesquiterpenes have become of increasing importance due to their potential to form secondary organic aerosol (Lee, Goldstein, Kroll, et al. 2006, Lee, Goldstein, Keywood, et al. 2006). Recently it was discovered that sesquiterpenes are emitted in significant amounts by Amazonian soil, influencing the reactive chemistry close to the rainforest floor (Bourtsoukidis et al. 2018). In addition, like monoterpenes, many sesquiterpenes are chiral and there have been few field experiments, which report measurements of enantiospecific sesquiterpenes. This thesis does not include data on sesquiterpenes; however, the same arguments for why it is important to differentiate between monoterpene enantiomers also stands for sesquiterpene enantiomers. Investigations should be performed in the future on the behaviour of sesquiterpene enantiomer emissions and concentrations in the atmosphere.

1.2.4. Emission of isoprenoids from vegetation

Plants have evolved to emit VOCs for three main known reasons: as products of processes related to plant growth, as a defence mechanism, and for reproduction (Peñuelas and Staudt 2010). More specifically, isoprenoids are emitted to attract pollinators, and as defence against biotic and abiotic stressors, which increase the presence of harmful reactive oxygen species (ROS) in the plant (e.g. H_20_2, ●OH, $O_2^{\bullet-}$, $^1O_2$) (Cruz de Carvalho 2008, Gill and Tuteja 2010, Peñuelas and Munné-Bosch 2005, Huang et al. 2019). The synthesis of the most emitted isoprenoid, isoprene, accounts for around 2% of carbon fixed through photosynthesis (Sharkey and Yeh 2001). Fascinatingly, this amount has been found to increase by up to 50% when plants are subjected to extreme stress, even though such a large emission resembles a significant loss of carbon and energy. The fact that such a high demand for carbon can be sustained and increased even when photosynthesis is limited, suggests that emitting BVOCs, namely isoprenoids, is of benefit to the plant.

1.3. The response of BVOC emissions to environmental stress

VOCs are known to play an important role in protecting vegetation from damage caused by various stress factors, for example, heat stress can cause an increase in the presence of ROS, which react with cell membranes and break down internal plant organs (Gill and Tuteja 2010, Huang et al. 2019). The production of volatile isoprenoids relieves heat stress, whereby ROS will react with the isoprenoids and be ejected from the plant through the stomata before the ROS has a chance to cause irreversible damage (Vickers et al. 2009, Huang et al. 2019). Such increases in VOC emissions to the atmosphere leads to increases in secondary organic aerosol (SOA), cloud condensation nuclei (CCN), and the prolonged atmospheric lifetime of methane if the local oxidation capacity is affected (Jokinen et al. 2015, Engelhart et al. 2008, Laothawornkitkul et al. 2009, Peñuelas and Staudt 2010). The consequences of which could lead to further climate change and increased global warming. Extreme weather events, such as drought, are expected to become more common in the future in important ecological regions such as the Amazonian rainforest. The effects of such events on VOC emissions will help in the development of models, which can be used to predict expected feedbacks from alterations in atmospheric abundances.

The effect of different environmental stresses on BVOC emissions has been well documented during many laboratory studies. However, in natural environments, plants will commonly experience conditions very different from those in the laboratory. For example, plants will commonly experience multiple stresses acting together such as drought, heat stress, and stress resulting from damage caused by herbivores. When multiple stresses act coincidentally on a plant, the effect can be additive or in some particular cases, the impact of one particular stress can dominate (Holopainen and Gershenzon 2010). So far, only a few studies have reported the stress response of an entire ecosystem (Pfannerstill et al. 2018, Seco et al. 2015, Tiiva et al. 2017). Few field studies have occurred during stress events due to the logistical issues of organising measurement campaigns during such events. The Biosphere 2 (Arizona, U.S.A) provides a unique opportunity to simulate extreme climate events in an enclosed tropical rainforest ecosystem. Further investigations in such sites are required to further the understanding of how emission trends change in natural environments. The next sub-chapters will explain how BVOC emissions are currently characterised.

1.3.1. Light and temperature

BVOC emissions have been known to increase with temperature for almost half a century (Dement, Tyson, and Mooney 1975). It is now understood that BVOC emission rates will vary exponentially with temperature (Guenther et al. 1995) because of 2 reasons. Firstly, higher temperatures will enhance enzymatic activity involved in BVOC synthesis up to an optimum temperature and secondly, increasing temperature will increase the vapour pressure of BVOC's allowing them to diffuse more easily (Staudt et al. 2017). Temperature also affects stomatal opening, which can restrict or allow certain emissions to pass out of the leaf (Urban et al. 2017). However, stomatal opening is believed to have little effect on the emissions of compounds with a low Henry's constant such as monoterpenes but has a significant effect on compounds with a high Henry's constant such as oxygenated monoterpenes and alcohols (Niinemets, Loreto, and Reichstein 2004). Global average surface temperature change is predicted to increase by 0.3 to 4.8 °C relative to 1985-2005, by the end of the century depending on a variety of scenarios (IPCC 2014). Heatwaves are already occurring more frequently and models predict the frequency to increase even further (Kleist et al. 2012, Perkins, Alexander, and Nairn 2012,

Perkins-Kirkpatrick and Gibson 2017). In 2003, it was predicted that a 2-3 °C increase in global average temperature would increase BVOC emissions by 30-45% (Peñuelas and Llusià 2003). Such an increase in BVOC emissions could deplete the number of hydroxyl radicals (OH) in the atmosphere, thereby suppressing the oxidation of methane, increasing its atmospheric lifetime and hence its radiative impact (Peñuelas and Staudt 2010). Furthermore, in polluted regions, the reaction of BVOCs with NO leads to the formation of ozone (Lelieveld et al. 2008). Ozone and methane are both important greenhouse gases, which can trap heat, which leads to further global warming. Additionally, an increase in global temperatures can directly influence vegetation's biochemical activity, resulting in increased active growth periods (Myneni et al. 1997).

As mentioned in section 1.2.4, the emission of isoprenoids can increase thermotolerance when a plant is subjected to prolonged heat stress (Sharkey, Wiberley, and Donohue 2007, Loreto and Fares 2007, Yáñez-Serrano et al. 2019). Increased isoprene emissions during recovery from prolonged periods of heat stress can last up to several days (Pétron et al. 2001). Enhanced Isoprene emission is controlled by isoprene synthase activity and DMAPP availability (Niinemets et al. 1999, Wiberley et al. 2008). It was reported that enhanced production of isoprene in two tropical plant species, due to heat stress, was found to involve an increase in the use of cytosolic pyruvate, thereby increasing the availability of DMAPP for the biosynthesis of isoprene (Yáñez-Serrano et al. 2019). Monoterpenes are also emitted from some plant species to prevent the cessation of photosynthesis when under stress and to protect internal cells from ROS (Peñuelas and Munné-Bosch 2005). Since some monoterpenes such as trans-β-ocimene and β-myrcene react quicker with ROS than other monoterpenes, their production pathway is favoured and enhanced when the plant is subjected to heat stress (Jardine et al. 2017). For monoterpene emitting plant species, the emission rate of monoterpenes was originally thought to be determined by diffusion and physical evaporation as the majority of emissions were believed to mainly originate from specialised storage pools (Guenther et al. 1993). The mathematical formulation for the temperature dependence of stored VOC emission was originally given as:

$$C_T = \exp\big(\beta(T - T_S)\big) \qquad (1)$$

where T and T_S are the actual temperature and standard temperature (e.g. 303 K), respectively, and β (K^{-1}) is an empirical coefficient, which is derived from the slope of the best-fit curve between temperature and emission rate. Equation 1 is still used to describe the temperature dependence of storage emissions of compounds such as monoterpenes. However, it is now known that monoterpenes are not always emitted from specialised storage pools and can instead be emitted *de novo* (Kuhn et al. 2004, Staudt et al. 2017). Therefore, the temperature dependence of *de novo* emissions such as isoprene and other de novo emitted VOCs, can now be used to model the temperature dependence of *de novo* emitted monoterpenes (Staudt et al. 2017, Guenther et al. 1993), given by:

$$C_T = \frac{\exp\frac{C_{T1}(T - T_S)}{RT_ST}}{1 + exp\frac{C_{T2}(T - T_M)}{RT_ST}} \qquad (2)$$

where T is the leaf temperature (K), R is the ideal gas constant (8.134 J K^{-1} mol^{-1}), T_S is the leaf temperature at a standard condition (e.g. 303 K), C_{T1} (J mol^{-1}), C_{T2} (J mol^{-1}), and T_M are empirically defined coefficients, derived from past measurements. The light-dependent term for *de novo* VOC emissions was originally given as (Guenther et al. 1993):

$$C_L = \frac{a\ C_{P1}\ PAR}{\sqrt{1 + a^2\ PAR^2}} \qquad (3)$$

Where PAR is the flux of photosynthetically active radiation (µmol m^{-2} s^{-1}), α (mol VOC mol^{-1} photons) and C_{P1} (m^2 s μmol^{-1}) are empirically defined coefficients, derived from past measurements. However, a correction was made to equation 3 (Monson et al. 2012) , which meant the term that describes light-dependent *de novo* emissions became:

$$C_L = \frac{a\ C_{P1}\ PAR}{\sqrt{1 + \frac{a^2\ PAR^2}{{C_{P2}}^2}}} \qquad (4)$$

Where C_{P2} (µmol m^{-2} s^{-1}) is another empirically defined coefficient.

1.3.2. Drought and flooding

Drought events are expected to become more frequent in the future due to climate change, posing a threat to the functioning of ecosystems and carbon sequestration (Bonan 2008, Hari et al. 2020, Reichstein et al. 2013, Lehner et al. 2006). Droughts are of particular concern to tropical rainforests as they are one of the biggest terrestrial carbon sinks and much of the sink capacity can be lost following a severe drought (Pan et al. 2011, Wigneron et al. 2020). A plant's fresh biomass is comprised of about 80-95% water, which is important for a range of processes including development and metabolism (Brodersen et al. 2019). To conserve water and prevent dehydration plants reduce their stomatal opening and reduce photosynthesis (Loewenstein and Pallardy 1998). Similar to drought, flooding is also expected to become a more frequent problem throughout the 21st century and beyond (IPCC 2014, Lehner et al. 2006). Flooding inhibits carbon gain and the uptake of oxygen in the roots thereby affecting the growth of the majority of terrestrial plant species. Tolerance to flooding is dependent on a plant's species and genotype and is influenced by a range of factors: the plant's age, time and duration of flooding, water condition, and environmental conditions (e.g. temperature) (Kozlowski 1997, Kreuzwieser, Papadopoulou, and Rennenberg 2004).

The emission rate of certain VOCs can be used as an indicator for plant stress severity (Werner et al. 2020, Monson et al. 2021, Jardine et al. 2017). Drought stress can lead to changes in the primary and secondary metabolism of plants, causing variations in the plant's emissions (Loreto and Schnitzler 2010). Since drought can lead to premature leaf fall, stored VOCs can be released upon biodegradation and released into the atmosphere. Salt and drought stress are interconnected as both are manifested as osmotic stress; therefore, the response of plants to both stresses is the same. In grey poplar, isoprene emission was sustained despite stomatal closure due to salt stress and a reduction in photosynthesis (Teuber et al. 2008). This was made possible by the use of alternative carbon sources such as the breakdown of starch or through respiration (Loreto and Schnitzler 2010). Curiously, past studies have revealed that monoterpene emissions can increase, decrease or remain unaffected by drought stress (Turtola et al. 2003, Kainulainen et al. 1992, Lavoir et al. 2009, Haberstroh et al. 2018, Ormeño et al. 2007). This might be because different plant species may have evolved different strategies for coping with stress, opting for either short or long-term responses (Yáñez-Serrano et al. 2019). Therefore, forming models that accurately predict how emissions change to drought and flooding is complex hence no such models yet exist. A different solution may be to study the total

atmospheric concentration of VOCs in an ecosystem, which is subjected to stress such as drought. Additionally, there have been no studies that have investigated if the chirality of plant emissions changes due to extreme stress events such as drought. Chapter 4 presents a study of how concentrations of isoprene and chiral speciated monoterpenes varied in a managed tropical mesocosm that was subjected to prolonged drought and eventually rewetted.

1.3.3. Herbivory

Insect herbivory is the predominant cause of damage to trees around the world (Michel, Prescher, and Schwärzel 2020, Kautz et al. 2017, Faiola and Taipale 2020). Biotic stressors, such as wounding caused by insects, can induce the emissions of VOCs, increasing emissions to the atmosphere, and can affect carbon sequestration in forests (Kurz et al. 2008, Ghimire et al. 2017, Amin et al. 2013, Faiola, Jobson, and VanReken 2015, Faiola and Taipale 2020). As already mentioned in section 1.3., increases in atmospheric VOC will generally increase the formation of SOA, however, insect herbivory has been reported to decrease the ratio of sesquiterpenes to monoterpenes emitted from Scots Pine, thereby decreasing the potential of the plant's emission profile to form SOA (Faiola et al. 2018, Griffin et al. 1999). Nevertheless, herbivory sometimes strongly suppresses isoprene emission (Copolovici et al. 2017, Brilli et al. 2009, Ye et al. 2019), and isoprene emission has been linked to the suppression of new particle formation and mass of SOA (McFiggans et al. 2019, Lee et al. 2016), thus, herbivory might sometimes favour SOA formation (Faiola and Taipale 2020). Until recently, a model that describes the effect of stress-induced VOC emissions from plants did not yet exist, since a consistent mechanism was not yet known. A new modelling approach to describing biotic and abiotic stress-induced *de novo* emissions has recently been proposed, which relies upon a collection of biosynthetic pathways and could be used to describe herbivory-induced *de novo* emissions for some groups of compounds (Grote et al. 2019).

1.4. Research objectives and thesis outline

BVOCs dominate the global atmosphere, accounting for ca. 85 – 87% of global VOC emissions (Sindelarova et al. 2014, Hoesly et al. 2018). Forests such as the Amazon rainforest are the biggest contributors of BVOC and are expected to face an increasing number of extreme climate events such as heatwaves and drought the rest of the 21st century (IPCC 2014). BVOC emissions are expected to vary greatly with prolonged stress; therefore, understanding how BVOCs are emitted is an important step in informing emission models for the accurate prediction of BVOC emissions. Current emission inventories do not differentiate between enantiomers despite curious regiospecific chiral signatures being measured above the Amazon rainforest and within the canopy of a boreal forest in Finland (Williams et al. 2007, Zannoni et al. 2020). Furthermore, biological systems are known to differentiate between enantiomers making it surprising that the resolution of enantiomers is seldom performed during atmospheric field studies (Degenhardt, Köllner, and Gershenzon 2009b). Therefore, to gain further understanding about the emissions of BVOC, chiral compounds must be resolved. Additionally, to gain more information about the emission and abundance of chiral VOC, more advanced techniques need to be developed and tested in the laboratory and field, which are able to perform real-time chiral analysis with a high level of accuracy.

The differences in emissions and ambient concentrations between enantiomers in forests are still poorly understood as most field and lab measurements do not resolve enantiomers and investigate them individually. This is because enantiomers have the same physical and chemical properties, such as rates of reaction with atmospheric oxidants. However, it is already known that enantiomers are treated separately during biological processes, which may lead to different emission characteristics. To contribute to the knowledge of how BVOC emissions vary with environmental drivers, a study of the chiral emissions from different locations within a homogenous Mediterranean maritime pine forest is included in this thesis. Observed differences in the chirality of the different forest compartments are presented and discussed in chapter 2. The experiment presented in this chapter was my first field campaign in which my contribution was collecting all of the air samples onto sorbent cartridges, as well as reviewing and discussing the data.

As severe climate events such as heatwaves and drought are expected to become more common due to climate change, it is important to understand how emissions of BVOCs will be affected. To better understand how the ambient concentrations of terpenoids are affected by drought, the ambient air within a tropical rainforest mesocosm was measured during a 3 month controlled drought experiment. The measured monoterpenes were resolved into their constituent enantiomers to reveal the individual responses of enantiomers. Further, atmospheric ^{13}C-labelling experiments were performed to differentiate between *de novo* and storage emissions. The study in chapter 4 investigates how drought affects ambient concentrations of terpenoids and provides further evidence for the differences between enantiomers. Chapter 5 focuses on the monoterpene emissions from two tropical plant species within the Biosphere 2 tropical rainforest during the same drought experiment as described in chapter 3. The species investigated were an upper canopy tree species, *Clitoria fairchildiana*, and an understory plant species, *Piper* sp. The method development and characterisation of the analytical equipment used in this thesis are presented in chapter 3.

The accurate assessment of chiral monoterpenes with GC-ToF-MS requires rigorous method development and extensive calibrations to identify and quantify trace-level compounds. A newly developed technique named cavity-enhanced chiral polarimetry (CCP) has been developed for the analysis of chiral VOCs. This technique does not require extensive calibrations since the measurements

are absolute and the polarimetric signal allows for the more accurate determination of enantiomers. Chapter 6 presents an experiment in which the abundance of chiral compounds emitted from a pine tree was thoroughly investigated before and after mechanical wounding. Offline measurements were performed using sorbent tubes and GC-ToF-MS, whilst online real-time measurements were performed with a brand new state-of-the-art technique known as cavity enhancedchiral polarimetry. The advantages and disadvantages of using either system measuring chiral VOCs are also discussed. Furthermore, a GC-CCP system was established for the first time and the first chromatogram was obtained.

Chapter 2: Compartment specific chiral pinene emissions identified in a Maritime pine forest

This chapter has already been published in Science of the Total Environment (STOTEN). I am the second author of the publication and my personal contribution to this work included contributing to the experiment conceptualisation and design, conducting the sampling at the experiment site, and assisting with the review and editing of the manuscript.

M. Staudt, **J. Byron**, K. Piquemal, J. Williams: Compartment specific chiral pinene emissions identified in a maritime pine forest, Science of the Total Environment, Volume 654, 1 March 2019, Pages 1158-1166, https://doi.org/10.1016/j.scitotenv.2018.11.146

Abstract. To track unknown sources and sinks of volatile organic compounds (VOCs) inside forest canopies we measured diel cycles of VOC exchanges in a temperate maritime forest at the branch, stem and ground level with special focus on the chiral signatures of pinenes. All compartments released day and night α- and β-pinene as major compounds. In addition, strong light dependent emissions of ocimene and linalool from branches occurred during hot summer days. In all compartments the overall emission strength of pinenes varied from day to day spanning 1 to 2 orders of magnitude. The highest pinene emissions from ground and stem were observed during high moisture conditions. Despite this variability stem emissions consistently expressed a different chiral composition than branch emissions, the former containing a much larger fraction of (−)-enantiomers than the latter. Pinene emissions from dead needle litter and soil were mostly enriched in (−)-enantiomers, while the chiral signatures of the ambient air inside the forest showed mostly intermediate levels compared to the emission signatures. These findings suggest that different organ-specific pinene producing enzymes exist in Maritime pine, and indicate that emissions from ground and stem compartments essentially contribute to the canopy VOC flux. Overall the results open new perspectives to explore chirality as a possible marker to recognize shifts in the contributions of different VOC sources present within forest ecosystems and to explain observed temporal changes in the chiral signature of pinenes in the atmosphere.

2.1. Introduction

Plants produce a large array of organic compounds whose vapour pressures are high enough (approx. ≥0.01 kPa) for them to become volatilized under ambient temperature conditions. All plant organs, namely flowers and fruits, foliage, stem, and roots can release volatile organic compounds (VOCs). Diverse ecological functions have been attributed to plant VOCs. The attraction of pollinators and seed dispersers by flower and fruit scents is an essential driver of sexual reproduction and evolution in many plant species. Furthermore, plant VOCs can serve as signals in interactions with biotic stressors and can even have toxic, repellent or aposematic effects against attackers and thereby contribute to limit damages to plants (Rowen and Kaplan 2016).

However, once emitted in the atmosphere the carbon skeleton of plant VOCs reacts gradually with oxidants to form progressively more oxidised species and ultimately CO_2. During oxidation, a substantial portion of intermediate products may be removed from the atmosphere via dry and wet deposition. In sunlit air containing nitrogen oxides, transient radicals from VOC oxidation generate tropospheric ozone, which is an important greenhouse gas and air pollutant (e.g. (Churkina et al. 2017)). In addition, more stable low volatility oxidation products can condense on existing atmospheric particles or even contribute to new particle formation (Jokinen et al. 2015), which may further act as cloud condensation nuclei. These secondary organic aerosols have important impacts on the Earth's radiative balance and therefore on climate forcing. In particular monoterpenes (C10) and other large reactive VOC molecules are prone to be strongly involved in aerosol formation over rural, forested areas (Jokinen et al. 2015, Zhang et al. 2018). Monoterpenes constitute the second largest class of highly reactive VOC on the global scale (Guenther et al. 2012), and they are particularly strongly emitted from coniferous forests (Kesselmeier and Staudt 1999).

Many monoterpene species and any VOC containing an asymmetric carbon center in its molecular structure exist in mirror image forms called (+) and (−) enantiomers or optical isomers. Enzymes often synthesize chiral-specific products and/or distinguish between the enantiomers of a chiral substrate (e.g. (Phillips, Savage, and Croteau 1999)). Biologically active molecules that are chiral can express an enantiomer-specific effectiveness in their receptors such as chiral olfactory receptors of insect antennae (e.g. (Wibe et al. 1998)). Alpha- and β-pinene are among the most common and abundant monoterpenes in the atmosphere. Each one naturally exists as a (+) and a (−) enantiomer that can be differentiated and detected in air (Williams et al. 2011). In the past, the monitoring of these enantiomers in the atmosphere revealed unexplained regional and temporal variation patterns in the atmospheric chiral composition over various forests (Williams et al. 2007, Song et al. 2011, Yassaa et al. 2012). For example, Williams et al. (2007) reported region-specific enantiomeric ratios for α-pinene in ambient air over tropical and boreal ecosystems, whereby the (−) form dominated over the tropical rainforest and the (+)-form over the Boreal forest. Furthermore, over the tropical forest variations in (−)-α-pinene correlated better with isoprene than with its own (+)-enantiomer. Song et al. (2012) monitored pinene enantiomers over a Mediterranean Stone pine forest during winter and summer and observed a marked diel cycle during summer but not during winter. All these variation patterns point to the existence of unknown pinene sinks and/or to multiple pinene sources that behave differently in response to environmental factors. In principle, enantiomers have the same reactivity towards atmospheric oxidants (OH, O_3 and NO_3) and therefore gas-phase stereo-selective air chemical sinks are unlikely to exist inside forest canopies (Williams et al. 2011). By contrast, the up-take of monoterpenes by soil and micro-organisms has been reported in several studies (Asensio et al. 2007, Aaltonen et al. 2013, Bamberger et al. 2011, Spielmann et al. 2017, Puentes-Cala et al. 2018), and this may be chirally specific if associated with stereo-selective sinks such as microbial enzymes. However,

the reported uptake rates are rather small (Asensio et al. 2007, Aaltonen et al. 2013), especially when compared with the large canopy fluxes from monoterpene-producing forest ecosystems. Thus, so far, the most plausible explanation of the mysterious diel cycles in the air is that distinctly different pinene sources co-exist in forest ecosystems, one stemming from a light-dependent de-novo synthesis pool predominantly active during day time and the vegetative period and one stemming from storages pools active throughout the course of day and seasons. Both putative sources might be present in the same species as for example evidenced from labelling experiments with Scots pine by (Lüpke et al. 2017), or be separated in different organs and/or organisms present in the forest ecosystems. In a previous study, we examined light and temperature responses of α-pinene enantiomers emitted from branches of three common evergreen Mediterranean woody plant species (Song et al. 2014). No clear divergence in the temperature and light responses of emissions was observed that could explain the temporal changes of enantiomeric ratios in ambient air over forests. Here we present results from an exploratory pilot study conducted in a Maritime pine plantation. We investigated diel cycles of terpene air concentrations and exchange rates at branch, stem and ground levels in order to see whether stereo-selective pinene sources/ sinks can exist in the different compartments of coniferous forests that could cause temporal and spatial variations of the enantiomeric signature of pinenes in ambient air.

2.2. Material and methods

2.2.1. Measurement site and meteorological conditions

The measurement site is part of the European program ICOS (Integrated Carbon Observation System) situated in the Landes forest of south-west France. It is located in a homogeneous 13-year old Maritime Pine (*Pinus pinaster Ait*.) plantation (44°29’39.69”N, 0°57’21.75”W, altitude: 37 m), about 50 km south-west of Bordeaux and 25 km east of the Atlantic coast. The soil is a typical sandy, acid podsol covered with a low sparse understory of moor grass (*Molinia caerulea*), heather (*Calluna vulgaris*) and gorse (*Ulex europaeus*). The canopy height of the forest was about 7 m and LAI around 2 (Kammer et al. 2018).

The measurement campaign lasted from 10th to 21st July. Weather conditions were very variable (Table 1). In the beginning of the measurement period, conditions were mostly overcast, humid with sporadic morning fog and drizzle, and moderately warm during day (20–23 °C) and night (15–18 °C). Subsequently, the weather became progressively drier, warmer with peak temperatures above 35 °C during daytime, ending with a brief thunderstorm in the evening hours. During the last days of the measurement campaign, the weather became again humid and only moderately warm (<25 °C, see Table 1). Generally, during most days of the campaign, the winds exhibited a typical day-night profile with calm nights and turbulent conditions during the day. These days were dominated by north westerly winds that became almost calm at night. In contrast, during the warmest period from 16th to 18th, the wind changed direction to south easterly and turbulence persisted throughout the night. Solar noon was at 14 h 09 local time.

2.2.2. VOC sampling and analysis

From 11th to 21th July, we measured nine diel cycles (24 h) of VOC exchanges and ambient concentration in three forest compartments namely: branch, stem and ground (litter and soil). In each compartment three diel cycles were measured consecutively, each time changing the compartment, sampled tree and underlying soil plot. Diel cycles are here after referred to as B1–B3 (Branch), S1–S3 (Stem) and G1–G3 (Ground), respectively. At the end of the campaign, additional measurements were made on bare soil (G4), on the same plot as G3 after having removed pine needle leaf litter and detritus the day before. For quantitative VOC measurement, 3 l of air was sampled at a flow of 150 ml min^{-1} onto cartridges packed with 180 mg Tenax TA (35 m^2 g^{-1}) and 130 mg Carbograph 1 (90 m^2 g^{-1}) sorbents. Air samples were taken at the entrance (ambient) and exit of the chambers, either alternately with a custom made auto sampler (Max Planck Institute), or simultaneously with two portable hand samplers (Gillian GilAir Plus). The auto sampler consists of a constant temperature magazine housing 20 cartridges, solenoid valves, a pump plus mass flow controller as well as a computer unit, which controls the sampling flow and sequence and records all sampling data. An empty cartridge is kept permanently in place and is used exclusively for bypassing and purging the system. Two ca. 5-m long PFA lines (1/4 in.) were connected on one end to the two inlet ports of the auto sampler and on the other end to the chamber in and outlets via two 3-way PTFE valves. The third spare port of the 3-way valves was used to insert adsorbent cartridges during manual sampling. The autosampler was programmed to start always first with ambient air before switching to chamber air, each time proceeded by a 5-min period of line purging. On most diel cycle measurements, ambient and chamber air was measured every 2 1/2 hours from 8 am to 7 am on the following day. Additional VOC samples of ambient and chamber air were taken with the hand samplers inbetween the regular sampling times. These extra samples were used for testing and adjusting the split-ratios of the GC–MS analysis or to fill data gaps in case regular samples were lost. They were also used to run some GC–MS analysis on a normal non-chiral column to endorse peak identification of semi volatile compounds (oxygenated monoterpenes and sesquiterpenes).

Table 1. Meteorological conditions during individual diel cycle measurements made from branch, stem and ground in July 2017 at the experimental site of Bilos in the forests of the Landes.

	Diel cycle	Date	PPFD [μmol s^{-1} m^{-2}]	Temperature [°C]		Relative humidity [%]		Rain [mm cum]		Wind speed [m s^{-1}]	
			Day ± SD (Cum * 10^6)	Day ± SD (Max)	Night ± SD (Min)	Day ± SD (Min)	Night ± SD (Max)	Day	Night	Day ± SD	Night ± SD
	Branch 1	14	956 ± 523 (41)	21.3 ± 1.6 (23.3)	15.0 ± 1.5 (13.2)	65 ± 8 (53)	92 ± 5 (98)	0	0	2.3 ± 1.0	1.3 ± 0.5
	Branch 2	17	1176 ± 540 (51)	30.2 ± 3.2 (33.4)	23.1 ± 3.0 (19.1)	47 ± 11 (36)	59 ± 5 (73)	0	0	2.1 ± 0.5	2.4 ± 0.3
	Branch 3	20	717 ± 262 (31)	20.4 ± 0.7 (21.6)	15.1 ± 1.2 (13.2)	65 ± 9 (56)	82 ± 7 (91)	0	0	2.6 ± 0.6	1.1 ± 0.5
	Stem 1	13	718 ± 277 (31)	20.4 ± 1.4 (21.9)	17.9 ± 0.4 (17.2)	78 ± 9 (69)	90 ± 2 (92)	0	0	2.2 ± 0.9	1.0 ± 0.4
	Stem 2	16	1477 ± 521 (64)	28.1 ± 3.4 (30.9)	21.3 ± 2.6 (17.9)	44 ± 11 (36)	76 ± 10 (88)	0	0	3.0 ± 0.8	1.7 ± 0.3
	Stem 3	19	835 ± 374 (36)	22.6 ± 1.4 (24.4)	18.9 ± 1.1 (17.1)	77 ± 8 (66)	90 ± 4 (96)	0.2	0.6	2.0 ± 0.7	1.7 ± 0.6
	Ground 1	12	767 ± 475 (33)	20.6 ± 0.8 (21.8)	17.9 ± 0.8 (16.8)	78 ± 6 (70)	91 ± 6 (98)	0	0.6	3.7 ± 1.1	0.7 ± 0.4
	Ground 2	15	1419 ± 489 (61)	23.0 ± 2.7 (25.5)	16.4 ± 2.1 (14.1)	63 ± 11 (50)	90 ± 8 (97)	0	0	2.2 ± 1.2	1.6 ± 0.3
	Ground 3	18	1324 ± 516 (57)	31.2 ± 4.6 (36.0)	20.0 ± 1.5 (18.5)	50 ± 14 (36)	91 ± 12 (99)	0.4	7.2	2.6 ± 0.7	1.8 ± 1.4
	Ground 4	20	717 ± 262 (31)	20.4 ± 0.7 (21.6)		65 ± 9 (56)		0		2.6 ± 0.6	

mainly sunny, mainly cloudy, cloudy with drizzle, sunny with morning fog, sunny with thunderstorm in the evening.

Cartridges were analyzed using a Shimadzu QP2010 Plus GC–MS equipped with a Shimadzu thermodesorber. Prior to analysis, cartridges were pre-purged for 3 min with dry N_2 to remove excess

water. VOCs were thermally desorbed from cartridges at 250 °C in a 30 ml min^{-1} He flow for 10 min and focused on a low-dead-volume cold trap filled with a bed of Tenax TA sorbent maintained at−10 °C. For thermal injection into the GC column, the cold trap was flash heated to 240 °C and then held for 5 min. Enantiomeric and non-enantiomeric VOCs were separated on a β-cyclodextrin column (30 m, 0.256 mm I.D., 0.25 µm film; J&W Scientific, CA, USA). The column temperature was initially held for 5 min at 40 °C, subsequently raised to 120 °C at 1.5 °C min^{-1},and then on to 200 °C at a rate of 20 °C min^{-1}. Thermal injection was done either in splitless mode or in split mode depending on the expected VOC concentration. Eluting VOCs were identified by comparison of mass spectra and arithmetic retention indices with commercial databases (NIST and Adams) as well as spiking with commercial pure standards (Fluka, Sigma) dissolved in methanol to achieve realistic concentrations. Liquid standards stepwise dissolved in methanol were also used to calibrate the GC–MS system. For unknown VOCs and for VOCs where no standard was available, we applied a mean calibration factor per compound class. Regarding VOC enantiomers, we have focused in the present study on those of α- and β-pinene, which could be well separated on our column and were predominant in all air samples.2.3. Enclosure systems (see Supplementary information 1 for photographs) Dynamic enclosure systems were used to measure the VOC exchange rates with unfiltered ambient air being drawn through the chambers so the chambers were operated at slight under-pressure. Each chamber was equipped with Teflon fittings and tubing and a small fan (motor outside) with Teflon blades that ensured mixing of the chamber air and sustained heat exchange. A quantum probe measuring the Photosynthetic Photon Flux Density (PPFD) was placed outside the chambers facing south and thermocouple inside to monitor chamber air temperature. CO2 gas exchange was measured by means of a LiCOR 6262 infra-red gas analyzer operated in absolute mode. Every 10 min air from the chamber outlet and inlet (ambient air) was alternately directed to the analyzer via a solid valve controlled by a Campbell data logger. The outlet air was taken via a T-fitting from the main line drawing air through the chambers, while the inlet air was taken from an extra line fixed close to the chambers. The data logger continuously recorded temperature and PPFD data as well as the LiCOR data, discarding the first 3 min of data after valve switching. H_2O data were not considered in this study, because during several diel cycles high humidity caused water condensation inside the main outlet lines and occasionally inside the chambers when the enclosed objects were very wet (G1 and S3).

The stem chamber consists of a 5 cm wide and 50 cm long stainless steel sheet, whose ends are bent to form a large U-shape with 3 cm height. The sheet is kept on the stem, vertically aligned and at 3 cm distance to the bark, and is fixed above and below by means of belt tensioners. A coated 50 µm thin FEP film surrounding the stem was clipped onto the steel sheet and the upper and lower ends of film were pressed to the stem with bungee cords. To prevent the film being drawn to the stem during operation, three 1mmdiameter flexible plastic rods were fixed outside around the chamber to the film and sheet through eyelets. The stem chamber enclosed stem sections with an estimated surface ranging between 2000 and 2400 cm^2 (Table S1Supplementary information 2). Once installed, the volume of then closed air around the stem was approximately 5.5 to 6 l. The stem chamber was run with an airflow ranging between 1.3 and 2.0 $lmin^{-1}$.

The ground chamber used in this study is a modified version of one first developed by Rayment and Jarvis (1997) for soil respiration. The chamber head and collar (diameter 25 cm) is made of stainless steel and was equipped with fittings and tubing in PFA Teflon. The chamber outlet port was connected inside to a T-fitting which held a ring of perforated PFA tubing horizontally over the soil. The chamber dimensions and air inlet port are designed to measure soil gas exchange by extracting ambient air above the soil at a rate of about 1 l min^{-1} without generating unwarranted under pressure or causing diffusive retro contamination of the entering air (see (Rayment and Jarvis 1997) for a detailed description). During the campaign, the chamber was operated at a rate of 1 to 1.5 $lmin^{-1}$. Before the

campaign, we tested the VOC behaviour in the chamber under various flow regimes using home-made diffusion tubes as artificial VOC sources. The collars of the chamber were installed on the ground at least 24 h before measurements started, on a spot without understory plants, between two trees within a tree row, and if possible adjacent to the tree used for branch and stem measurements. In these areas the ground was heavily covered with needle litter and coarse detritus and remained undisturbed by human movement (Table S1 Supplementary information 2). To install the chamber, we removed litter and coarse detritus from the soil (mostly sand mixed with small detritus and humus particles), pressed the collar slightly in the soil and gently put back litter and detritus. Litter and soil were wet during the first and last cycle measurements (G1, G4) while they were rather dry during the second and third one (G2, G3). Prior to measurements the chamber head was put on the collar, which was filled with water to ensure tightness.

The branch enclosure was a cylindrical chamber of 15 cm diameter and a volume of approximately 3.5–5.5 l. The chamber head consists of a PTFE Teflon disk that housed the external fittings and fan motor. A cylindrical frame suspended a PFA bag (50 µm) inside was clamped to the head. The frame consisted of two Plexiglas rings interconnected with 3 thin (5 mm) metal braces that were adjusted in length to accommodate for differences in branch size. Small plastic clips were used to fix the PFA bag outside to the braces thus keeping the bag away from the enclosed branch when air was pulled through the chamber. The chamber airflow was kept at rates between 3 and 5.5 l min^{-1} depending on the branch size and time of day. A terminal southern-exposed shoot at 4 to 5 m height, comprising two most recent needle age classes (Table S1 Supplementary information 2) was installed in the chamber the day before measurements and kept open until the chamber was flushed with air. Once the chamber was flushed with air the distal end of the Teflon bag was gently wrapped and loosely tightened around the bare shoot basis.

2.2.3. Data treatments

The VOC exchange rate was calculated from the VOC concentration differences between outgoing (chamber) and incoming (ambient) air multiplied by chamber flow and divided by the enclosed area or dry biomass. For the enclosed area, we used ground surface for soil/litter, needle and stem surface for branch and stem exchange rates (Table S1 supplementary information 2). Stem area was calculated from the height and circumference of the stem section and needle area from dry weight using the mean needle area dry weight ratios reported by (Porté et al. 2000) for the same site. It should be noted that the roughness of the pine bark confers the pine stem a higher surface than the calculated one. The enantiomeric fraction (chiral composition) of α-pinene and β-pinene is presented as the % fraction of the (−) enantiomer to the sum of both (−) and (+) enantiomers for each of the two structural isomers.

Unpaired t-tests (or Mann-Whitney rank sum tests if tests for normality and equal variance failed) were used to test whether the enantiomeric fractions of pinenes differed between the air leaving the enclosure systems and the air entering the enclosure systems (surrounding ambient air). Furthermore, one way ANOVAs (or Kruskal-Wallis tests) were applied to test whether the enantiomeric fractions and the ratios of α-pinene to β-pinene (sum of both enantiomers) were different among the individual diel pinene emissions cycles i) of the three trees for a given compartment, and ii) of the three compartments for a given tree. For ANOVA tests we used only emission data measured by day, because during several diel cycles emissions were very low by night close to zero or even negative

(apparent VOC deposition). Holm-Sidak (orDunns) tests were applied for pairwise comparisons. All statistical tests were run with SigmaStat software (Jandel Scientific Inc.).

2.3. Results

Alpha- and β-pinene were among the strongest emitted VOC from all forest compartments (Fig. 1a–c). They were by far the major compounds emitted from stem and ground during day and night accounting for about 80–90% of the total measured VOC release (for more detailed information see Table S2 Supplementary information 2). Similar high proportions of pinenes were also found in the VOC emissions from branches during night time hours. However, during daytime hours, large amounts of β-ocimene and linalool, plus minor amounts of other ocimene isomers and 1,8-cineol emerged in branch emissions. These apparent light-dependent emissions were not observed in ground and stem emissions. They dominated the VOC release from branches by day on the second and third diurnal cycles and in particular on B2 when the weather was sunny and hot with maximum emissions of almost 2000 ng m^{-2} s^{-1}. Besides, some weak VOC deposition events were indicated for the stem and the ground compartments with apparent deposition rates of up to 10 ng m^2 s^{-1} for light dependent monoterpenes during the G3 cycle; and low rates of b1 ng m^2 s^{-1} for various VOC during the G2 and S2 cycle.

Regarding the chiral signatures of α- and β-pinene, ambient and chamber air always contained more (−) enantiomers than (+) enantiomers (Fig. 1d–i). Especially in β-pinene the (−) enantiomer was predominant, and its (+) form almost never exceeded 15%. Nevertheless, consistent differences in the chiral compositions of pinenes can be seen between ambient and chamber air, as well as within and among compartments and days. The amplitude of chiral composition variation was much higher in the chamber outlet air than in the surrounding ambient air proving that during passage the air became either enriched or depleted in an enantiomeric form. Compared to ambient air, chamber air with branches was consistently enriched in (+)-pinene enantiomers, while the chamber air with stems was consistently enriched in (−)-pinene enantiomers. The air leaving the ground chambers contained also more (−)-enantiomers with the exception of G2, during which it became enriched in (+)-α-pinene and enriched in (−)-β-pinene.

For each tree, the pinene emissions from stems were significantly more enriched in (−)-enantiomers than the emissions from their branches (Table 2), despite the variable weather conditions and large differences in the overall emission strength. However, within each compartment the chiral signatures of pinene emissions were different among trees/days depending on the compound and compartment (Table 2). For example the (−)-α-pinene fractions of pinene emissions differed significantly among the branches of the three trees but not their (−)-β-pinene fractions. Also the ratios of the structural isomers α-pinene to β-pinene were not always the same for pinene emissions of a given compartment. Thus, both stem and branch emissions of tree 2 (B2, S2) had significantly greater α−/β-pinene ratios than the emissions of the two others.

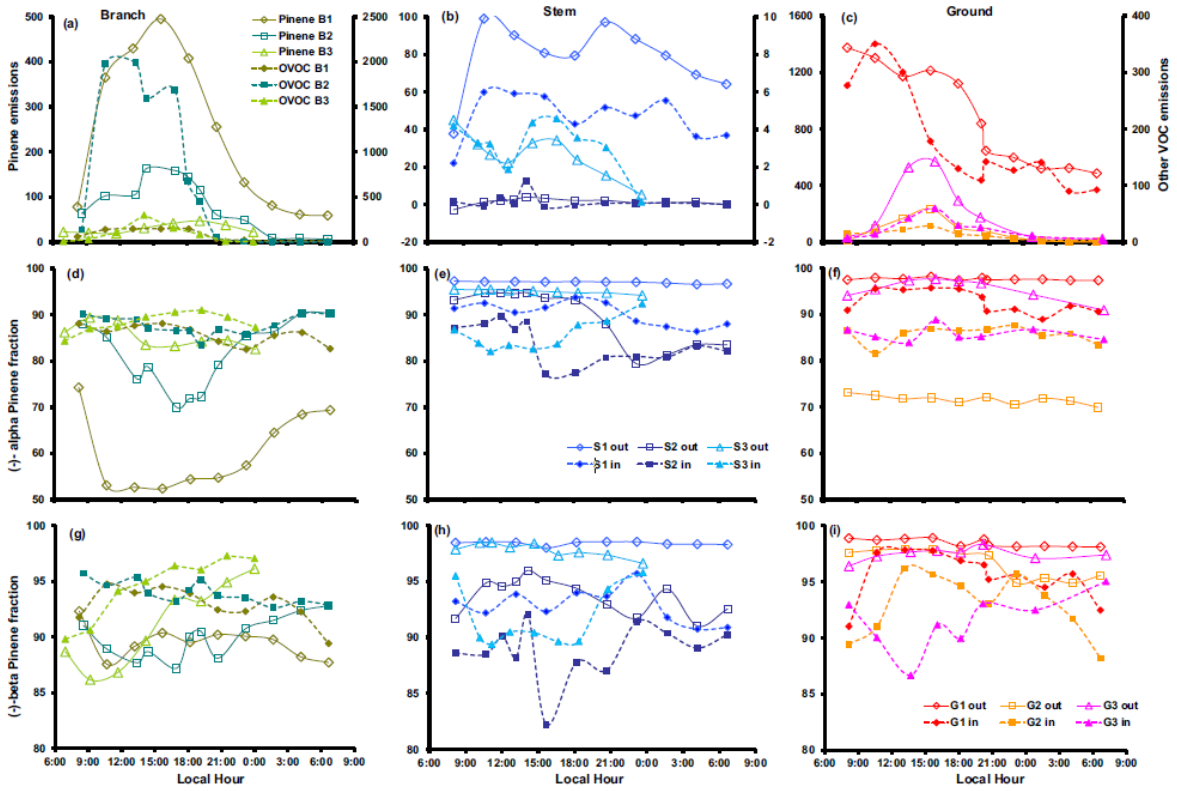

Figure 3. Diel variations of VOC emissions ((a), (b), (c)) and the chiral composition ofα-pinene ((d), (e), (f)) and β-pinene ((g), (h), (i)) in air measured in the different forest compartments, each on three different days: Branches (B1–B3: (a), (d), (g)); Stems (S1–S3: (b), (e), (h)); Ground (G1–G3: (c), (f), (i)). Emission rates are given for the sum of α- and β-pinene enantiomers ("Pinene", open symbols solid lines) and the sum of all other emitted VOC ("OVOC", closed symbols broken lines) expressed in ng per sec and square meter of enclosed total needle area (branch); stem area (stem) and ground area (ground). The enantiomeric composition is presented for the air leaving the chambers ("out", open symbols solid lines) and the ambient air entering the chambers ("in", closed symbols broken lines) as the % fraction of the (−) enantiomer to the sum of both (−) and (+) enantiomers. Note the different Y-scales used for the enantiomeric compositions of α- and β-pinene.

Besides, the intra-day enrichments of the enantiomers in the air of the chambers were primarily associated with the emission strength during the course of diel cycles. The chiral fingerprints of chamber air were always significantly different from that of the corresponding ambient air by day when emissions were high ($P < 0.05$ for B3 and $P < 0.01$ for both (−)-α-pinene and (−)-β-pinene fractions of all other cycles), whereas they were closer and frequently not significantly different by night when emissions were very low (e.g. B2, B3, S2, S3). Compared to chamber air, the enantiomeric composition of pinenes in ambient air varied little over the course of the days and showed no recurrent diel temporal variation or spatial gradient inside the canopy. Nevertheless, on some days the chiral signature of the surrounding ambient air showed enrichment patterns in accordance with local emissions. For example on B1 and B2, when(+)-α-pinene emissions from branches were apparently strong (Fig. 1a), the (−)-α-pinene fraction of ambient air tended to decrease by day (Fig. 1d), while in contrast it tended to increase on B3 when (+)-α-pinene emissions from branches were apparently low. Likewise, during the diel cycles G1 and S1, ambient air in the low forest compartments was particularly enriched in (−)-enantiomers by day (Fig. 1e, f, h, i) in agreement with the strong local emissions of (−)-pinene enantiomers observed on these days (Fig. 1b, c).

Table 2. Characteristics of α- and β-pinenes emissions measured during individual diel cycles on branches, stems and ground plots (forest floor close to the stems) of different trees in a Maritime pine forest. (−)-α-Pinene fraction and (−)-β pinene fraction are the percentage fractions of the (−)-enantiomers in the emissions of α- andβ-pinene respectively, andα-/β-pinene ratio is the ratio of total α- to total β-pinene emissions. All values are means ± SD of n=5 measurements made by day. ANOVA and Kruskal Wallis statistics were used to test whether ratios and fractions are different among i) individual cycles of a given forest compartment (lines); ii) among individual compartments of a given tree (columns). P-values indicate the overall probability of the test results (ns: not significant if $P \geq 0.05$). Superscript letters indicate which of the cycles differs at $\alpha < 0.05$: upper case letters for differences between compartments (columns) and lower case letters for differences among trees (lines). More detailed information on VOC emissions and measurement conditions are given in Table S2 Supplementary information 2.

Cycle/tree	1	2	3		1	2	3		1	2	3	
	(−)-α-Pinene fraction [%]			P_{tree}	(−)-β-Pinene fraction [%]			P_{tree}	α-/β-Pinene ratio			P_{tree}
Branch	53 ± 2^{Aa}	$76 \pm 6^{AB\ b}$	85 ± 4^{Ac}	<0.001	89 ± 1^{A}	88 ± 1^{A}	89 ± 3^{A}	ns	0.3 ± 0.1^{Aa}	1.4 ± 0.3^{Ab}	0.6 ± 0.2^{Aa}	<0.001
Stem	97 ± 1^{B}	97 ± 2^{B}	96 ± 1^{B}	ns	98 ± 1^{B}	99 ± 1^{B}	99 ± 1^{B}	ns	1.2 ± 0.1^{Ba}	4.7 ± 0.9^{Bb}	1.7 ± 0.1^{Ba}	<0.001
Ground	98 ± 1^{Ba}	72 ± 1^{Ab}	97 ± 2^{Ba}	<0.001	99 ± 1^{Ba}	98 ± 1^{Bb}	98 ± 1^{Bab}	0.027	0.9 ± 0.2^{ABa}	1.4 ± 0.1^{Ab}	1.9 ± 0.2^{Bc}	<0.001
$P_{compartment}$	<0.001	0.001	<0.001		<0.001	<0.001	0.008		0.002	<0.001	<0.001	

Accordingly, for a given compartment, ambient air mixing ratios of pinenes (Fig. 2) were frequently lowest during daytime on the days of lowest emissions (i.e. B3, S2, G2). The overall highest mixing ratios were recorded over the ground on G1 reaching several ppb throughout day and night. During most other diel cycles pinene mixing ratios reached maximal values by night and minima by day with lowest values (≪1 ppb) observed in the upper branch compartment. However, on B2 and S2 pinene mixing ratios remained low also during night. Both days were characterized by hot, dry and windy night conditions (Table 1).

Within each compartment, pinene emission rates largely varied from one day to another spanning more than one order of magnitude in the case of stem and ground emissions (Fig. 3). Temperature is known to be the principal factor controlling terpene emissions from plants and is the sole factor taken into account to predict storage derived non-light dependent monoterpene emissions. Typically, these emissions increase exponentially with temperature increase with a slope of about ≈ 0.1 $°C^{-1}$ (coefficient β; Guenther et al., 2012). In the present study, the observed day-to-day variation in the overall strength of pinene emissions was mostly unrelated to temperature changes (Fig. 3). Even within the diel cycles, the proportion of the observed emission evolution explained by temperature (or its co-varying environmental factors) was variable. Good temperature relationships with typical slopes can be seen for pinene emissions from branches on B1 ($R2 = 0.86$, $\beta = 0.12$ $°C^{-1}$) and B2 ($R2 = 0.72$, $\beta = 0.12$ $°C^{-1}$) and the pinene emissions from stem on S2 ($R2 = 0.78$, $\beta = 0.10$ °C−1) although emissions were very low that day. Diel changes in pinene emissions from the ground scaled also well with temperature on G2 ($R2 = 0.84$) and G3 ($R2 = 0.87$) but with much steeper slopes (β=0.27 and 0.23 $°C^{-1}$). However on G1, emissions were only poorly correlated with temperature ($R2 = 0.57$, $\beta = 0.16$ $°C^{-1}$) and no or little apparent relation to temperature showed the diel evolutions of pinene emissions from stem on S1 (R2=0.22) and S3 (R2=0.08) and from the branch on B3 ($R2 = 0.12$). These days were characterized by relatively small diurnal-nocturnal temperature amplitudes under cloudy and humid weather conditions (Table 1).

2.4. Discussion

The significant enrichments of the air inside the branch and stem chambers by either (−) or (+)-pinene enantiomers (Table 2) must be linked to different emission sources. Monoterpene synthases are more specific for optical isomers than for structural isomers with respect to their products (Degenhardt, Köllner, and Gershenzon 2009a). For example in Norway spruce, (Martin, Fäldt, and Bohlmann 2004)

isolated and characterized a terpene synthase producing both (−)-α- and (−)-β-pinene but no enzyme producing both (−) and (+) enantiomers. Accordingly, in Maritime Pine at least two pinene synthases should exist, one producing mainly (−) enantiomers in stem tissues and one in branch tissues producing mainly (+) enantiomers. Because branches are composed of both stem and needle organs, it is likely that the (+)-pinene source is localized inside the needles and that these dominated whole branch emissions. Given that in branch emissions the (−)-α-pinene fractions varied among the days/trees more than their (−)-β-pinene fractions (Table 2), we speculate that several isoenzymes exist in Maritime pine foliage that also differed in the proportions of α- to β-pinene they produce. Genetic variations in the terpene production of conifers have been frequently reported (i.e. chemotypes) including *P. pinaster* (Tognetti et al. 2000, Blanch et al. 2012). More recently, Song et al. (2014) observed clear between-tree differences in the signature of optical and structural monoterpene isomers emitted from a Mediterranean oak species. However, even though inherent factors may have contributed to shape the optical and structural composition of pinene emissions from individual trees, the consistent difference between the chiral signatures of branches and stems suggest that it might be common in Maritime pine populations, possibly a trait that has been conserved during species evolution. If this is confirmed by future studies, it would be interesting to know whether this trait has ecological implications in the tree's interactions to other organisms. For example the olfactory receptors of bark beetles are stereoselective (Reddemann and Schopf 1996, Wibe et al. 1998), and therefore variations in the chiral signature of forest air may play a role in host tree and organ recognition.

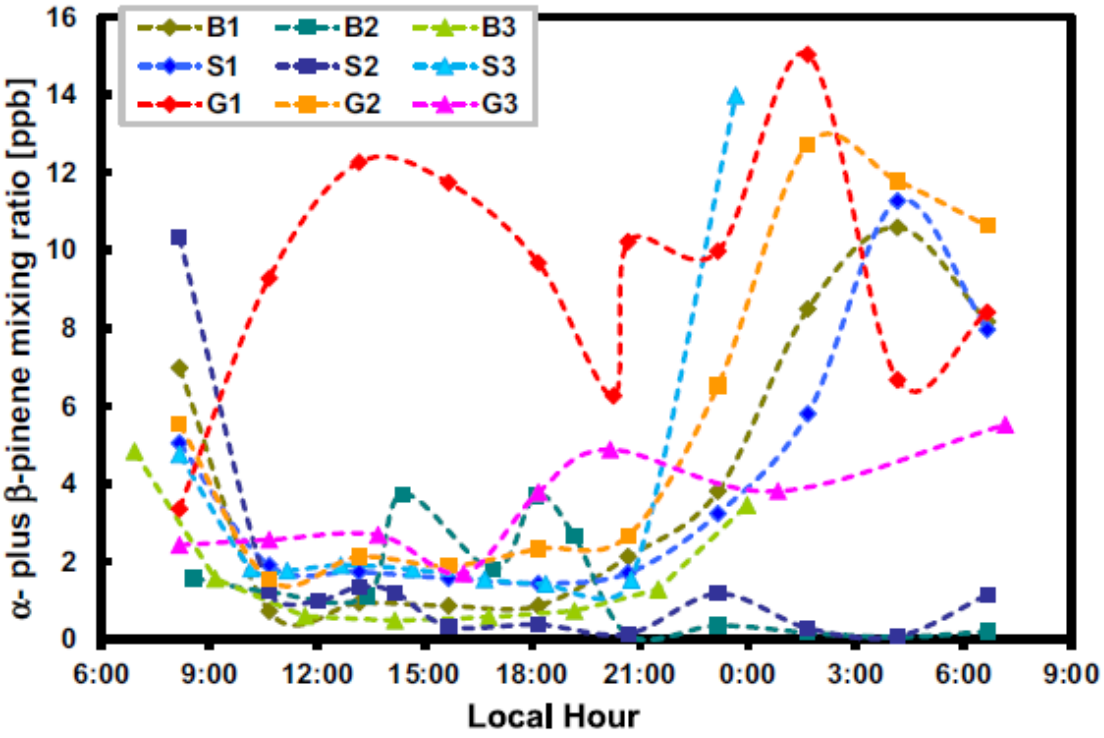

Figure 4. Diel variations of the pinene mixing ratios (sum of α- and β-pinene) in ambient air at different levels inside the canopy of a Maritime pine plantation (S: Stem level, B: Branch level, G: Ground level).

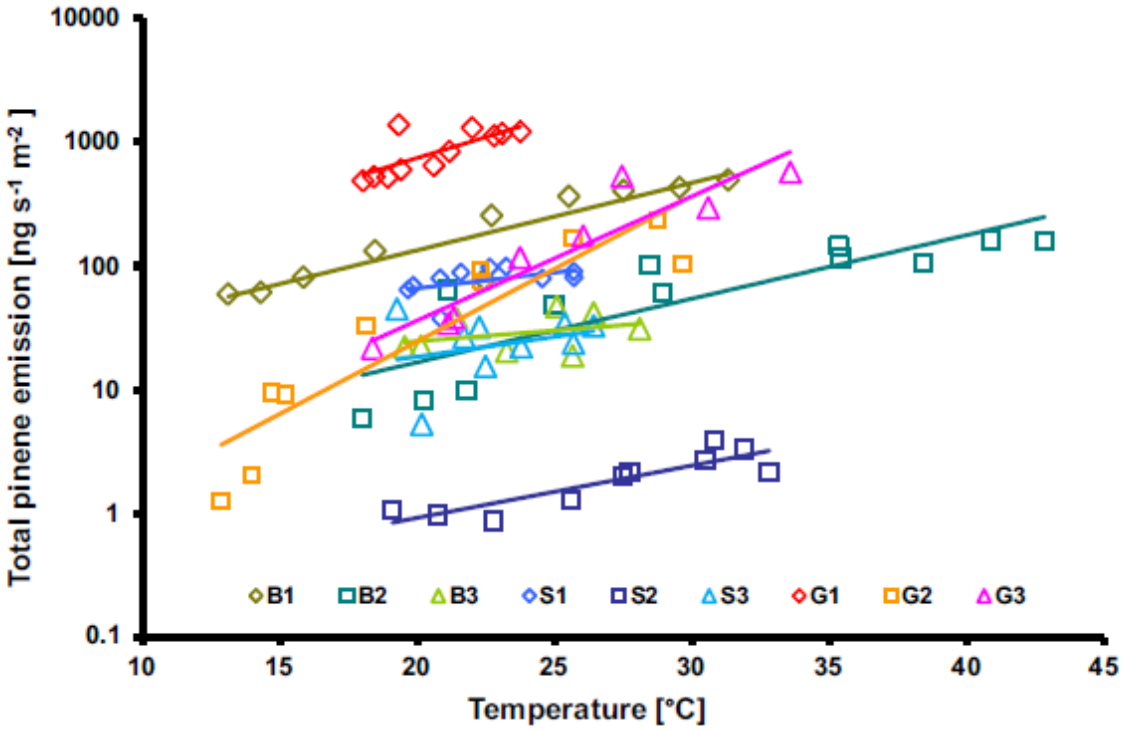

Figure 5. Log-linear plot of pinene emission (sum of α- and β-pinene) against temperature data of individual diurnal cycles measured on different days and in different compartments of a Maritime pine plantation: B1–B3: Branch; S1–S3: Stem; G1–G3: Ground (i.e. soil plus litter). Lines show best fit results assuming an exponential emission-temperature relationship. Emission rates are expressed per m^2 of enclosed stem, soil and total needle areas for stem, ground and branch measurements respectively. In S2, two data points showing negative emissions (apparent VOC uptake) were omitted.

The enantiomeric signature of pinenes released from the ground was always different to that of the surrounding ambient air but the enrichment pattern were less uniform than for stem and branch emissions, possibly because the ground chambers enclosed the largest pool of potential VOC sources and sinks including diverse soil horizons, microbial communities, litter and detritus from several trees in variable decomposition states. Nevertheless, β-pinene emissions from all three G-cycles were strongly enriched in its (−)-enantiomer in contrary to branch emissions. This may imply that a large portion of (+)-β-pinene comes from an ongoing production in living needle tissues that ceases only when needles drop to the forest floor and decay. However, the ground emissions of α- pinene do not entirely support this claim, because only G1 and G3 emissions were strongly enriched in its (−)-form, whereas α-pinene emissions on G2 had a chiral signature similar to branches. It is improbable that an additional unknown stereo-selective (−)-α-pinene sink existed in the in the G2 lot and was particularly active on that day, since we found no evidence of strong pinene deposition in any of the G-cycles even after removal of litter and detritus. Thus, we conclude that either other stereo selective sources than needle litter played a role in ground emissions of G2 or the plot contained larger amounts of needle litter from a (+)-α-pinene chemotype.

The mixing ratios of pinenes in ambient air inside the canopy (cf. Fig. 2) showed during most diel cycles typical day-night profiles similar to those observed previously by Kammer et al. (2018) at canopy height. This resulted from the variation of turbulent mixing with the free troposphere, which was frequently lower during night time allowing the build-up of high pinene concentrations (cf. Table 1). However, weather and associated turbulent conditions were quite variable during the campaign. Therefore and because the emission strength of pinenes in the forest compartments apparently varied strongly from one day and enclosed object to another, the enantiomeric composition of pinenes in

ambient air showed no regular recurrent variation pattern as observed above the canopies of Mediterranean and boreal conifer forests by Song et al. (2012) and Yassaa et al. (2012). Nevertheless some enrichment pattern in ambient air was likely influenced by local emissions, because several within- and between-day variations of the enantiomeric signature of ambient air coincided with the observed variations in the strength of the enantiomeric specific local emissions. However, the chiral signatures of ambient air remained always in between those of the specific emissions at all levels, during daytime on all days with the exception of S2. Consequently, significant (−)-pinene sources must have contributed to shape the chiral signature in the forest air even in the upper branch compartment where (+)-pinene emissions were apparently predominant, provided that no unknown stereo-selective sink existed inside the canopy. We found no evidence of strong stereo-selective uptake of pinenes on branch, stem and ground surfaces and stereo-selective chemical sinks are unlikely to exist in forest canopies, because enantiomers should express the same chemical reactivity to atmospheric oxidants (Williams et al. 2011). Therefore, the relatively large and consistent presence of (−)-pinenes in ambient air indirectly corroborates the strong albeit highly variable (−)-pinene emissions observed at stem and ground levels.

This conclusion assumes however, that the quantities and chiral compositions of pinene emissions measured on these few trees/plots were representative for the site. Yet to our knowledge, no published data are available for litter and stem emissions from *P. pinaster* and only four studies concern the branch emissions. Among these, one studied the enantiomeric composition of pinene emissions from Maritime pine (Yassaa et al. 2001). The reported mean fractions of 73% (−)-pinene and 96% (−)-β-pinene are close to our values of 72.7% (−)-α-pinene and 89.7% (−)-β-pinene (means of all branch measurements). Literature values of absolute pinene emission rates from *P. pinaster* branches are rather variable, as in our study. (Simon et al. 1994) observed low rates of 0.1 to 0.4 μg h^{-1} g^{-1} compared to the values reported in Blanch et al. (2012) ranging between 2 and 12 μg h^{-1} g^{-1} (mean at standard conditions: 7.8 μg h^{-1} g^{-1}). In a more recent screening study of VOC emissions from tree species in Turkey, (Aydin et al. 2014) found values of about 0.6 ± 0.3 μg h^{-1} g^{-1} for pinene emissions from Maritime pine branches. In our study, daily mean emission rates of pinenes were 4.7, 1.6 and 0.6 μg h^{-1} g^{-1} DM for B1, B2 and B3 respectively.

Studies reporting VOC emissions from conifer stems are very scarce. In a boreal forest, (Vanhatalo et al. 2015) continuously measured monoterpene emissions from a scots pine stem during early spring. Mean rates were around 1 ng s^{-1} m^{-2}. However, these authors observed transient high emissions after freeze–thaw cycles of up to 50 ng s^{-1} m^{-2} corresponding to 500 ng s^{-1} m^{-2} when temperature normalized to 30 °C. In a later study at the same site, (Rissanen et al. 2016) surveyed stem monoterpene emissions during May/June and observed regular diel cycles with rates ranging between 0 and 20 ng s^{-1} m^{-2}. In the present study, pinene emissions from Maritime pine stems varied between −2 and 99 ng s^{-1} m^{-2} with daily means of 78 (S1), 1.5 (S2) and 26 (S3) ng s^{-1} m^{-2}.

A larger body of literature is available on VOC emissions from conifer litter and forest floors though none for Maritime pine. In the aforementioned boreal Scots pine forest, monoterpene emissions from the ground ranged approximately between −10 and 250 ng s^{-1} m^{-2} ground area (Aaltonen et al. 2013) with peak emissions occurring during early summer. In alpine coniferous forests (Greenberg et al. 2012) measured low soil monoterpene emissions of up to 0.1 ng s^{-1} m^{-2} and (Gray, Monson, and Fierer 2014) of around 0.2 ng s^{-1} m^{-2} (max 1.2 ng s^{-1} m^{-2}). In an earlier study made in a temperate Sitka spruce forest, (Hayward et al. 2001) reported 30 °C-normalized monoterpene emissions of about 10 ng s^{-1} m^{-2} soil. Further, several studies investigated VOC emissions from conifer litter and soil in the laboratory. (Faiola et al. 2014) measured soil and litter emissions from a temperate mixed coniferous forest and recorded monoterpene emissions ranging between 7 and 70 ng s^{-1} m^{-2} soil. (Gray, Monson,

and Fierer 2010) screened VOC emissions from decomposing litter of various tree species including the two pine species *Pinus contorta* and *P. ponderosa*, for which monoterpene emission rates of respectively 2.3 and 4.3 μg h^{-1} g^{-1} litter were observed. (Isidorov et al. 2010) followed emissions from Scots pine and Norway spruce litter over a 16-month period and found rates ranging between 0.2 and 7.5 μg h^{-1} g^{-1}. In our study daily mean emission rates per ground area were 890, 72 and 199 ng s^{-1} m^{-2} ground area, hence were considerably higher than most of the emission rates observed in previous field studies. This was partly due the huge amount of litter and detritus that covered the soil around the stems (Table S1 Supplementary information 2). When expressed on a litter dry matter basis, daily mean rates of G1, G2 and G3 amount to only 2.0, 0.1 and 0.3 μg h^{-1} g^{-1}. However, two observations indicate that litter was not the only source of pinenes in the Maritime forest floor: first, after removal of litter and coarse detritus bare soil still emitted pinenes in significant amounts albeit at about 5-fold lower rates (Table S2 Supplementary information 2). Second, pinene emissions from ground plots increased far more strongly with increasing temperatures compared to pinene emissions from stems and branches and to monoterpene emissions from storage pools in general ((Staudt et al. 2017) and references therein). As outlined by Gray et al. (2014), this strong temperature dependence could be a result of both biotic (e.g., root and microbial metabolisms) and abiotic processes (e.g., increased evaporation of stored compounds).

Together, the variable emission rates we observed from branches, stems and ground during summer in a temperate Maritime pine forest are in the range of those reported in the literature for the same or other coniferous species. Given that at our site the canopy LAI was relatively modest (ca. 2), stems and the largest part of branches were bare of live needles, and large parts of the underlying soil heavily covered with litter, we conclude that ground and stem emissions significantly contributed to the whole canopy pinene flux. This is consistent with the relatively large presence of (−)-pinenes in ambient air measured during most days of the campaign. A remaining question is why within a compartment, pinene emissions were so variable from one day/tree to another spanning more than one order of magnitude in case of stem emissions. Inherent differences in the tree's capacity to produce and release terpenes might be one reason as indicated from qualitative differences in the tree's emission spectra such as the α-/β-pinene ratios (see above and Table 2). However, it seems unlikely to us that genetic variability among planted trees of the same age would alone cause 10-fold differences in the emission rates that also responded differently to environmental factors such as temperature (Fig. 3). The variability in the relationships of pinene emissions to temperature within and among the compartments implies that external factors other than temperature must have influenced pinene emissions. Terpene emissions from conifer organs are susceptible to change rapidly and profoundly due to sudden outgassing of VOCs or outflow of oleoresin from internal storage pools. Resin secretion has reported to happen spontaneously at specific points of exudation of pine organs (Eller, Harley, and Monson 2013). However, emission bursts can easily be triggered by mechanical stress caused by natural factors such as wind, animals and herbivores attacks or by artefacts as for example the mounting of enclosure systems on pine branches. After a single mechanical stress event, emissions rapidly decrease in an exponential decay approaching near pre-stress levels after several hours (Niinemets et al. 2011). If in our study mechanical stress had occurred during chamber installation prior to diel cycle measurements, emissions would be enhanced at the beginning of the cycles (Fig. 1) generating a “N” sign data distribution in emission-temperature plots (Fig. 3). Such a data distribution is indeed seen for S3 and G1 but not for other cycles with particular high emissions or poor temperature correlation. Therefore, and because chambers have been installed with much care at least the day before measurements started, we conclude that non-natural resin outflow by accidental mechanic stress was not the main cause for the observed temperature independent emission variability. All diel cycles with poor temperature correlation coincide with humid weather

conditions and small day-night temperature amplitudes (Fig. 3, Table 1). During these cycles, surfaces were partly or constantly moisture saturated and even wet due to drizzle, morning fog and dew or previous rain events. A variety of studies made on conifers have observed terpene emission bursts during and after natural or artificial wetting at branch (Lamb et al. 1985, Janson 1993), soil/litter (Warneke et al. 1999, Greenberg et al. 2012, Faiola et al. 2014) and canopy levels (Helmig et al. 1998, Schade, Goldstein, and Lamanna 1999, Mochizuki et al. 2014). The mechanisms leading to these emission bursts are not exactly known. Warneke et al. (1999) hypothesized that after wetting VOC adhering on surfaces during dry conditions dissolve in the aqueous phase and subsequently evaporate. While such a transfer may be important for oxygenated VOC such as acetone, it is likely less relevant for non-oxygenated monoterpenes that have a very low water solubility. Uneven hydration and swelling of epidermal and underlying tissues could favor outgassing and outflow of oleoresin from storage organs either by lowering their resistance and/or by increasing the pressure in storage organs. Moisture and plant water status has been shown to influence the oleoresin exudation pressure in pine stems (Rissanen et al., 2016 and references therein) and the hydration of leaf cuticles is known to reduce their mechanic resistance (Khanal and Knoche 2017). Concerning forest floors, other additional emission enhancing effects of moisture may come into play such as the filling of the air spaces by water and changes in the metabolic activities of microorganisms in soil and litter (Bigg 2004, Bourtsoukidis et al. 2018). Thus, we conclude that a large portion of the observed strong day-to-day variations in pinene emissions was due to high moisture conditions leading to wetting of surfaces. This is an aspect that is not currently considered enough in VOC research, despite the numerous independent studies that describe its large effect on biogenic VOC emissions. Because in many forest ecosystems surfaces are regularly wetted, more research should be devoted to understand and predict the effects of wetting on biogenic VOC emissions

2.5. Conclusions

The results of our pilot study clearly demonstrate that stereo selective compartment specific pinene sources can exist in coniferous forest. Notably branch emissions expressed a different chiral composition than stem and ground emissions. Compared to emissions, the chiral signature of the ambient air inside the canopy showed intermediate values with minor within-day and between-day variations likely reflecting variable turbulent mixing and the enantiomeric specific emissions produced in the specific compartments. Both, ambient air and chamber measurements indicate that at the study site litter/ground and stem emissions significantly contributed to the overall VOC flux especially under high moisture conditions. Thus, our findings provide new encouraging perspectives to explain previously observed temporal changes in the chiral signature of pinenes over conifer forests, and to further explore chirality as a possible marker to recognize shifts in the contributions of different hitherto neglected VOC sources/sinks present within forest canopies such as stem and ground emissions. If enantiomeric signatures help characterizing net VOC exchanges at the biosphere atmosphere interface we can use them to determine their influence on local air chemical processes, as for instance SOA formation under variable weather conditions (Kammer et al., 2018). Future studies should investigate the chiral signatures of compartment emissions on a larger number of individuals, ideally continuously and simultaneously accompanied by ambient air measurements at different canopy heights. Such a thorough protocol is still difficult to realize, since the measurement of enantiomers requires time-consuming high performance chromatography and VOC accumulation during sampling to detect trace levels. Perhaps in future, improvements in the performance of fast GC combined with ultra sensitive PTR techniques may overcome these constraints.

Supplement. Supplementary data to this article can be found online at https://doi.org/10.1016/j.scitotenv.2018.11.146.

Data ownership. All data contained within this paper is under the ownership of Centre national de la recherche scientifique (CNRS).

Chapter 3: Offline GC-TOF-MS and Online GC-MS characterisation during the B2WALD campaign

Abstract. A new system was characterised to assess the array of monoterpenes in the enclosed atmosphere of the Biosphere 2 tropical rainforest, branch cuvettes, and soil chambers. For the accurate study of the enantiomeric excess of volatile organic compounds (VOCs), effort was taken to effectively optimise the detector system and establish an oven temperature program, which can clearly resolve both chiral peaks. Furthermore, throughout this work, thorough efforts were undertaken to produce accurate calibrations of monoterpenes and to optimise the performance of the analytical system for the reliable study of their atmospheric abundance and fluxes. In addition to monoterpenes, VOCs ranging in volatility from C4 to C15 can be measured. The system consists of three sections: pre-concentration and thermal desorption, gas chromatographic separation, and analyte ion detection. Helium 6.0 was used as the carrier gas in each stage of the system. In addition to this, three different sampling systems were used for the automatic collection of air onto the sorbent tubes.

3.1. Offline sampling, pre-concentration and thermal desorption

3.1.1. Offline sampling with absorbent cartridges

Sorbent tubes, also referred to as sorbent cartridges or sampling cartridges, are a well-established method for the sampling of VOCs, including the study of monoterpenes (Song et al. 2011, Song et al. 2014, Woolfenden 1997). Sorbent tubes, in principle, have the same functionality as cold sorbent traps in the pre-concentration stage, in that they are trapping a range of compounds on a multi-bed absorbent for later desorption. The main difference, being that sampling tubes are not cooled to low temperatures whilst trapping occurs. This results in the equilibrium between the analyte compounds and the sorbent being dependent on ambient temperature. Different combinations of sorbent materials are available for packing into the tube. The types of sorbents are categorized into porous polymers (e.g. Tenax® TA), graphitized carbon blacks, and carbon molecular sieves.

3.1.1.1. Development of new sorbent tubes

Before use in the B2WALD campaign, an investigation was performed into how suitable the existing cartridges were for the B2WALD campaign. Initially, two different sets of inert lined fused silica lined stainless steel tubes (Silcosteel® (Restek, USA)) were used which contained different sequential absorbent beds. Both sets of sorbent tubes had been made and packed in house at the Max Planck Institute for Chemistry (MPIC) for previous uses. All sorbent tubes used were 89 mm long with a diameter of 6.4 mm and an internal diameter of 5.3 mm. The sorbent bed in the first set of cartridges consisted of 180 mg Tenax® TA 60/80 (35 $m^2 g^{-1}$) followed by 130 mg of Carbograph™ 1 (90 $m^2 g^{-1}$). The sorbent bed in the second set of cartridges consisted of 130 mg of Carbograph 1 followed by 130 mg of Carbograph™ 5 (560 m^2/g). The size of the Carbograph™ particles was in the range of 20-40 mesh. The Carbograph™ 1 was supplied by L.A.R.A s.r.l. (Rome, Italy) and Alltech (Deerfield, IL, USA) supplied the Tenax® TA (Kesselmeier et al. 2002).

Over time, Tenax® TA can undergo degradation into various products due to numerous thermal cycles and also due to exposure to various oxidants such as the OH radical and ozone (Klenø et al. 2002). As different sorbent tubes are used at different times and different amounts, the amount of degradation is non-uniform across the sorbent tube set. Therefore, the absorption capacity of each tube can vary with respect to other tubes in the same set. This can potentially result in increasing deviations between sorbent tubes when they are filled with the same concentration of analyte. Therefore, new sorbent tubes were produced for comparison with the old sorbent tubes for quality control.

The new sorbent tubes were manufactured in house at the MPIC to compare the absorption of monoterpenes between the old sorbent tubes and the new sorbent tubes. It should be noted that the two sets of sorbent tubes contained different sorbent material, a different ratio of their two sorbents and a small but different amount of total sorbent material. In addition, the new sorbent tubes were made of stainless steel whereas the old sorbent tubes were made from inert lined fused silica lined stainless steel tubes (Silcosteel® (Restek, USA)). The new sorbent tubes contained 150 mg of Tenax® TA followed by 150 mg of Carbograph™ 5 TD (560 m^2/g).The size of the Carbograph™ particles was in the range of 20-40 mesh. The Carbograph™ 5 was supplied by L.A.R.A s.r.l. (Rome, Italy) and and Buchem BV (Apeldoorn, The Netherlands) supplied the Tenax®.

To test the strength of absorption of monoterpenes onto the new and old sorbent tubes, 3 old Carbograph™ 1 and Tenax TA sorbent tubes and 3 new Carbograph™ 5 TD and Tenax TA sorbent tubes were filled with 2 litres of the same concentration of the 162 component Apel-Riemer-2017 gas calibration standard diluted with synthetic air (**Fig. 1**).

The deviation between the old cartridges was greater than between the new cartridges, likely due to the cartridges being used different amounts over their lifetimes, which would cause different rates of thermal degradation of the sorbents. For the old Tenax® TA and Carbograph™ 1 sorbent tubes, both enantiomers of camphene appear in significant quantities, despite camphene not being present in the calibration standard. Whereas, for the new Tenax® TA and Carbograph™ 5 sorbent tubes, both enantiomers of camphene are negligible. Furthermore, the new Tenax® TA and Carbograph™ 5 sorbent tubes show a greater response for (-)-β-pinene than the old Tenax® TA and Carbograph™ 1 sorbent tubes, with (+)-β-pinene remaining at a relatively constant and low amount over both sets off sorbent tubes. Therefore, it is hypothesized that there is isomerization occurring within the sorbent tubes when they are heated to the desorption temperature. If there are metal particles from manufacturing, trapped with the sorbent in the sorbent tubes, the surface of the particles could be acting as a catalyst for the isomerization to occur. Notably, the enatiomeric excess of (-)-limonene was greater for the old sorbent tubes then for the the new sorbent tubes (**Fig. 3**). To eliminate the effect of the type of steel on the enantiomeric ratio of limonene, 5 silicosteel tubes were manufactured with exactly the same sorbent bed as the stainless steel tubes. **Fig. 1** shows the comparison of the area under the curve of different monoterpenes between the inert coated sorbent tubes and the sorbent tubes without inert coating. No significant difference was seen between inert coated and non-inert-coated sorbent tubes.

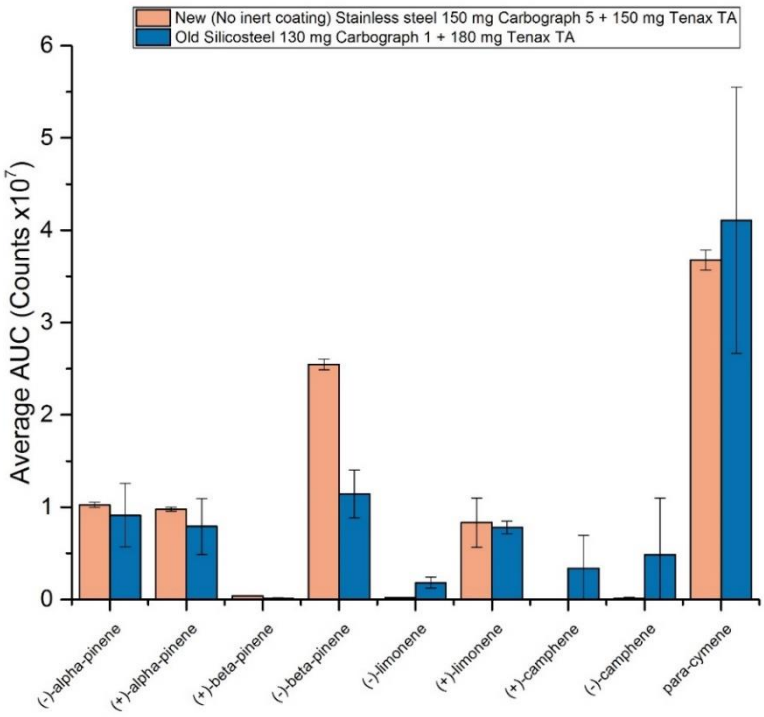

Figure 1. Comparison of the area under the curve (AUC) of an array of terpenes sampled on to two different cartridge sets. The error bars represent 1σ.

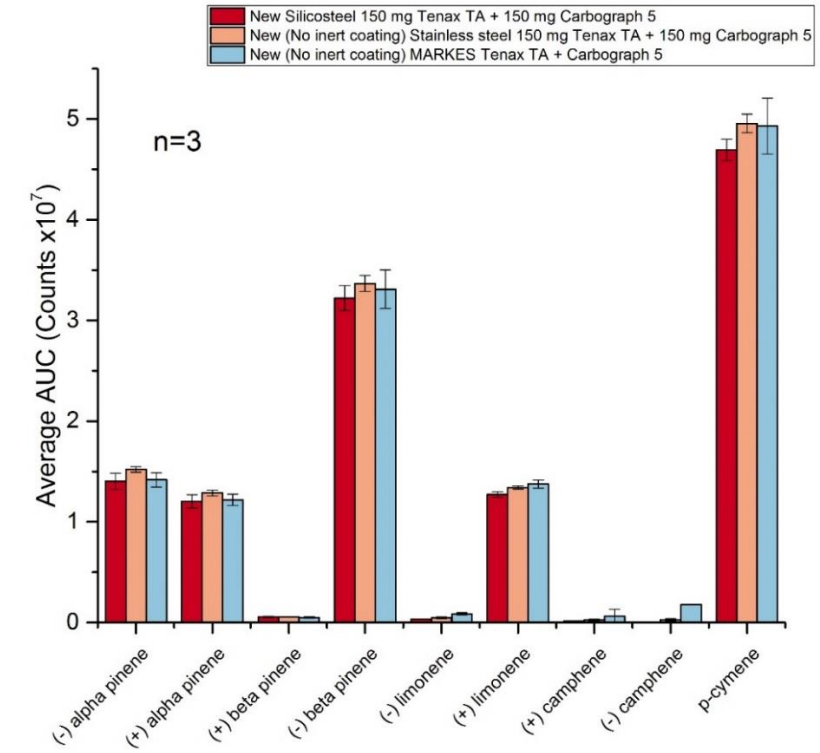

Figure 2. Comparison of the area under the curve (AUC) of an array of terpenes sampled onto 3 different sets of newly made cartridges. The error bars represent 1σ.

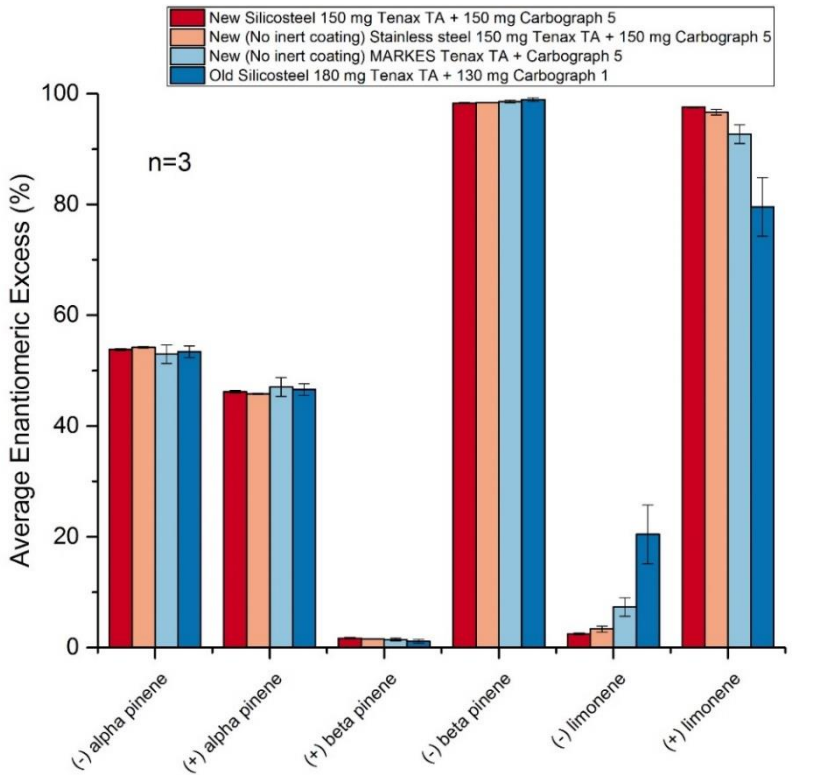

Figure 3. Comparison of the enantiomeric excesses of 3 common monoterpenes between all sets of tested cartridges. The error bars represent 1σ.

3.1.1.2. Sorbent tube contamination

To remove contamination and to condition the cartridges between uses, they were placed in a thermal conditioner (TC, TC-20, MARKES International Ltd. U.K.) for 1 hour at a temperature of 300 °C. The tubes were conditioned with Nitrogen 6.0 regulated at a pressure of 30 psi, which is approximately equivalent to a flow rate of 90 ml min^{-1}. The tubes were placed in the TC so that the flow was in the opposite direction to the normal sampling flow. This is especially important for the tubes containing both Tenax® TA and Carbograph™ as Carbograph™ has a greater sorbent strength than Tenax® TA and so the conditioning flow is opposite to the sampling flow so that the species absorbed by Tenax® TA are not pushed onto the stronger absorbing Carbograph™ (Woolfenden 2010). A drawback of using Tenax® TA as a sorbent is that it can thermally degrade into benzene and toluene, resulting in benzene and toluene peak artefacts commonly appearing in chromatograms corresponding to those sorbent tubes (Woolfenden 1997). Other common contaminants include phthalates and silicon containing compounds (Fankhauser-Noti and Grob 2007, Varaprath, Stutts, and Kozerski 2006). The silicon containing compounds likely arise from the silanised glass wool that is use in the cartridges to contain the sorbent bed but also the stationary phases of some analytical columns breakdown to produce siloxanes (Varaprath, Stutts, and Kozerski 2006). It should be noted that if further in-house cartridges are assembled, it would be better to use quartz wool to avoid the siloxane contamination.

3.1.2. Preconcentration of analytes

When performing thermal desorption, focusing of the analyte compounds onto adsorptive material, prior to desorption, is necessary for achieving a desirable narrow injection bandwidth. Focusing the analyte on a cold trap, ensures that all of the compounds can be introduced as close to the same instant as possible to the chromatographic column, resulting in sharper chromatographic peaks and a decrease in the detection limit of the analyte (Werkhoff and Bretschneider 1987). Adsorptive material, for example, glass wool, Carbograph™ and Tenax TA®, packed into a quartz tube (known as a cold trap or sorbent trap) is a well practiced method for pre-concentration, with different sorbents possessing different properties for trapping different compounds (Woolfenden 2010). When a sample is passed over the adsorptive material, a fraction of the analyte will be retained on the surface of the material, due to physical interactions, whilst allowing the most common and volatile constituents of air (e.g. O_2, N_2 and Ar) to pass through unretained.

The retained fraction of analyte can be increased by simultaneously cooling the cold trap whilst trapping the analyte. The thermal desorber used for this work relies on thermoelectricity for the cooling and heating of the cold trap. The Peltier effect, caused when a voltage is applied over a junction between two different conductors, removes the need for cryogenic trapping using liquid nitrogen as relied upon by other systems. This gives the advantage of being able to run a large set of samples automatically without the need to interrupt and replenish the level of liquid nitrogen.

3.1.2.1. Preconcentration and thermal desorption with MARKES instrument

Pre-concentration and thermal desorption was achieved using a two stage automated thermal desorber (TD100-xr, MARKES International Ltd. U.K.). Nitrogen is connected to the “Pneumatic gas” inlet at the rear of the unit. Within this system, nitrogen has the function of switching the pneumatic valves and creating a small positive pressure in the focusing trap box to prevent the formation of ice around the Peltier cell due to the entry of moisture from the laboratory. If ice was allowed to build up

around the Peltier cell, then the rapid heating of the focusing trap could be disturbed and the trap could overheat.

A constant desorption program was used throughout this work with the exception of the desorption split ratio. The split ratio was chosen when considering the concentrations of the sample expected to have been collected on the cartridge. The sample is first dry purged without heating with a flow of 50 ml min^{-1} in the opposite direction to the direction of sampling to remove excess water. The sample on the sorbent tube is thermally desorbed at a temperature of 250 °C, with flow of 50 ml min^{-1} for 10 minutes. All of the sample is then transferred and preconcentrated onto a quartz cold focusing trap (Material emissions, MARKES International Ltd., U.K.) at 30 °C.

The quartz cold trap contains a 2 mm diameter x 60 mm long bed of sorbent supported by quartz wool. The system thermoelectrically cools the absorbent trap using a 2-stage Peltier cell to create a heat flux away from the focusing trap. Under ambient temperatures, the Peltier cell can uniformly lower the temperature of the 60 mm sorbent bed to a minimum of -30 °C and a maximum of +50 °C. Following tube desorption, the cold focusing trap is purged for 1 minute with a flow of 50 ml min^{-1} directed towards the trap vent. The cold trap is then rapidly heated at 100 °C s^{-1} to 300 °C. The sample is then swept from the focusing trap with a total flow of 3.5 ml min^{-1}, including a split flow of 2 ml min^{-1} and a septum purge flow of 1 ml min^{-1}, for 5 minutes and injected into the separating column. Since installation, the septum purge had been portioning flow downstream of the cold trap and, therefore, sample too. The benefit of this configuration is that when different splits are used, the retention times should stay constant for the same GC oven temperature program. However, since one split is always used for a sample set, the configuration was changed so that the septum purge would take place upstream of the cold trap so that no sample would be lost to the septum purge. This results in the total desorption flow only being a sum of the split flow and column flow.

3.2. Online and offline gas chromatographic separation

Online and offline gas chromatographic separation was achieved using an online Agilent 6890A GC and an offline Agilent 7890B GC respectively, with similar temperature programs. The equilibration time of the oven temperature was set to 0 minutes and a constant flow mode was used for all programs. To achieve chiral and volatile separation of the analyte compounds, a 30 m MEGA-DEX DMT-Beta column with 0.25 mm internal diameter and a 0.25 µm film thickness was used. The column has a chiral stationary phase of permethylated beta-cyclodextrin. The initial pressure, average velocity and hold up time were 32.06 psi, 32.83 cm s^{-1} and 1.37 min respectively. The column flow was 1 ml min^{-1}. The temperature programs used are summarised in **Table 1 and 2**.

Table 1. GC oven program used by the offline Agilent 7890B GC.

Rate (°C min^{-1})	Temperature (°C)	Hold time (min)
	40	5
4	220	5

Total runtime: 55.0 minutes

Table 2. GC oven program used by the online Agilent 6890A GC.

Rate (°C min^{-1})	Temperature (°C)	Hold time (min)
	40	5
4	150	
30	200	

Total runtime: 55.0 minutes

3.3. Detection, identification and calibration

3.3.1. Time of flight mass spectrometry

Offline detection of the separated analyte compounds was achieved using a Time-of-Flight-Mass Spectrometer (TOF-MS, BenchTOF, MARKES International Ltd., U.K.) (**Fig. 4**). The BenchTOF has a dual ionization feature allowing for the simultaneous acquisition of two chromatograms at two different ionization energies. For this thesis work, 70 eV and 14 eV were always used.

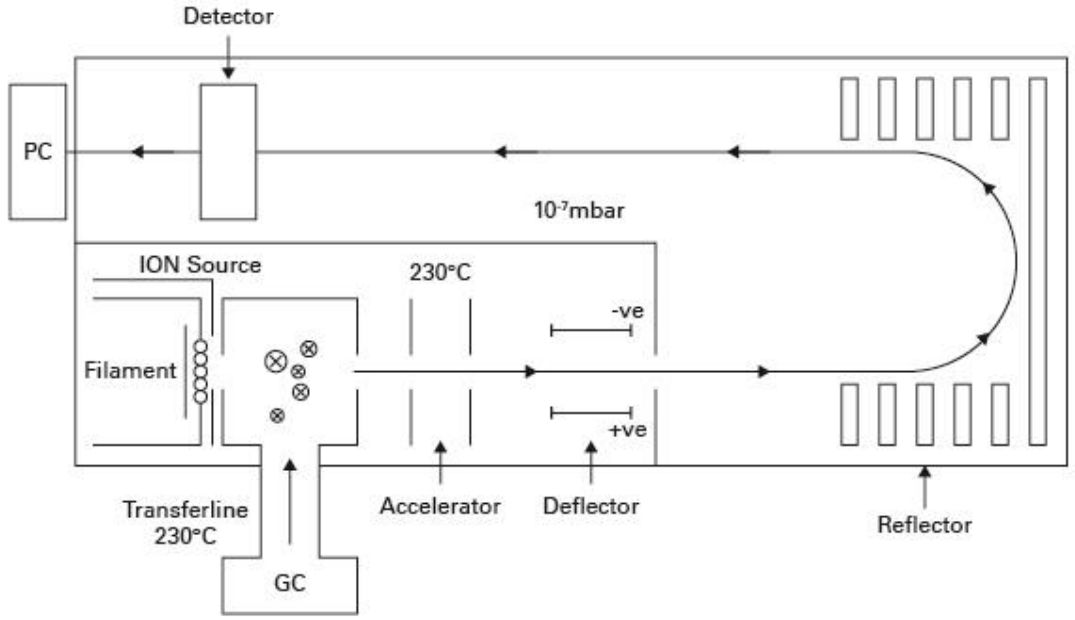

Figure 4. Schematic of the time of flight mass spectrometer (ToF-MS).

The mass range that is recorded by the TOF-MS was set from 40 to 600 m/z and the data rate was set to 4 data points per second which was later changed to 2.5 data points per second. The data rate was changed as the TOF scans through the entire mass range at a frequency of 10 KHz, thus when the data rate is set to 4 data points per second, the result is 2500 scans combined together each second. Whereas when the data rate is set to 2.5 data points per second, this results in 4000 scans combined together each second. Achieving a greater amount of combined scans will result in a greater sensitivity, but also less data points on the peak. The filament voltage was set between 1.7 V and 1.8 V.

3.3.2. Identification of compounds

Extensive method development was undertaken prior to the B2 WALD measurement campaign to achieve the best possible separation of peaks in the chromatograms obtained with the GC-MS. When operating the GC-MS with a chiral column installed, finding the optimum conditions for resolving individual peaks becomes more difficult since the number of monoterpene peaks almost doubles compared to chromatograms that do not resolve for enantiomers. Initially peak identification was

performed by running the GC-MS in scan mode and comparing with the National Institute of Standards and Technology (NIST) mass spectra library. The comparison of the obtained mass spectra with the NIST library is performed with the MARKES Chromspace or TOF-DS softwares. Later, peak identification was confirmed using the offline GC-TOF-MS. Whilst operating the offline GC-TOF-MS in tandem ionisation mode, two separate chromatograms are acquired simultaneously for the 14 eV and 70 eV ionisation energies. The data rate for acquisition is set to 4 Hz and the recorded mass range was set from 43 to 600. To identify the compounds in the sample, the Apel-Reimer 2019 BVOC mixture calibration gas was sampled onto a cartridge and desorbed into the GC-ToF-MS system. The compounds were identified by comparing the acquired mass spectra with the NIST library. Since enantiomers produce identical mass spectra, the headspace of enantiomerically pure liquid standards was passively sampled onto sorbent cartridge to identify the elution order of enantiomers. Since the online GC operated with a quadrupole in selected ion mode, only several ions were measured and therefore a comparison with the NIST library could not be made. To identify the compounds measured by the online GC, a calibration standard gas with the same mixture but less concentrated than the Apel-Reimer 2019 BVOC mixture was used. A less concentrated mixture was used so that it could be injected directly onto the cold trap instead of first being diluted. This was done to save time when calibrating the GC as sampling diluted gas onto the cold trap takes 10 minutes; whereas injection of the mixture straight onto the cold trap could be done in > 1 minute and the concentration scaled up to be equal to a diluted mixture which had been sampled for 10 minutes. Since both the online and offline GCs used the same oven programme and type of chromatographic column, the resulting chromatograms could be compared to identify the peaks (**Fig. 5 & 6**).

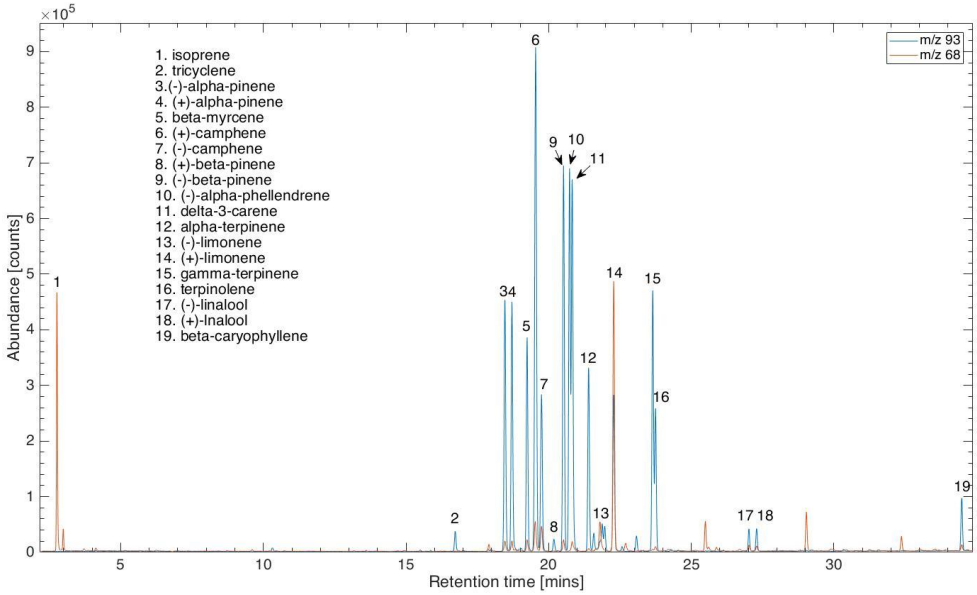

Figure 5. Chromatogram obtained by injecting a sample from the Apel-Reimer 2019 BVOC mixture into the GC-ToF-MS with identified terpenoid peaks.

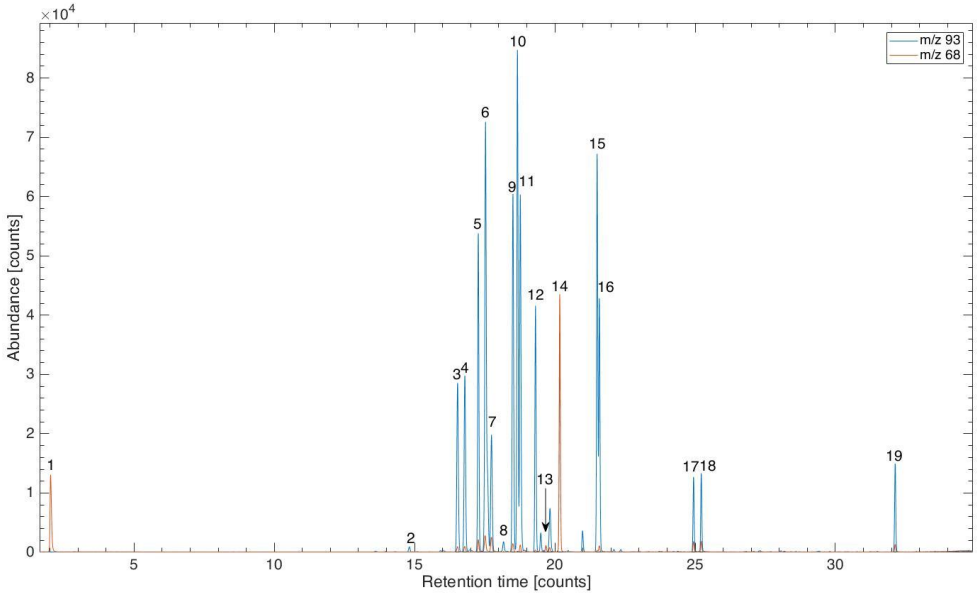

Figure 6. Chromatogram obtained by injecting a sample from the Apel-Reimer Biosphere 2 2019 BVOC mixture into the GC-MS with identified terpenoid peaks.

3.3.3. Online GC calibration

Before the start of the B2 WALD campaign, the response of the GC-MS system was characterised to ensure the calibrations were accurate and samples would fit onto the linear response. This was achieved by performing 6 step-wise increases of the standard gas injection time onto the cold trap, thereby performing 6 calibration steps and then repeating each step 3 times (**Fig. 7B**). During the campaign, the Online GC-MS was routinely retuned approximately every week followed by a brief linearity check, which was performed by performing the 1st, 3rd and 5th calibration steps, repeating twice (**Fig. 7B**). To correct for the systematic decrease in sensitivity following the retuning, in between every 10 atmospheric measurements, 2-3 calibrations were performed of the second calibration step (**Fig. 7A**). A line was then plotted through each set of calibration points; the time of each atmospheric sample measurement was then put into the equation of the calibration line to solve for the MS response at the corresponding point in time (**Fig. 7C**). The sensitivity of the MS decreased unexpectedly after the 4th retune (day of year (doy) 275) and unexpectedly increased again (doy 315), due to an error in the optimisation of the quadrupole mass spectrometer. Since the sensitivity was fully characterised throughout the entire measurement period and the linearity was routinely checked, the calibrated measurement data was deemed to be unaffected by the sensitivity fluctuation.

To calculate the limit of detection (LOD), the signal height and the corresponding average noise level from the same chromatogram for each calibration level was taken. To obtain the average noise level, suitable retention time regions were chosen, over a range of time with no peaks, and the sum of the noise height was calculated and divided by the number of data points within the chosen region. The LOD was then calculated at each calibration level for each species of interest using equation (1). The average LOD for each compound was then calculated from the LODs at each calibration level using the equation:

$$LOD = 3 \times \frac{\overline{Noise} \times MR}{Peak\ signal\ height} \quad (1)$$

The calculated LOD's were in the range of 0.2 - 4.3 pptv for the monoterpenes as listed in **Table 3 and 4**.

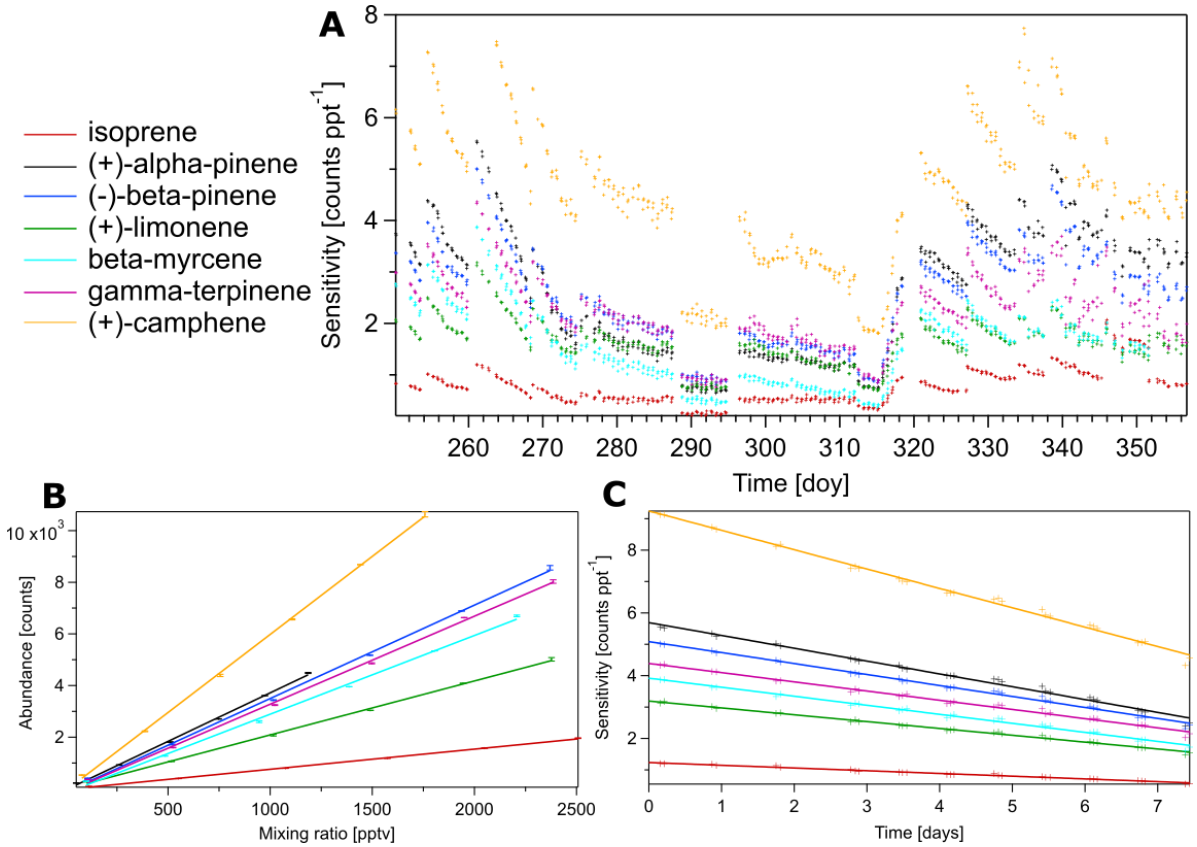

Figure 7. **A**. Comparison of how the online GC-MS sensitivity varied over the B2WALD measurement campaign for some selected monoterpenes and isoprene. For the sake of clarity, only some monoterpenes are shown. **B.** Calibration curves showing that the response was linear for the monoterpenes until at least 2400 pptv. **C.** The systematic sensitivity decrease between mass spectrometer retunes was characterized by performing 3 calibration points every 10 samples. A linear fit was applied to the sensitivity drop to correct the sampled data. The error bars represent the standard deviation between measurements.

3.3.4. Offline GC-ToF-MS calibration

The BenchTOF system was routinely auto-optimised and recalibrated with Apel-Riemer 2019 BVOC gas calibration standard before every set of samples, whenever there was a change to any part of the entire TD-GC-TOF system and, for a large sample set, after 2 weeks of continuous use. To monitor the detector response when desorbing a set of samples, sorbent tubes containing the same concentration of compounds from the gas standard bottle were placed in the sequence, normally after every 5 samples. To calibrate the samples, the average response was used from the two calibration cartridges either side of the sample in the sequence.

The auto-optimisation adjusts the voltages within the BenchTOF and normalises the baseline and detector response for optimum performance, therefore a linear calibration is performed after each

auto-optimisation (**Fig. 8**). When operating in tandem ionisation mode, it is necessary to optimise at both of the ionisation energies to get the best signal. To conduct a calibration, sorbent tubes were filled with the calibration standard that had first been diluted with synthetic air to obtain mixing ratios (MRs) more relevant to those seen in experimental samples. The flow from the Apel-Reimer-2019 gas standard bottle was controlled using a mass flow controller (MFC) using flows in the range of 10 - 30 ml min^{-1} and the flow from the synthetic air bottle was controlled using another MFC in the range of 1000 – 5000 ml min^{-1}. A portable pump used for sampling cartridges was set to 200 ml min^{-1} was used to regulate the diluted flow of calibration gas through the cartridge. Using the calibration measurements and extracting the chromatogram of the most abundant ionisation fragment for the corresponding species, the response factors (RFs), limits of detection (LODs) and the linearities (R^2) could be determined. For each species, the RFs were calculated by integrating the corresponding peak curve to obtain the area under curve (AUC), plotting against their corresponding mixing ratios and taking the gradient.

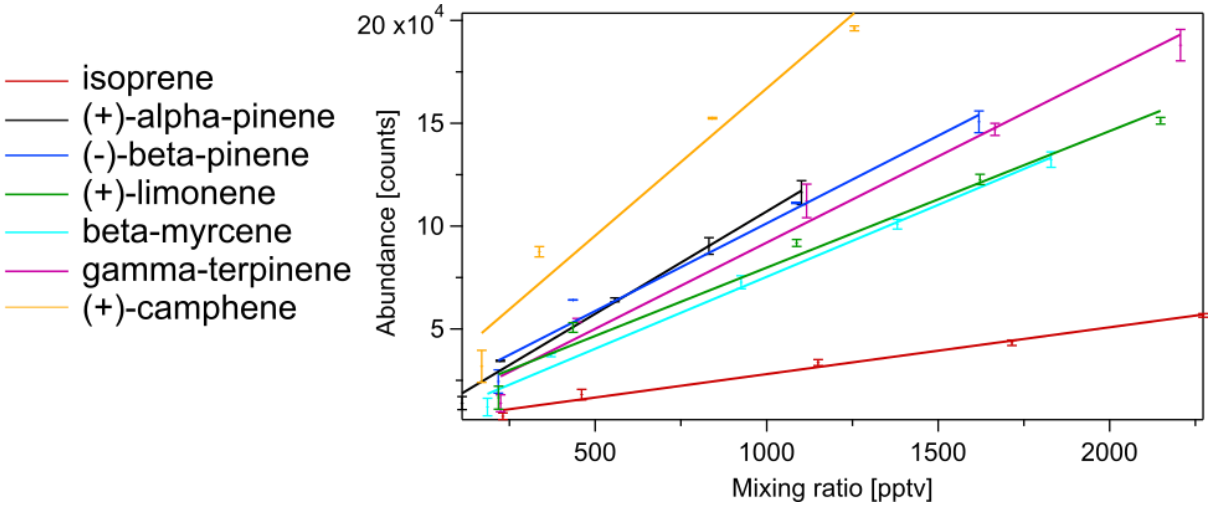

Figure 8. Calibration curves for some selected monoterpenes and isoprene obtained using the GC-ToF-MS. The error bars represent 1σ.

Table 3. Calculated RF's, R^2 values and LOD's for online GC-MS for the terpenes in the Apel-Riemer-Biosphere2-2019 gas standard during the B2WALD campaign.

Compound	m/z fragment	LOD (pptv)	RF ± uncertainty (counts $pptv^{-1}$)	R^2
isoprene	68	1	0.78 ± 0.04	0.999
(-) – α – pinene	93	0.6	3.77 ± 0.20	0.999
(+) – α – pinene	93	0.6	3.74 ± 0.19	0.998
(+) – camphene	93	0.3	6.03 ± 0.31	0.999
(-) – camphene	93	0.3	6.02 ± 0.31	0.999
β-myrcene	93	0.4	3.03 ± 0.16	0.997
(+) – β – pinene	93	0.2	3.60 ± 0.19	0.999
(-) – β – pinene	93	0.2	3.60 ± 0.19	0.999
Δ-3-carene	93	3.5	3.69 ± 0.19	0.998
α – terpinene	93	0.5	2.42 ± 0.13	0.998
(-) – limonene	68	4.3	2.04 ± 0.11	0.997
(+) – limonene	68	0.4	2.08 ± 0.11	0.999
γ – terpinene	93	0.3	3.38 ± 0.18	0.999
terpinolene	93	0.5	2.51 ± 0.13	0.997
(-) – linalool	93	27.3	1.49 ± 0.08	0.992
(+) – linalool	93	27	1.52 ± 0.08	0.993
β – caryophyllene	93	24.5	1.66 ± 0.09	0.988

Table 4. Calculated RF's, R^2 values and LOD's for offline GC-ToF-MS for the terpenes in the Apel-Riemer-2019 gas standard.

Compound	m/z fragment	LOD (pptv)	RF ± uncertainty (counts $pptv^{-1}$)	R^2
isoprene	68	60.2	29 ± 3	0.987
(-) – α – pinene	93	3.4	118 ± 13	0.994
(+) – α – pinene	93	3.3	114 ± 13	0.993
(+) – camphene	93	0.7	185 ± 20	0.953
(-) – camphene	93	0.4	197 ± 22	0.991
β-myrcene	93	5.5	73 ± 8	0.991
(+) – β – pinene	93	0.7	119 ± 13	0.995
(-) – β – pinene	93	1	107 ± 12	0.965
Δ-3-carene	93	4.7	113 ± 12	0.988
α – terpinene	93	3.7	57 ± 6	0.986
(+) – limonene	68	2.8	76 ± 8	0.978
γ – terpinene	93	1.1	88 ± 10	0.981
terpinolene	93	4.3	68 ± 7	0.99
(-) – linalool	93	6.0	100 ± 11	0.976
(+) – linalool	93	5.7	104 ± 11	0.975
β – caryophyllene	93	12.7	12 ± 1	0.95

Chapter 4: Chiral monoterpenes reveal forest emission mechanisms and drought responses

This chapter has already been published as a preprint in Research Square and is undergoing peer review. I am the first author of the publication and my personal contribution to this work included having the idea to measure isoprene and chiral compounds in the air with GC-MS during the campaign, to measure chiral compounds in the air during $^{13}CO_2$ labelling, and to sample chiral compounds from soil chambers. I also measured atmospheric isoprene and chiral compounds with GC-MS throughout the whole campaign, analysed the GC-MS data, prepared the figures, and wrote the manuscript.

J. Byron, J. Kreuzwieser, G. Purser, et al.: Chiral monoterpenes reveal forest emission mechanisms and drought responses, 13 August 2021, PREPRINT (Version 1) available at Research Square [https://doi.org/10.21203/rs.3.rs-770148/v1]

Abstract. Monoterpenes exist in mirror image forms called enantiomers, but their individual formation pathways in plants and ecological functions are poorly understood, as enantiomers are usually measured and modelled together. Here we present enantiomerically separated atmospheric monoterpene and isoprene data from an enclosed tropical rainforest ecosystem without photochemistry during a four-month controlled drought and rewetting experiment. Surprisingly, the enantiomers showed distinct diel emission peaks, which responded differently to progressive drying. Isotopic labelling established that vegetation emitted (-)-α-pinene mainly *de novo* while (+)-α-pinene was emitted from storage pools. As drought stress increased, (-)-α-pinene emissions shifted to storage pools, which are released later in the day, favouring cloud formation. The α-pinene enantiomers each correlated better with other monoterpenes than with each other, indicating different enzymatic controls. These results show that enantiomeric distribution is key to understanding the processes driving monoterpene emission from ecosystems and to predicting atmospheric feedbacks in response to climate change.

4.1. Introduction

Monoterpenes ($C_{10}H_{16}$) are emitted in large quantities by vegetation to the atmosphere (>100 Tg C yr^{-1}), where they react with hydroxyl radicals and ozone to form new particles and hence influence clouds formation impacting the Earth's radiative budget and climate change (Jokinen et al. 2015, Engelhart et al. 2008, Laothawornkitkul et al. 2009). Little attention has been given to their different chiral forms ((+) and (-)), as both monoterpene enantiomers have identical physical properties and rates of reaction with OH and O_3 (Zannoni et al. 2020); therefore, most atmospheric field and modelling studies do not differentiate them. However, this implicitly assumes that the sources and sinks of both enantiomers are identical, even though the individual enantiomer production pathways and drivers are uncertain. Recent forest measurements showed unequal (non-racemic) concentrations of enantiomers that sometimes do not even correlate with each other (Williams et al. 2007, Song et al. 2014), indicating distinct source mechanisms. Although some reports suggest that the biosynthesis of enantiomers is homogenous throughout an individual plant(Song et al. 2014), leaves, bark and soil litter within a homogenous forest have distinct chiral signatures (Staudt et al. 2019), strongly suggesting that the emission and removal processes of these chiral species (and hence monoterpenes generally) are not adequately understood.

Isoprene emission is better understood than monoterpene emission, with generally precise model-prediction and measurement agreement (Sharkey and Yeh 2001, Karl et al. 2007). Isoprene synthesis occurs by the 2-C-methyl-D-erythitol 4-phosphate (MEP) pathway, where photosynthetically assimilated CO_2 is converted to the isoprene precursor, isopentenyl diphosphate, and directly emitted from the leaf (*de novo* emission)(Sharkey and Yeh 2001). Monoterpene synthesis also occurs by the MEP pathway, but some monoterpenes are synthesized by the mevalonate pathway. Both pathways result in the production of isopentenyl diphosphate, which combines with its isomer, dimethylallyl diphosphate, to form the common monoterpene precursor geranyl diphosphate (GPP) (Pazouki and Niinemets 2016, Croteau 1987). Enzymes known as terpene synthases transform GPP into an array of monoterpenes such that chiral monoterpenes produced by a particular enzyme are typically in one chiral form, (-) or (+)(Phillips, Savage, and Croteau 1999, Degenhardt, Köllner, and Gershenzon 2009b). Monoterpenes can be emitted by *de novo* emission, or released from storage pools, thus, decoupled from time of biosynthesis. Broad leaf plant species typical of the tropics usually store monoterpenes non-specifically throughout the leaves, mainly in the lipid phase but also a small amount in the aqueous phase within the leaf (Niinemets, Loreto, and Reichstein 2004, Niinemets and Reichstein 2002). The processes regulating monoterpene production and potential storage likely determine the plant's overall chiral emission signature, and it is unclear how these will change in response to extreme climate events such as drought. Droughts are expected to become more frequent throughout the 21st century(IPCC 2014), causing disruptions to the functioning of ecosystems(Bonan 2008) and emissions of volatile organic compound from forests(Loreto and Schnitzler 2010). Reported monoterpene emission responses to drought are highly variable and dependent on the individual plant, making empirically based achiral emission inventories intractable (Lavoir et al. 2009, Ghirardo et al. 2010, Lüpke et al. 2017). However, since chiral compounds link directly to the underlying enzymatically driven processes they could form the basis of an improved emission scheme.

We separated and measured the enantiomers for α-pinene, camphene and limonene as well as measuring (-)-β-pinene, γ-terpinene, and isoprene at hourly intervals over almost four months within the enclosed Biosphere 2 Tropical Rain Forest (B2-TRF) by on-line gas chromatography-mass spectrometry (GC-MS) (**Fig. 1**). Trans-β-ocimene and β-myrcene were also detected but could not be resolved using the method for the online GC-MS. The B2-TRF was continually flushed with outside air and all incident light wavelengths below 385 nm were filtered by the internal mylar sheet within the surrounding glass panels (Finn 1996). After three weeks of ambient measurements to establish the normal pre-drought condition (day of year (doy) 252–280), a 9.5-week drought was imposed to cause

physiological change and drive differential responses in the biochemical processes (doy 281-337). The subsequent drought stage developed two phases (mild and severe drought), with respect to two relative humidity minima, soil moisture decline, and vegetation response. At the end of the drought, water was added to the deep soil for 12 days (doy 337-346), followed by "rain" delivered from overhead sprinklers (doy 347-356). Isotopically labelled $^{13}CO_2$ was twice added to the enclosed atmosphere during pre-drought and severe drought, enabling differentiation between *de novo* and storage pool emissions using an off-line GC-isotope ratio MS (GC-IRMS). ^{13}C labelling combined with long-term atmospheric flux monitoring allowed us to precisely determine how drought impacts fluxes and sources of distinct monoterpene enantiomers.

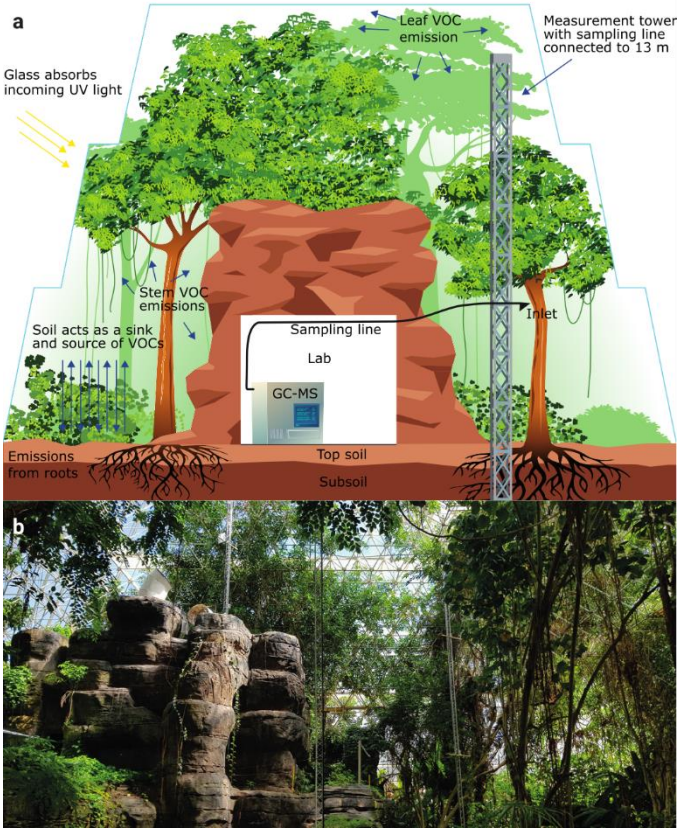

Figure 6. a. Schematic of the Biosphere 2 Tropical Rainforest biome. **b**. A photograph taken from within the biome (Photo J. Byron).

4.2. Results

4.2.1. Distinct trends of enantiomers

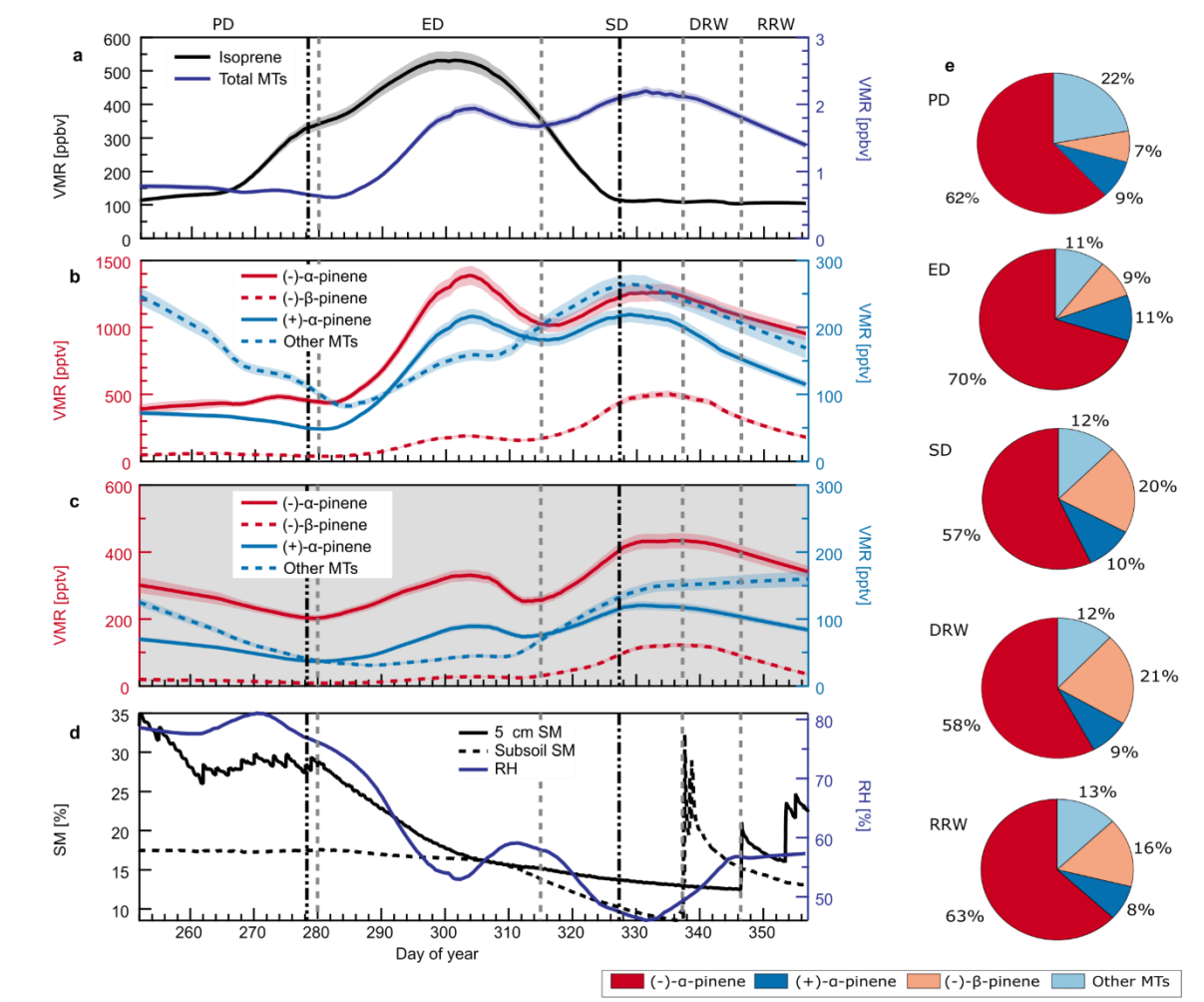

Figure 2. Long-term total monoterpenes (MTs) and isoprene trends throughout the experiment show strongly differing trends for monoterpene enantiomers, especially during daylight hours. Monoterpene and isoprene data is divided into 5 stages, indicated by the grey dashed lines: pre-drought (PD), early drought (ED), severe drought (SD), deep-water rewet (DRW) and rain rewet (RRW). The timing of the $^{13}CO_2$ pulses is indicated by the black (···) lines. **a**. Daytime isoprene and total monoterpene volume mixing ratios (VMR). The shaded region around the line represents the absolute measurement uncertainty. **b**. Daytime (-) and (+) alpha-pinene and other monoterpenes. **c**. Night-time (-) and (+) alpha-pinene and other monoterpenes. **d**. soil moisture (SM) and relative humidity (RH). Note different scales for enantiomers. **e**. Pie charts showing the daytime composition of the enantiomeric monoterpenes during each stage. Note different scales for enantiomers. The shaded region around the line represents the absolute measurement uncertainty. Other monoterpenes includes (-)-camphene, (+)-camphene, (-)-limonene, (+)-limonene and γ-terpinene.

Total monoterpenes (consisting of (-)-α-pinene, (+)-α-pinene, (-)-β-pinene, (-)-limonene, (+)-limonene, (-)-camphene, (+)-camphene, and γ-terpinene) stayed relatively constant during pre-drought but peaked after 33 days (in Early Drought) and again, more strongly, after 66 days (in Severe Drought) (**Fig. 2a**). During deep-water rewet, when water was reintroduced to the lowest soil levels, the total monoterpene concentrations started to decrease. This decrease continued after rain (rain-rewet), but did not quite recover to pre-drought levels by the end of the measurement period. The same pattern of two concentration peaks (corresponding to mild and severe drought periods) was also observed when the enantiomeric monoterpenes were separated; however, the enantiomer peak sizes showed strongly contrasting behaviour. Daytime concentrations of (-)-α-pinene were higher in the mild drought, whereas for (-)-β-pinene the severe drought concentrations were 10 times that of the mild

(**Fig. 2b**). The (+)-α-pinene peak concentrations were approximately equal in both mild and severe stress conditions. For nighttime concentrations (-)-α-pinene, (+)-α-pinene, and (-)-β-pinene all showed higher concentrations during severe drought (**Fig. 2c**). After rewetting by rain, nighttime values of (-)-β-pinene, (-) and (+)-α-pinene all returned to pre-drought levels (**Fig. 2c**). Although daytime concentrations of the enantiomers also all decreased from their severe drought maxima they did not reach pre-drought levels. Another clear contrast in behaviour was that the enantiomers correlated well during nighttime, while during daytime they exhibited independent patterns (when *de novo* emissions were important) (**Ext. Data Fig. 1**). Strikingly, the current monoterpene emission model-based expectation that drought would elicit equivalent responses in (-) and (+)-α-pinene was not true.

Although (-)-α-pinene consistently dominated the total monoterpene emissions, (-)-β-pinene overtook (+)-α-pinene to become the second most abundant monoterpene during severe drought (**Fig. 2e**). Thus, the ratio of (+)-α-pinene to (-)-β-pinene could be used as a proxy of drought severity in this experiment. It should be noted that fluxes of monoterpenes from the soil did not affect these enantiomeric ratios as samples taken periodically throughout the experiment showed that the soil maintained a modest steady uptake of enantiomeric monoterpenes throughout (**Ext. Data Fig. 2**).

These responses in monoterpenes were in contrast to isoprene. During pre-drought, isoprene in the tree canopies increased by a factor of 3 over 26 days, reaching average concentrations of ~ 300 ppb (**Fig. 2a**), likely because the top soil moisture (5 cm SM) decreased from 35% to 26% and the strong soil uptake of isoprene weakened before the drought started (Pegoraro et al. 2005, Pegoraro et al. 2006). By the severe drought period the top soil moisture had decreased from ~28% to 15%, whilst average isoprene concentrations decreased and plateaued at ~100 ppb, equivalent to initial pre-drought values. This means that in the severe drought the monoterpene to isoprene ratio was significantly higher than under mild drought.

4.2.2. Distinct enantiomer emission sources

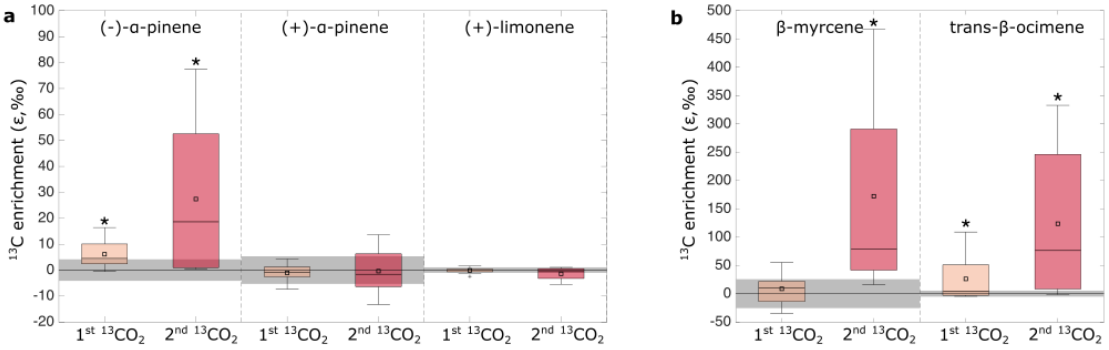

Figure 3. Carbon sources (*de novo* or storage) for monoterpene emissions were clearly separated by $\varepsilon^{13}C$ values of monoterpenes and their enantiomers after ^{13}C-enriched CO_2 was added during one morning in pre-drought (1^{st} $^{13}CO_2$) and severe drought (2^{nd} $^{13}CO_2$) phases. $^{13}CO_2$ gas was introduced into the atmosphere so that plants taking up CO_2 and directly producing immediate monoterpene emissions (*de novo*) would produce emissions enriched in ^{13}C. Therefore, emissions that did not become enriched in ^{13}C came from storage pools. **a**. Enrichment of chiral monoterpenes. **b**. Enrichment of non-chiral monoterpenes. Grey shading represents the standard deviation of the $\varepsilon^{13}C$ values of the compounds in ambient air when there is no $^{13}CO_2$ pulse. The black line through the grey boxes represents the mean. The box plots present median, and 25^{th} and 75^{th} percentiles. The small squares represent the mean and the whiskers represent the maximum and minimum acquired data points that are not considered outliers. Significantly ^{13}C-enriched values are indicated by the asterisk (*) above the box (i.e. results are significant if $P \leq 0.05$).

On two days during the experiment (pre-drought and severe drought), CO_2 labelled with the heavy ^{13}C isotope ($^{13}CO_2$) was introduced into the B2-TRF atmosphere to distinguish between *de novo* and storage type monoterpene emissions (**Fig. 3**). For (-)-α-pinene, the emissions became more enriched

in ^{13}C during both pulses. Atmospheric samples taken post-pulse show that, on average, the baseline $\varepsilon^{13}C$ values of (-)-α-pinene did not decline rapidly to pre-pulse values. This shows that (-)-α-pinene emissions are predominately *de novo* but that a small fraction also enters the storage pools from which it is emitted after the labelled CO_2 is flushed from the TRF. In contrast, no significant incorporation of ^{13}C was observed for (+)-α-pinene and (+)-limonene, indicating that these enantiomers were generated separately and emitted primarily from storage pools (Asensio et al. 2007). Therefore, the daytime increases of these monoterpenes during drought (**Fig. 2b**) comes from an increase in storage pool emissions.

The observed increases in $\varepsilon^{13}C$ values clearly indicate that fresh photosynthetic carbon was directly used to produce (-)-α-pinene, trans-β-ocimene and β-myrcene. The incorporation of ^{13}C by (-)-α-pinene, trans-β-ocimene and β-myrcene increased during the second pulse, likely because more freshly assimilated carbon is used for the production of these specific compounds. Trans-β-ocimene and β-myrcene are important emissions since they react quicker with harmful reactive oxygen species than other monoterpenes. This agrees with measurements from the Amazon rainforest, where emissions of ocimene and β-myrcene increased from heat stressed leaves (Jardine et al. 2017).

4.2.3. Distinct diel cycles of enantiomers

Two distinct types of diel cycle were observed during pre-drought. One, followed by (-)-α-pinene and (-)-β-pinene, was aligned to photosynthetically active radiation (PAR) and assimilation rate (A); while the second, followed by (+)-α-pinene and (+)-limonene, was aligned to atmospheric water potential (AWP) and temperature. Current atmospheric models predict all monoterpene emissions as a function of temperature and light and therefore would erroneously place peak monoterpene emission midway between the real peaks, and be unable to reproduce the drought induced changes revealed by resolving enantiomers (Guenther 1997).

During pre- and mild drought, (-)-α-pinene and (-)-β-pinene peaked with maximum assimilation rate (*A*) between 11:00 and 12:00. In contrast, (+)-α-pinene and (+)-limonene peaked between 14:00 and 15:00, coincident with maximum temperature and atmospheric water potential (**Fig. 4c**). With the transition into severe drought, the (-)-α-pinene and (-)-β-pinene diel cycles shifted progressively later in the day, merging with the diel cycles of (+)-α-pinene in the afternoon, while the assimilation rate (A) declined (less carbon uptake by the vegetation) and atmospheric water potential (AWP) and PAR decreased. With rewetting the assimilation rate began to recover (increased carbon uptake), concurrent with a shift in peak (-)-α-pinene and (-)-β-pinene from 14:00 back to 12:00. Hence, the shift of the daily maximum of (-)-α-pinene to the afternoon with progressive drying potentially suggests that the emissions are less *de novo* and more storage pool in character (**Fig. 4a**). Since the diel cycles of (-)-β-pinene followed the same temporal pattern as (-)-α-pinene, it is likely that (-)-β-pinene also transitioned from *de novo* emission to storage pool emission.

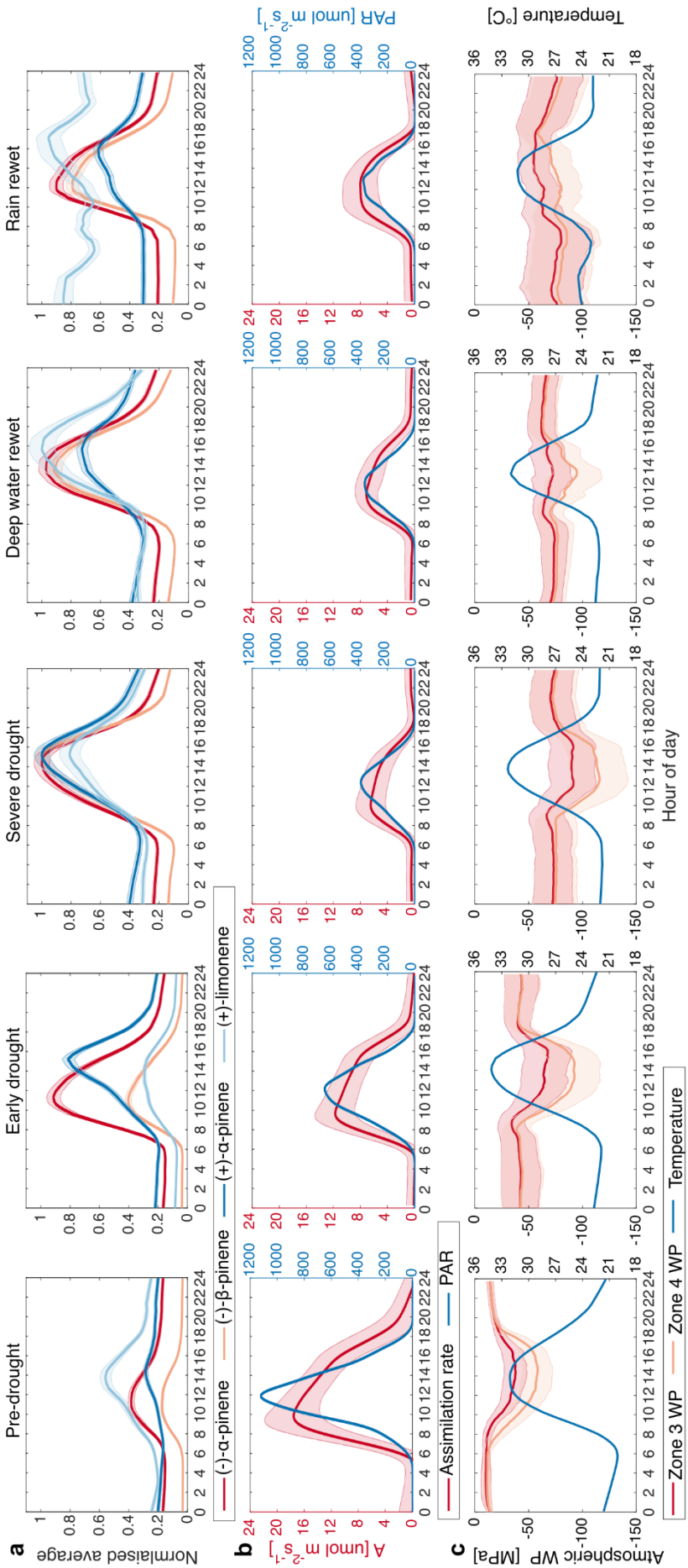

Figure 4. Comparison of diel cycles of selected monoterpenes and their enantiomers with light, temperature and soil moisture across the experiment suggest emission driver changes in some monoterpenes. **a**. Average diel cycles for (-) and (+)-α-pinene, (-)-β-pinene and (+)-limonene. The monoterpene diel cycles were normalized by their respective maxima across all averaged diel bins, which was found to be during SD for both compounds. The shaded region around the lines is the average absolute uncertainty. **b**. Assimilation (A) and photosynthetically active radiation (PAR). The shaded region around the assimilation rate line represents 1σ. **c**. Atmospheric water potential (AWP) and temperature. Zones 3 and 4 were the uppermost sections of the rainforest enclosure (**Ext. Data Fig. 3**). The shaded region around the atmospheric water potential lines represents 1σ.

Monoterpenes are generally stored in the lipid phase rather than the aqueous phase within the leaf (Niinemets, Loreto, and Reichstein 2004, Niinemets and Reichstein 2002). Monoterpenes are relatively water insoluble and partition rapidly between the aqueous and gas phase, according to their Henry's constant (Sander 2015). The aqueous phase storage is small and empties quickly in the morning when the stomata open and water is lost from the leaf to the atmosphere therefore any monoterpene emissions from the aqueous phase are likely to be negligible (Niinemets, Loreto, and Reichstein 2004). Monoterpenes possess large octanol/water partition coefficients (K_{ow}) (≈ 20000–30000), meaning they can be stored in relatively large quantities in the lipid phase from where they are more slowly emitted to the atmosphere (Niinemets, Loreto, and Reichstein 2004). A plausible explanation of the emission behaviour is that throughout the measurement period, (+)-α-pinene and (+)-limonene were stored in the lipid phase, leaking slowly into the atmosphere peaking later in the day than the *de novo* emissions. As photosynthesis decreased and biomass degradation increased, the emission character of (-)-α-pinene and (-)-β-pinene transitioned from mainly *de novo* synthesis to emission from storage pools.

By grouping enzymes, which share similar attributes (i.e. light and temperature dependency, major monoterpene product), a three enzyme group – two reservoir model can explain the observed isoprene and monoterpene emissions (**Ext. Data Fig. 4**). Isoprene is generated by light activated isoprene synthase (enzyme group 1) and (-)-α-pinene and (-)-β-pinene are generated by light activated enzyme group 2 and emitted directly (*de novo*). However, both (-)-α-pinene and (-)-β-pinene are also partitioned to the lipid phase where they are released upon drought stress. Enzyme group 3 is responsible for synthesizing (+)-α-pinene and (+)-limonene continuously without light activation, which also partition to the lipid phase.

The changes in ecosystem emissions in relation to potential particle formation and growth are important since increased condensation nuclei (CCN) production efficiency, cloud formation and subsequent rain would represent a possible negative biosphere-atmosphere feedback to the drought. In early drought *de novo* monoterpene emissions increase. High fluxes of reactive isoprene will act to suppress OH radical levels above the canopy allowing the less reactive monoterpene emissions to reach higher, cooler altitudes, where the newly formed aerosols may invigorate convection (Abbott and Cronin 2021). In severe drought, isoprene emissions, which do not produce particles or extremely low volatile organic compounds (ELVOC) efficiently, decrease, whereas monoterpene emissions increase further. Among the monoterpenes, the most prolific increase is of α-pinene, which oxidizes to ELVOC and particles with high yield. The results presented here are therefore consistent with the negative feedback mechanism hypothesized above. Furthermore, the shift in monoterpene emissions during drought to later in the afternoon means they are released in periods when higher sensible heat flux and turbulence which would facilitate the transport of monoterpene rich air parcels to the levels of cloud formation.

The emission characteristics of enantiomers were deciphered because the B2-TRF provides a unique venue to conduct a drought under controlled conditions, with comprehensive biological measurements, in addition to atmospheric isotopic labelling in an environment of greatly reduced atmospheric chemistry. These results show that the degree of drought stress in a tropical rainforest can be gauged by either the afternoon-to-morning ratios of (-)-α-pinene or by the fractional contribution of (-)-β-pinene to the sum of monoterpenes, which almost tripled from pre- to severe drought. Unexpectedly, the (-) enantiomers from different monoterpenes exhibited the same diel behaviour whereas opposite enantiomers from the same monoterpenes exhibited different diel cycles. It is remarkable that the *de novo* and storage pool sources of monoterpene emissions from an ecosystem, and the carbon cycling changes in response to drought, can be assessed externally from air measurements provided that individual enantiomers are considered. This underlines that a new enantiomerically specific approach to emission modelling, based on the enzyme group model proposed here, would be more accurate and biologically founded than current approaches (Messina et al. 2016), in particular with regards to a possible feedback between emission composition and

particle production efficiency. We conclude that enantiomerically resolved monoterpenes are required to accurately assess how key tropical regions, such as the Amazon rainforest, emit monoterpenes and respond to the predicted increase in future extreme drought events.

Additional Information. Supplementary Information is available for this paper.

Correspondence and requests for materials should be addressed to jonathan.williams@mpic.de

4.3. Methods

4.3.1. Tropical rainforest mesocosm (TRF)

The tropical rainforest mesocosm at the Biosphere 2 covers ca. 1950 m^2 and is representative of a managed tropical rainforest ecosystem similar to those found in South America. It is contained under a 26700 m^3 glass ziggurat enclosure (Pegoraro et al. 2005) (Fig. 1). Within the enclosure, there are 95 species of tropical plants, including 23 species of trees and 67 species of understory plants. The most dominant species are *Clitoria fairchildiana*, *Phytolacca dioica*, *Arenga pinnata*, *Ficus benjamina*, *Syngonium podophyllum*, *Piper* sp., *Musa* sp. and *Pachira aquatica*. To recreate real rainforest conditions, such as low light intensity beneath the canopy, larger trees and understory plants (*Musa* sp., *Piper* sp., *Hibiscus rosa-sinensis*) were planted around the edges of the glass enclosure to block out direct sunlight. The soil profile consists of an up to 4 m deep subsoil layer and a, 70–100 cm, variable topsoil layer(Pegoraro et al. 2006). Located at the centre of the rainforest is a small artificial "mountain" within which a laboratory was constructed to house the on-line GC-MS and where the ambient temperature and humidity inside could be controlled.

4.3.2. Drought experiment

This experiment was conducted during the Water, Atmosphere, and Life Dynamics campaign. Prior to the commencement of the drought period, the tropical rainforest was wetted from above with a sprinkler system to simulate rainfall, using ~20,000 liters of water 3 times a week. After watering on 7th October 2019 the rainforest biome was left to dry. During some stages air handler units were employed for the removal of humidity by condensation, otherwise the rainforest biome was left to dry naturally, until 3rd December 2019. The first water to the rainforest was introduced at the bottom through a network of drainage pipes under the soil on top of the concrete and steel structure underlying Biosphere 2. The rainforest was again watered from above using the sprinkler system, on 12th December 2019, 19th December 2019, and every 2 days afterwards. The rainforest temperature was controlled throughout the experiment and the temperature at 13 m was on average between 28 and 32 °C during daylight hours and between 21 and 24 °C during nighttime hours.

The photosynthetically active radiation (PAR), temperature and relative humidity (RH) were recorded every 15 minutes using sensors connected to a datalogger (PAR sensors (Apogee SQ110, Campbell Scientific, Logan, UT, USA), temperature and RH with Vaisala HMP 45c sensors (Vaisala Oyi., Vantaa, Finland; purchased through Campbell Scientific). Sensors reported every 15 minutes to a centralized CR1000 datalogger (Campbell Scientific, Logan, UT, USA) with an AM16/32B multiplexer (Campbell Scientific, Logan, UT, USA). The dataloggers were connected to a centralized database with NL100 communications modules (Campbell Scientific, Logan, UT, USA) and the data is available through the Biosphere 2 website (www.biosphere2.org/data-models/rainforest-data). The PAR sensor was located at 13 m on the central measurement tower and the humidity and temperature sensors were located at a height of 13 m on the north-eastern measurement tower together with the sampling inlet. The soil moisture data presented in Fig. 2D is an average of measurements that were recorded every 15 minutes from four different soil pits (soil moisture and temperature sensors (Truebner SMT100, Truebner Gmbh, Neustadt, Germany) and water potential sensors (TEROS 21, Meter Group, Pullman, WA, USA) in all four pits at 5 cm depth and at the soil-concrete interface (subsoil bottom)). Since the sensors are 30 mm wide and inserted vertically into the soil with the soil depth indicated at the midpoint, each depth is ± 1.5 cm.

The rainforest enclosure acted as a semi-enclosed system where there was constant air exchange with the outside environment. The air-exchange rate from the tropical rainforest enclosure was measured

using sulfur hexafluoride (SF6) at low ppb levels as a tracer gas, as it is completely anthropogenic and its concentration is < 10 ppt in background air and therefore it is only be affected by leakage and flushing. More information on using SF6 as a tracer gas in the tropical rainforest mesocosm at the Biosphere 2 can be found elsewhere (Pegoraro et al. 2005). Once the percentage exchange rate of SF6 was obtained and interpolated, the measured data was corrected by using the equation

$$VMR_c = VMR_u + (VMR_u * ER)$$

Where the VMR_u was the uncorrected data, ER was the exchange rate percentage and VMR_c was the corrected data. The incoming VMR of all VOCs were assumed negligible.

4.3.3. Determination of isoprene and monoterpene ambient mixing ratios

From 9th September to 23rd December 2019, the ambient air from the 13 m high within Biosphere 2 rainforest was continuously drawn at a flow of approximately 800 ml min^{-1} through a main Teflon inlet line which comprised of 37 m of 0.625 cm (¼ “) Teflon tubing. 13 m was chosen as the sampling height as this was the height within the enclosure that had the greatest leaf area index. The main inlet line was fitted with a (Cole Palmer, EW-02915-31) filter. After approximately 26 m, a t-piece was connected to the main inlet line which was connected to a thermal desorption unit (TD) (TT247-xr, MARKES International Ltd., U.K.) using 7 m of = 3.175 mm (1/8 “) Teflon tubing. All sampling lines were insulated and heated to 50 °C to avoid water condensation within the lines. The line to the TD was continuously purged to avoid the sampling of a dead volume with a pump situated the behind the TD in the flow path. During sampling, the pump behind the TD drew air from the main inlet line at flows ranging between 70 and 200 ml min^{-1} for 10 minutes. The collected air was sampled first through a water condenser (kori-xr, MARKES International Ltd., U.K.). This allowed for the removal of water whilst leaving the target VOCs unchanged. The dehumidified sample was then pre-concentrated onto a cold injection trap at 30 °C (Material emissions, MARKES International Ltd., U.K.). After sampling, the injection trap was purged for 1 minute with helium with a flow of 50 ml min^{-1} before being rapidly heated to 300 °C and desorbed for 3 minutes. The sample was removed from the cold trap with a Helium flow of 3 ml min^{-1} including a split flow of 2 ml min^{-1} and injected into the separating column.

The rainforest ambient air was analysed using a Gas Chromatograph (GC) (6890A, Agilent Technologies, U.K.). The carrier gas used was research 6.0 grade helium (Airgas®, USA.) Separation of the sampled compounds was achieved using a 30 m β-DEX™ 120 column (Sigma-Aldrich GmbH, Germany) with 0.25 mm internal diameter and a 0.25 µm film thickness. The temperature program used was as follows, 40 °C for 5 minutes then 40 °C to 150 °C at 4 °C min^{-1} and 150 °C to 200 °C at 30 °C min^{-1}. The column flow was set to 1 ml min^{-1}.

The GC was coupled with a quadrupole mass spectrometer (MS) (5973N, Agilent Technologies, U.K.), operated in selected ion mode for the identification of mass ions 68, 69, 93, 94, 119, 120, 136, 137 each with a dwell time of 60 ms.

The identification of the target compounds was achieved by first operating the MS in scan mode to obtain full mass spectra to be able to compare with the NIST 70 eV electron ionization library. For further confirmation, a gas standard mixture (Apel-Riemer Environmental Inc., 2019) containing the target compounds was injected into the GC-MS system. The same gas standard mixture was also injected onto sorbent cartridges and subsequently desorbed into a GC - time of flight - mass spectrometer (GC-TOF-MS) operated with identical conditions to the online GC-MS. Using liquid standards, the headspace of the individual compounds was taken onto sorbent cartridges and also desorbed into the GC-TOF-MS. The retention times from the chromatograms of the individual compounds was then crosschecked with the chromatogram of the gas standard mixture.

The MS was tuned on a weekly basis and the linearity was checked throughout the campaign. The gas standard mixture was injected into the system after each tuning and after 10 samples were analysed. Routine calibrations were performed by initially flushing the TD system with the gas standard mixture at a flow of 20 ml min^{-1} for 2 minutes in order to remove the dead volume. The calibration gas was then injected with a flow of 20 ml min^{-1} for 5 minutes directly onto the cold injection trap within the TD. The calibration gas sample was then treated with the same TD-GC-MS parameters as the routine sampling. This step was repeated three times before sampling continued. The MS responses to the injected calibration gas samples were then plotted against the time since the last MS tune to track the MS sensitivity drop, which allowed for the correction and calibration of the raw data. To check the linearity, the same procedure was used with the calibration gas injection time being increased in stepwise intervals of 2.5 minutes from 0.5 to 12.5 minutes.

4.3.4. Data management

The highest individual VMRs measured were in excess of 3 ppb for (-)-alpha-pinene and 400 ppt for (+)-alpha-pinene were measured during ED (**Ext. Data Fig. 5 and 6**). However, to evaluate the general trends of all measured compounds through each stage, the hourly total monoterpene and isoprene data was smoothed by applying a Savitzky-Golay filter to keep long term trends whilst removing short term fluctuations. The dataset was further split into daytime and nighttime, using photoactinic radiation (PAR) data collected at the point of measurement. The smooth function (MATLAB) was then used to suppress noise in the trend line for each compound and the uncertainties were propagated using the same functions. To obtain average diel cycles for each compound, and the average composition all data in each of the five stages of the campaign were taken. A moving median calculation with a window length of 5 was applied to each group. The diel cycles were averaged over 435, 526, 349, 136 and 193 data points for PD, ED, SD, DRW and RRW respectively. β-Myrcene, (+)-β-pinene, α -terpinene and terpinolene, were also observed but not included as they amounted to an average of less than 5 % of the average total monoterpene for the entire measurement period. Ocimene was also observed but not calibrated with the on-line GC-MS system.

The atmospheric water potential was calculated from the Vaisala temperature and relative humidity measurements according to:

$$\psi\,(Pa) = -\frac{RT}{V_w^0}\ln\left(\frac{\%RH}{100}\right)$$

where Ψ is the water potential (in Pa), R the gas constant (8.3144 J mol^{-1} K^{-1}), T the temperature (°C), V_w^0 the molar volume of water at 293 K, and %RH is the relative humidity (%)(Lambers and Oliveira 2019). Zone 3 and 4 are the two height zones that contain the majority of the canopy in the Biosphere 2 rainforest (**Ext. Data Fig. 3**). The environmental conditions were averaged over all the sensors that were located within these zones. Net ecosystem exchange (NEE) was calculated every 15 minutes based on the change in moles of CO_2 within the rainforest ecosystem and the amount of CO_2 lost or gained with the air-exchange with the outside:

$$NEE = \frac{\left((CO_2^t - CO_2^{t-1}) + \left(CO_2^{27m} - CO_2^{Outside}\right) * ER\right)}{Area}$$

where CO_2^t, CO_2^{t-1}, CO_2^{27m}, and $CO_2^{outside}$ are the moles of CO_2 at the time calculated, previous time-step, 27m or top of the rainforest where the air flows out, and the outside air coming into the rainforest. Area stands for the soil surface area of the rainforest. The moles of CO_2 were calculated based on the ideal gas law and the CO_2 concentration:

$$moles\ of\ CO_2\ = \frac{V * P}{(273.15 + T_{Ave}) * R} * \frac{[CO_2]}{10^6}$$

where V denotes the representative volume for the CO_2 measurement (either the rainforest volume fraction or the volume of air exchanged), P denotes the pressure (measured inside and outside the Biosphere 2 rainforest using WeatherHawk WXT 530, Vaisala Oyi., Vantaa, Finland), T_{Ave} denotes the average air temperature for the measurement zone or the outside air temperature (measured using HMP45c temperature and humidity sensors (Vaisala Oyi., Vantuu, Finland), R denotes the gas constant, and $[CO_2]$ denotes the CO_2 concentration measured inside Biosphere 2 with GMP343 CO2 sensors (Vaisala Oyi., Vantuu, Finland) and outside Biosphere 2 with GMP220 sensors (Vaisala Oyi., Vantuu, Finland) and inside the air inflow with an Aerodyne Dual QCL (Aerodyne Research Inc., Billerica, MA, USA). The ecosystem assimilation (A, μmoles m^{-2} s^{-1}) was calculated from the Net Ecosystem Exchange (NEE) and assuming that the nighttime respiration (R) was representative for the daytime respiration (a reasonable assumption in tropical forest ecosystems(Restrepo-Coupe et al. 2013, Hutyra et al. 2007)):

$$A = NEE - R$$

4.3.5. $^{13}CO_2$ pulse labelling experiment

The $^{13}CO_2$ pulses were carried out on 5th October at 8:00 am (MST) and 23rd November 2019 at 9:00 am (MST) to coincide with peak photosynthetic activity (Rascher et al. 2004). A deliberate effort was made to proceed with the pulse experiments on days with high amounts of direct sunlight, when there would be a high rate of photosynthesis, to maximize CO_2 uptake. During the first pulse, the rainforest was fumigated with 10 lpm of 99% $^{13}CO_2$ (Millipore Sigma, Burlington, MA, USA) for 15 minutes. In order to balance reduced carbon assimilation rates during the drought, 20 lpm of 99% $^{13}CO_2$ was released over 15 minutes during the second pulse. The $\delta^{13}C$ value of atmospheric CO_2 within the rainforest was monitored throughout each pulse using a Tunable Infrared Laser Direct Absorption Spectrometer (TILDAS, Aerodyne Research, Billerica, MA, U.S.A). After 4 hours during the first pulse, and 5.2 hours during the second pulse, the flow of air through the rainforest was increased and, at midday, windows were temporarily removed from the enclosure of the B2-TRF and excess $^{13}CO_2$ was ventilated to the outside air, so that the entry of ^{13}C into the mesocosm could be more accurately traced back to a fixed point in time.

4.3.6. Determining enantiomer 13C isotope ratios

Pairs of monoterpene enantiomers abundant in the air were analysed in the TRF ecosystem in a height of 13m at the atmosphere tower. 5, 16, 36, 11 and 14 glass cartridges were sampled during pre-pulse, first pulse, first post-pulse, second pulse and second post pulse respectively. For terpene accumulation, ambient air was drawn through glass cartridges filled with about 100 mg Tenax (Sigma, Germany) as an adsorbent at a controlled flow rate of 200 ml min^{-1} for 90 min using a handheld pump (SKC ltd., Dorset, U.K). Glass cartridges were kept at 4 °C until analysis. The samples were analyzed at the university of Freiburg on a system consisting of a gas chromatograph (GC 7980, Agilent Technologies, Germany) coupled to a mass selective detector (MSD 5975C, Agilent Technologies, Germany) and equipped with a thermodesorption unit (TDU, Gerstel, Germany) and a cold injection system (CIS, Gerstel, Germany). For analysis of ^{13}C isotope ratios, this system was coupled to an isotope ratio mass spectrometer (IRMS, Isoprime precisION, Elementar Analysesysteme GmbH, Langenselbold, Germany) via a combustion furnace (GC 5 interface, Elementar Analysesysteme GmbH,

Langenselbold, Germany). For analysis, air sampling glass cartridges were heated to 220 °C for 5 min to thermodesorb terpenes and channel them into the CIS which was kept at -70 °C. By heating the CIS to 240 °C for 3 min, terpenes were directed onto the GC separation column (BetaDex 120 Chirality, 60 m x 250 µm x 0.25 µm, Supelco, USA) with a He stream of 1 ml min^{-1}. The oven program started at 45 °C which was kept for 1 min, temperature was then stepwise increased to 60 °C, 150 °C and 210 °C at rates of 2 °C min^{-1}, 1 °C min^{-1} and 3.5 °C min^{-1}, respectively. The eluate was split and ca. 10 % was directed into the MSD for terpene identification and quantification. For this purpose, the MSD was run in SIM mode detecting m/z 68, 93, 119 and 136. The remainder eluate passed the combustion furnace where at a temperature of 850 °C the terpenes were oxidized to form CO_2 and H_2O. After elimination the H_2O by a Nafion water trap, the $^{13}C/^{12}C$ ratios of the CO_2 were measured by the IRMS.

4.3.7. Statistical information

The t-tests used on the data presented in figure 3, were one-tailed, two sample unequal variance t-tests that were performed using the MATLAB R2017B software (**Ext. Data Table 1**).

4.3.8. GC-IRMS data processing

^{13}C isotopologues elute slightly faster from the GC than their ^{12}C counterparts, meaning that $\delta^{13}C$ values are not homogenous across the peak(Ricci et al. 1994). For chromatographically unresolved compounds such as (-)-α-pinene, integrating from the beginning of the peak to the trough between it and the subsequent unidentified coeluting peak results in $\delta^{13}C$ values that appear artificially enriched in ^{13}C. Absolute $\delta^{13}C$ values for such compounds cannot be reported. We therefore report relative offsets between measured $\delta^{13}C$ values during the $^{13}CO_2$ pulses and ambient conditions

$$\varepsilon^{13}C = \frac{\left(\frac{^{12}C}{^{13}C}\right)_{pulse}}{\left(\frac{^{12}C}{^{13}C}\right)_{ambient}} - 1$$

While the relative abundance of (-)-α-pinene to its coeluter changes its apparent $\delta^{13}C$ value, we are confident that these chromatographic effects cannot account for the relative ^{13}C-enrichment of this compound during the $^{13}CO_2$ pulses for two reasons. First, the ^{13}C-enrichment of the samples from the $^{13}CO_2$ pulses are significantly enriched relative to the variability in ambient $\delta^{13}C$ values, which are subject to a greater range of relative peak heights. Second, ^{13}C enrichment is only apparent during the $^{13}CO_2$ pulses when (-)-α-pinene is integrated in various combinations with the other three peaks in the coeluting hump, but not when any of these other peaks are individually integrated trough-to-trough (**Ext. Data Fig. 6**).

There is no indication that (+)-α-pinene becomes enriched in ^{13}C during either $^{13}CO_2$ pulse. However, given its small size and poor resolution from the preceding unlabelled peak, we cannot definitively rule out slight ^{13}C-enrichment for (+)-α-pinene. Myrcene, trans-β-ocimene, and (+)-limonene all have well resolved fronts and poorly resolved tails. These compounds display either high ^{13}C-enrichment during the $^{13}CO_2$ pulses (trans-β-ocimene during both pulses, myrcene during the second) or no

enrichment at all (myrcene during the first pulse, (+)-limonene during both). Since these chromatographically similar peaks only display large ^{13}C-enrichment in some compounds and not others, we consider apparent presence or absence of label uptake to be robust results for these compounds (**Ext. Data Fig. 8 & 9**).

4.3.9. Soil uptake and emission of monoterpenes experiment

For the investigation of how monoterpenes are taken up and emitted by the soil, 3 soil chambers made from polyvinyl chloride were placed on pre-installed soil collars around the B2-TRF (***Ext. Data Fig.* 2**). Using sorbent cartridges, samples were taken from the atmosphere, located at the inlet (MR_{atm}) of the soil chamber, and at the same time from the outlet (MR_{soil}). Samples were collected at 200 ml min^{-1} for ~ 10 minutes using a handheld pump (SKC ltd., Dorset, U.K). The sorbent cartridges were made from inert coated stainless steel (SilcoNert 2000 (SilcoTek™, Germany)). The sorbent consisted of 150 mg of Tenax® TA followed by 150 mg of Carbograph™ 5 TD (560 m^2/g).The size of the Carbograph™ particles was in the range of 20-40 mesh. The Carbograph™ 5 was supplied by L.A.R.A s.r.l. (Rome, Italy) and Buchem BV (Apeldoorn, The Netherlands) supplied the Tenax®.

Chapter 5: Chiral terpenoid emissions of two tropical plant species in response to an extended experimental drought

This chapter is a paper in preparation and is planned to be submitted as a manuscript for peer review. I am the first author and my personal contribution included sampling the emissions from the plants, measuring the collected air samples with GC-TOF-MS, analysing the GC-TOF-MS data, preparing the figures and writing the manuscript.

Abstract. Drought affects the regular functioning of internal plant processes and emissions of volatile organic compounds (VOCs) to the atmosphere. Terpenoids are a family of VOCs that are synthesized by plants to protect against stress and to maintain photosynthesis. However, there is still not a holistic understanding of how drought affects plant terpenoid emissions, as various results have been published reporting increases whilst other studies have reported decreased or unaffected emissions. Here we present enantiomerically separated monoterpene and linalool emissions from two tropical plant species: an upper canopy species, *Clitoria fairchildiana*, and an understory species, *Piper* sp. measured in a managed indoor tropical rainforest during a 9.5-week drought and rewetting experiment. The dominant monoterpene emitted from *C. fairchildiana* was consistently found to be ocimene throughout the entire measurement period, whereas, the dominant monoterpene from *Piper* sp. varied among an array of compounds. Unexpectedly, (-)-α-pinene and (+)-α-pinene emissions from *Piper* sp. changed similarly to each other, but monoterpene emissions *C. fairchildiana* did not co-vary with each other. In contrast, the emissions of (-)-linalool and (+)-linalool did not co-vary with each other for both plant species. The monoterpene emissions from *C. fairchildiana* were found to be more dependent than *Piper* sp. on plant water potential. Monoterpene emissions for both species increased during drought; however, the greatest increase in monoterpene emissions for *Piper* sp. occurred during early drought whereas for *C. fairchildiana* it was during severe drought. Overall, these results suggest a strong positive effect of drought on terpenoid emissions from tropical plant species.

5.1. Introduction

Extreme climate events such as drought are expected to become an increasingly common occurrence throughout the 21st century (IPCC 2014), weakening carbon sequestration and regular functioning of forest ecosystems (Bonan 2008, Reichstein et al. 2013). Carbon in the form of CO_2 is uptaken by forests and used in the synthesis of a multitude of biogenic volatile organic compounds (BVOCs), some of which are stored in specific or non-specific storage, whilst other BVOC's are emitted from the leaf directly following synthesis (*de novo* emission) (Niinemets, Loreto, and Reichstein 2004, Niinemets and Reichstein 2002). BVOC's are emitted from plants to attract pollinators, as a defence against biotic and abiotic stressors and for processes related to plant growth (Peñuelas and Staudt 2010). One such group of BVOCs is known as monoterpenes ($C_{10}H_{16}$), which are commonly emitted by many different plant species (Kesselmeier and Staudt 1999). Once monoterpenes enter the atmosphere, they can undergo reactions with atmospheric radicals to eventually form secondary organic aerosol and cloud condensation nuclei (Engelhart et al. 2008). Therefore, understanding how monoterpene emissions change when a plant experiences stress events such as drought is vitally important for predicting feedbacks on the climate.

Monoterpene emissions from different plant species do not have the same response to drought stress (Staudt et al. 2002, Ormeño et al. 2007, Blanch, Peñuelas, and Llusià 2007). It has been shown that monoterpene emissions from plants increase, decrease or stay unaffected by drought stress with the length of drought and experimental procedure being important factors in observed differences in addition to the physiology of the plant species. Measurements of monoterpene emissions from drought-stressed *Quercus ilex*, *Citrus sinensis*, *Fagus sylvatica, Quercus suber*, and *Cistus ladanifer* found that drought stress restricts monoterpene emissions (Bertin and Staudt 1996, Blanch, Peñuelas, and Llusià 2007, Staudt et al. 2002, Hansen and Seufert 1999, Haberstroh et al. 2018). Whereas, water stress experiments on *Pinus halepensis*, *Cistus albidus*, and *Salvia officinalis* showed that water stress increased monoterpene emissions, which were significantly correlated to the plant water potential (Ormeño et al. 2007, Blanch, Peñuelas, and Llusià 2007, Radwan, Kleinwächter, and Selmar 2017). In contrast, water stress did not significantly affect the monoterpene emission rate of *Rosmarin officinalis*, and *Cistus monspeliensis* and the emissions were not significantly correlated to the plant water potential (Nogués, Medori, and Calfapietra 2015, Ormeño et al. 2007). Since monoterpene emissions from these species are not dependent on photosynthesis and they have large storage pools for monoterpenes, their emissions remained stable. Similarly, the monoterpene emission rate of *Quercus coccifera* was found to remain stable under water stress (Ormeño et al. 2007), directly disagreeing with another study on the same species which found that water stress inhibited monoterpene emission after one week (Llusià and Peñuelas 1998). Many of the species that have already been studied for how their monoterpene emissions respond to drought stress have been boreal and Mediterranean species. However, tropical forests are an important source of BVOC to the atmosphere (Guenther et al. 2012) with little research performed so far on how the emissions from tropical plant species will respond to reduced water availability. Thus, more experiments must be performed on tropical plant species that can explain how their monoterpene emissions respond to drought.

Some, but not all, monoterpenes contain an asymmetric chiral centre, which means they exist as two mirror-image forms ((-) and (+)) known as enantiomers. Of the plant species that have been studied so far during drought experiments, monoterpene emissions have not been resolved for the individual enantiomers. This is because, firstly, it is commonly assumed that sources and sinks of enantiomers are identical since they possess the same chemical characteristics such as vapour pressure and atmospheric lifetimes. Secondly, resolving enantiomers with a gas chromatograph-mass spectrometer system requires a specialist chromatographic separating column and extensive method development

as resolving enantiomers almost doubles the number of terpenoid peaks in a given time period in the chromatogram, leading to an increased risk of co-elution and poor chromatography. However, some studies have already shown that there is still much to be learnt about the emission of enantiomers (Staudt et al. 2019, Zannoni et al. 2020, Williams et al. 2007). Branch, stem, and soil emissions samples taken from a homogenous Mediterranean maritime pine forest, showed unexplainable differences in the enantiomeric percentages of α-pinene (Staudt et al. 2019). Additionally, regional differences were observed as samples taken from the air above the amazon rainforest contained more (-)-α-pinene than (+)-α-pinene, whereas the opposite was seen for samples taken within a boreal rainforest (Williams et al. 2007). Further, (-)-α-pinene correlated better with a totally different compound than it did with (+)-α-pinene, hinting that the sources of enantiomers are not always identical (Williams et al. 2007). Surprising chiral composition changes of α-pinene was also seen on a 325 m measurement tower in the Amazon rainforest, (+)-alpha-pinene dominating at 40 m and 80 m and (-)-α-pinene dominating at 150 m and 320 m (Zannoni et al. 2020). Since these studies show that little is still known about the differences in emissions of enantiomers, it is important for more studies to be performed which resolve enantiomers, which can better inform models, which predict how monoterpenes are emitted.

In this study, two species of tropical plants were chosen, a canopy species, *Clitoria fairchildiana* (**Fig. 1a**), and, an understory species, *Piper* sp. (**Fig 1b**) in an enclosed experimental forest. Since these two species occupy different spaces within the forest (canopy vs. understory), it is hypothesized that because *C. fairchildiana* is a larger woody tree with deeper roots than the herbaceous *Piper* sp., monoterpene emissions from *C. fairchildiana* are more tolerant to drought than monoterpene emissions from *Piper* sp. The monoterpene emissions were tracked on selected days throughout a 9.5-week drought experiment to see how the individual monoterpene species and enantiomer emissions respond to drought and how these results compare with drought experiments that have been performed on other plant species.

Figure 1. Photographs taken from within the Biosphere 2 tropical rainforest. **a**. *Clitoria fairchildiana* (photo K. Kuhnhammer). **b**. *Piper* sp. grove (Photo J. Byron).

5.2. Methods and materials

5.2.1 Drought experiment

The intermittent sampling of the air from branch cuvettes throughout an extended drought and rewetting was an experiment conducted as part of the Biosphere 2 Water, Atmosphere, and Life Dynamics (B2-WALD) campaign. The project took place inside the artificial rainforest in Biosphere 2, Oracle, AZ (USA) (Pegoraro et al. 2006, Pegoraro et al. 2005). The project began in August 2019 with a pre-drought phase, followed by drought, rewetting and recovery periods. Before the drought period began, sprinklers wetted the tropical rainforest from above to simulate rainfall, using ~20,000 liters of water 3 times per week. The final watering before drought occurred on 7th October 2019 after which the rainforest biome was left to dry. At times during the measurement period, air handler units were used to remove humidity by condensation, otherwise, the rainforest biome was left to dry naturally, until 3rd December 2019. Near the end of the drought period, water was introduced to the rainforest at the bottom through a network of drainage pipes that lie under the soil and on top of the steel and concrete structure, which underlies the Biosphere 2. The recovery period began with rain from above using the sprinkler system on 12th December 2019, 19th December 2019, and every 2 days afterward.

5.2.2 Monoterpene sampling

To understand how BVOC emissions are impacted by drought and rewetting, the two highest monoterpene emitting species were chosen: one upper canopy tree species (*Clitoria fairchildiana*) and one understory species (*Piper* sp.). Species were also selected according to representativeness (i.e. presence within the forest) of the ecosystem, site distribution, and accessibility (**Fig. 2**). Four *C. fairchildiana* trees and four *Piper* sp. plants were chosen and one branch cuvette was placed on each tree and plant. Cartridges were also used to sample the air from an empty cuvette, which would be used as a background measurement. The air from an empty cuvette was sampled at the same time as the air from the *C. fairchildiana* and *Piper* sp. cuvettes.

Species-specific separate cuvettes made of FEP film (FEP film (85905K64, McMaster Carr, Atlanta, GA, USA) were installed to reduce dead space as much as possible within the chambers. Fans were installed in chambers to ensure air homogenisation inside chambers. Terostat (Terrostat-II, Kahmann & Ellerbrock GmbH & Co. KG, Bielefeld, Germany) and rubber bands were used to seal the chambers. Humidified zero-air with defined CO_2 concentration, matching the average atmospheric concentrations in the Biosphere 2 rainforest (500 ppm), was transported into the chambers with a constant flow of 11 l min^{-1} via flow controllers (MC-2SLPM-D/5M, Alicat Scientific, Inc., Tucson, AZ, USA). Lines were heated to reduce condensation. Relative humidity and temperature were measured on the Northeast (NE) measurement tower at 3 and 13 m (**Fig. 2**), which was the approximate height of the bulk of the *Piper* sp. and *C. fairchildiana* vegetation, respectively. Leaf chambers were held under slight but constant overpressure during the experiments, reducing the risk of leaks influencing the measurements. Chambers were connected to the sorbent cartridges via. PFA-tubing (1/4" OD x 1/8" ID, Ametak, Nesquehoning, PA, USA). Chamber air was drawn through inert coated stainless steel cartridges (SilcoNert 2000 (SilcoTek™, Germany)) which were filled with about 150 mg Tenax® TA followed by 150 mg of Carbograph™ 5 TD (560 m^2/g).).The size of the Carbograph™ particles was in the range of 20-40 mesh. The Carbograph™ 5 was supplied by L.A.R.A s.r.l. (Rome, Italy) and Buchem

BV (Apeldoorn, The Netherlands) supplied the Tenax®, Samples were collected at 200 ml min^{-1} for between 20 and 60 minutes using a handheld pump (SKC ltd., Dorset, U.K).

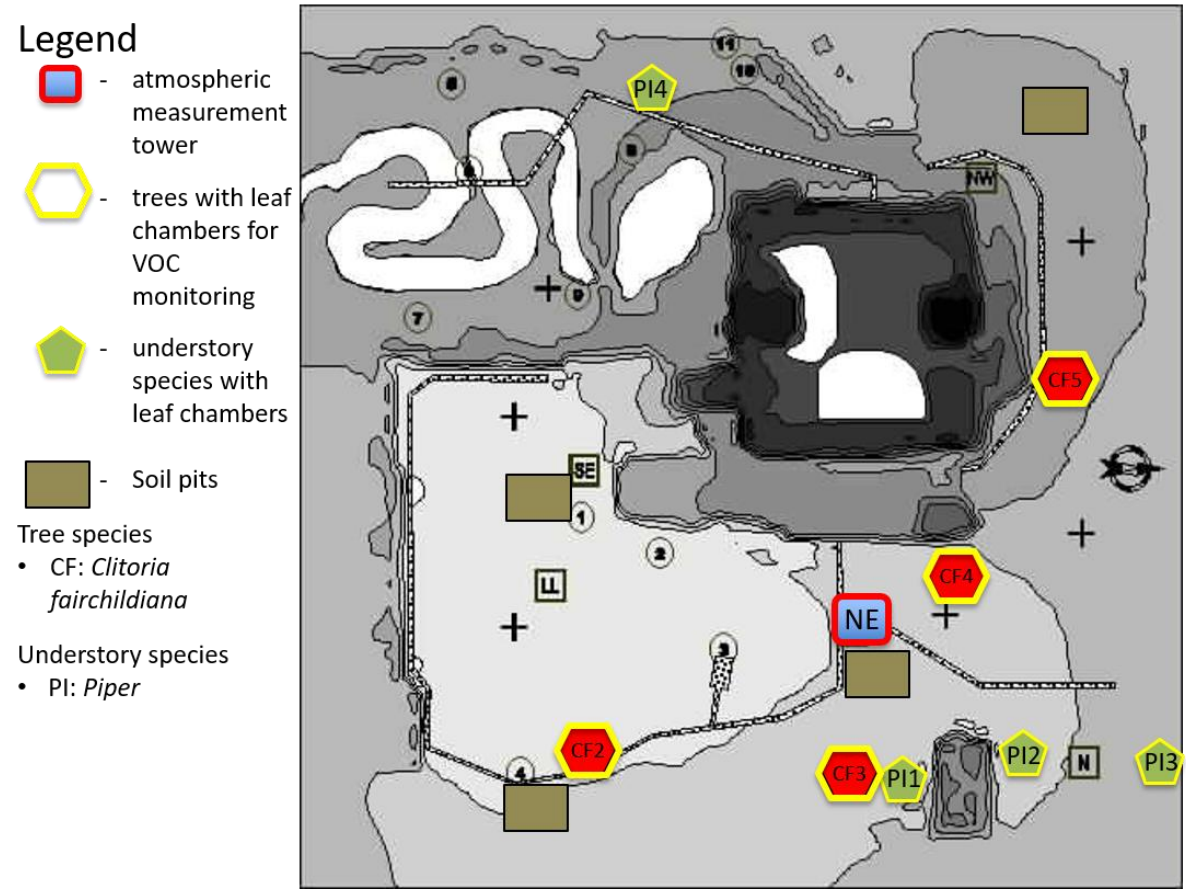

Figure 2. Map of the Biosphere 2 tropical rainforest indicating the location of the plants that were used in this investigation, as well as the northeast (NE) atmospheric measurement tower and the soil pits.

5.2.2. Monoterpene analysis

The sampled cartridges were analysed at the Max Planck Institute for Chemistry in Mainz, Germany using a gas chromatograph (Agilent 7890B, Agilent Technologies, U.S.A) coupled with a time of flight – mass spectrometer (BenchTOF Select, MARKES International, UK) (Zannoni et al. 2020). Samples desorption was performed using a two-stage automated thermal desorber (TD100-xr, MARKES International, U.K.). The carrier gas used was helium 6.0. The sample was swept from the adsorbent tube at a temperature of 250 °C and a flow of 50 ml min^{-1} for 10 min, and was pre-concentrated onto a cold trap (materials emissions, MARKES International, U.K.) at 30 °C. The cold trap was then purged with helium for 1 min with a flow of 50 ml min^{-1} before being rapidly heated to 300 °C. The sample was removed from the cold trap with a flow of 3 ml min^{-1} and injected into the column. The separation of the sampled compounds was achieved in the first dimension using a 30 m β-DEX™ 120 column with 0.25 mm internal diameter and a film thickness of 0.25 µm. The temperature program used was as follows, 40 °C for 5 minutes then 40 °C to 150 °C at 4 °C min^{-1} and 150 °C to 200 °C at 30 °C min^{-1}. The column flow was set to 1 ml min^{-1}. Detection was achieved using a time of flight mass spectrometer (Bench TOF-Select, MARKES International, U.K.). The common ion fragment m/z 93 was extracted from the total ion count to uncover the peaks of the monoterpene. Identification was achieved using a

standard gas mixture (Apel-Riemer 2019) BVOC gas calibration standard containing all monoterpenes other than ocimene. Individual liquid standards were also used to identify the individual monoterpenes and their enantiomers. Calibration was achieved by filling sorbent cartridges with the standard gas diluted with synthetic air and placing a calibration sorbent cartridge after every 5 sample cartridges within the desorption sequence. The area of the peaks found in the calibration cartridges were averaged together and used to calibrate the peaks of the samples cartridges that were desorbed between the calibration cartridges. All monoterpenes were calibrated individually to their corresponding peaks within the standard gas, other than ocimene, which was calibrated to α-pinene. The flux of monoterpenes, *F*, was calculated with the equation:

$$F = \frac{n}{A} \times (VMR_p - VMR_e)$$

where *n* is the molar flow rate, *A* is the leaf area, VMR_p is the volume mixing ratio in the plant chamber and VMR_e is the mixing ratio in the empty chamber. When a cartridge measured from the empty cuvette was not available, the median mixing ratio of the particular compound across all empty cuvette cartridges was used as the background value.

5.2.3. Meteorological measurements

The photosynthetically active radiation (PAR), temperature and relative humidity (RH) were recorded at 15-minute intervals with sensors connected to a datalogger (PAR sensors (Apogee SQ110, Campbell Scientific, Logan, UT, USA), temperature and RH with Vaisala HMP 45c sensors (Vaisala Oyi., Vantaa, Finland). Sensors reported every 15 minutes to a centralized CR1000 datalogger (Campbell Scientific, Logan, UT, USA) with an AM16/32B multiplexer (Campbell Scientific, Logan, UT, USA). The dataloggers were connected to a centralized database with NL100 communications modules (Campbell Scientific, Logan, UT, USA) and the data is available through the Biosphere 2 website (www.biosphere2.org/data-models/rainforest-data). The PAR sensor was located outside the Biosphere 2 enclosure and the humidity and temperature sensors were located at a height of 3 m and 13 m on the north-eastern measurement tower together with the sampling inlet (**Fig. 2**). The soil moisture data were averaged over 15-minute intervals across four soil pits (**Fig. 2**) (soil moisture and temperature sensors (Truebner SMT100, Truebner Gmbh, Neustadt, Germany) and water potential sensors (TEROS 21, Meter Group, Pullman, WA, USA) in all four pits at 5 cm, 10 cm, 20 cm, 50 cm, and 100 cm depths and at the soil-concrete interface (Soil bottom)). Since the sensors are 30 mm wide and inserted vertically into the soil with the soil depth indicated at the midpoint, each depth is ± 1.5 cm.

5.2.4. Water status measurements

Individual leaves were selected for water potential measurements in accordance with the following: 1) suitable leaf dimension for leaf water potential to be accurately determined using a Scholander style pressure bomb (Scholander, 1965), 2) spatial location within the rainforest biome, and 3) compatibility with other data collection goals of the B2 WALD campaign.

Predawn water potential (Ψ_{pd}) and midday water potential (Ψ_{md}) measurements were made on 10 days throughout the experiment, with both Ψ_{pd} and Ψ_{md} measurements made during the early drought, severe drought, and rain rewet phases (25-10-19, 01-11-19, 08-11-19, 15-11-19, 24-11-19),

deep re-wet (03-12-19, 06-12-19), and rain phase (13-12-19). For *C. fairchildiana*, two additional Ψ_{pd} occurred during the pre-drought phase (25-09-19 and 01-10-19), and for *Piper* sp. one additional Ψ_{md} during the deep re-wet (01-12-19). Predawn measurements were taken starting around 5:30 in August and later around 6:30 by December, because sunrise shifted to later in the morning. Midday measurements were taken from 10:00 to 11:00; despite these times not corresponding to true midday, previous studies in the Biosphere 2 tropical rainforest biome found that plant activity decreased after 11:00, as temperature and relative humidity increased (Rascher et. al. 2004). Thus, the aim was to collect samples when water potential values were most negative, just before stomatal closure. For both predawn and midday measurements, all leaves were collected within 30 minutes from start to finish.

For *C .fairchildiana*, large branches were collected from the rainforest canopy, from which 3-5 leaves were measured from each branch. When whole branches were not collected, cut leaves were placed into ziplock bags and sealed for a couple of minutes until the measurement was made. Freshly cut leaves, or leaves from the sealed bags, were placed into the PMS Scholander type pressure bomb (PMS Instrument Company, OR, USA), and nitrogen gas was slowly added to the chamber until water appeared from the cut end of the leaf. From the same branches, and for both predawn and midday, we also collected 3 leaves for measuring relative leaf water content. Leaves were placed immediately into ziplock bags and sealed. The fresh leaves were weighed within an hour of harvest and then dried at 40 °C for 48 hours before being weighed again. Relative water content (RWC) was calculated as

$$RWC = \frac{W_{wet} - W_{dry}}{W_{wet}}$$

where W_{wet} and W_{dry} are the dry leaf weight and wet leaf weight, respectively.

5.3. Results

5.3.2. Meteorological conditions and soil moisture level

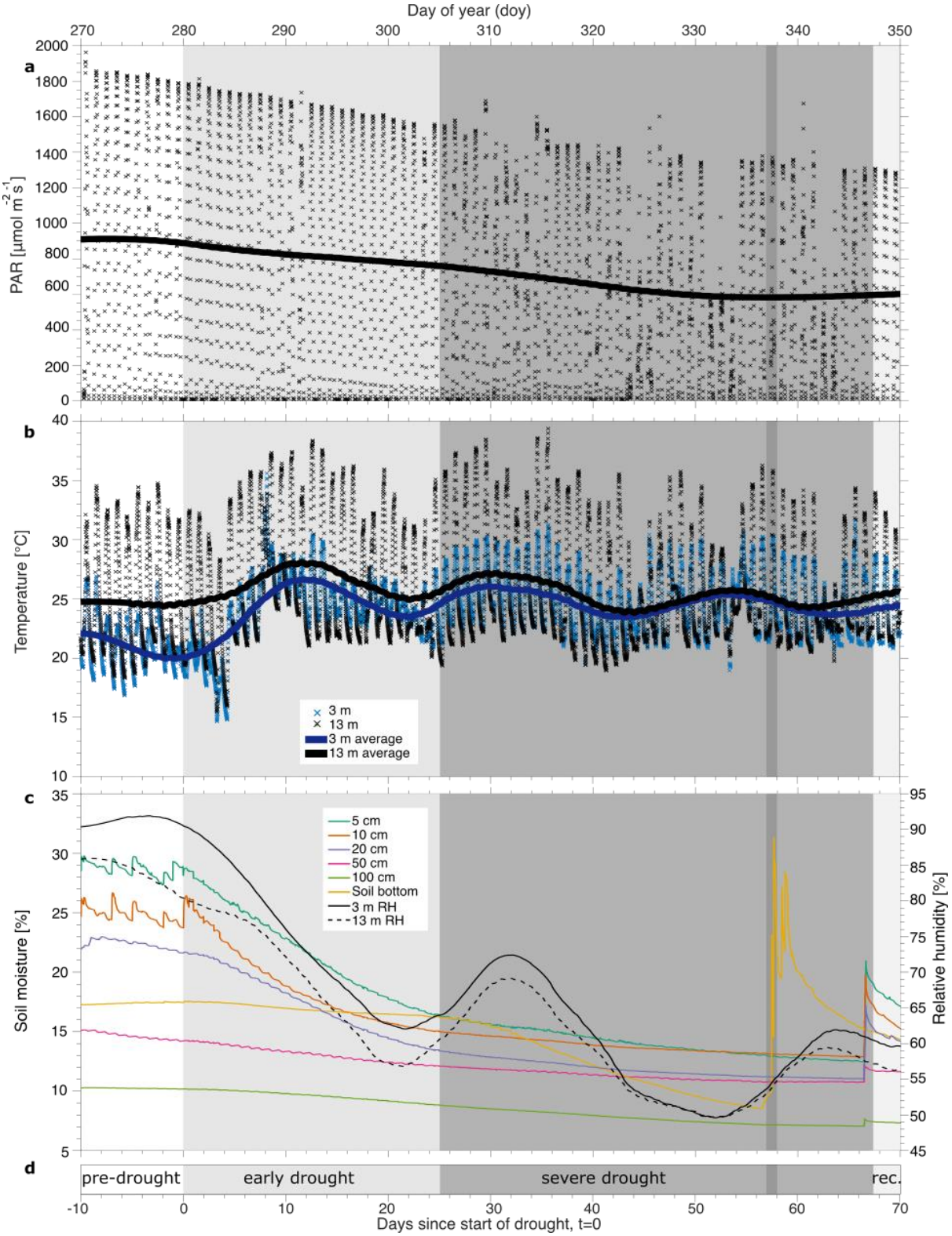

Figure 3. **a**. Smoothing mean for incident outside photosynthetically active radiation (PAR). **b**. Smoothing mean for the 3 m and 13 m temperature on the northeast measurement tower. The bulk of *Piper* sp. and *C. fairchildiana* vegetation was located near the northeast measurement tower at 3 m and 13 m heights, respectively. **c**. Soil moisture measured at 6 different depths within the soil and smoothing mean for the 3 m and 13 m relative humidity (RH). Soil bottom refers to the bottom of the subsoil. The symbols (x) indicate the measured values measured at 15 minute intervals. **d**. Drought phases.

The grey background shadings in (**a-c)** correspond to the phases in (**d**). The vertical dark grey line indicates the deep soil rewetting. rec. stands for recovery.

On average, according to the season, the photosynthetically active radiation (PAR) declined steadily throughout the entire measurement period from 909 to 602 µmol m^{-2} s^{-1} (**Fig. 3a**). In general, the temperature fluctuated at heights of 3 m and 13 m throughout the entire measurement period (**Fig. 3b**). Initially, higher temperatures were measured at 13 m than 3 m as expected; however, the average daily temperatures became more similar as the drought progressed. Daily maximum temperatures for each phase of drought are shown in **Table 1**. The minima in the average temperature corresponded with the increases in relative humidity (**Fig. 3b-c**). Declines in soil moisture were observed at all soil depths, after the start of drought (**Fig. 3c**). The soil moisture at 5 cm, 10 cm, 20 cm, 50 cm, soil bottom declined across the early drought and severe drought, by 15 %, 11 %, 10 %, 3 % and 8 %, respectively. The only depth which responded to the deep rewetting was the soil bottom, whilst all depths, except the soil bottom, responded to the rain rewetting. The average relative humidity declined following the same pattern for 3 m and 13 m, declining during the early drought over 20 days, then increasing over 12 days before declining further during the severe drought over 20 days. The relative humidity already started to increase after the deep rewet despite the shallow soil layers not increasing in moisture content, indicating that the relative humidity likely increased due to an increase in transpiration from the deep-rooted plants.

Table 1. Maximum measured temperatures in each phase of drought at 3 and 13 m on a measurement tower.

Height (m)	Maximum ambient temperature (°C)				
	Pre-drought	Early drought	Severe drought	Deep water rewet	Rain rewet
13	34.8	38.6	39.4	35.9	34
3	26.9	35.6	31.3	31.7	28.8

5.3.3. Different emission responses to long term drought

From October 2019 to December 2019, samples were intermittently collected onto sorbent cartridges from leaf cuvettes attached to 4 different *C. fairchildiana* trees and 4 different *Piper* sp. plants. The average distribution of the measured monoterpenes for 4 measured *C. fairchildiana* trees is shown in **Fig. 4a** and for 4 measured *Piper* sp. plants in **Fig. 4b**. For the *C. fairchildiana* and *Piper* sp. datasets, the monoterpene emissions detected were: (-)-α-pinene, (+)-α-pinene, (-)-β-pinene, (+)-β-pinene, (+)-limonene, β-myrcene, γ-terpinene, terpinolene, and α-terpinene. In addition, ocimene was only seen in a few *Piper* sp. chromatograms in very low amounts, therefore it was omitted from the analysis of *Piper* sp. Whereas, Ocimene was detected in almost all the *C. fairchildiana* chromatograms. Throughout the majority of the measurement period, the most abundant monoterpene that was measured from *C. fairchildiana* was ocimene (>47%) until the rain rewet phase (day of year (doy) 347 and 348) when α-pinene became the most abundant (>35%). However, for *Piper* sp., over the whole measurement period, there was not a consistently dominating monoterpene (**Fig. 4b**). Interestingly, as the drought progressed the relative amount of α-terpinene increased up to doy 315 and then started to decrease again. In addition, the emission of γ-terpinene decreased to zero after doy 294 but had resumed emission again by doy 339 coinciding with the deep rewet phase.

The total monoterpene emission patterns for both plant species were different when compared with each other through the measurement period (**Fig. 5a**). *Piper* sp. emitted almost no monoterpenes until average emissions started to increase on the 12^{th} day of drought up to an average maximum of ~30x10^{-}

^{3} nmol m^{-2} s^{-1} before steadily decreasing and plateauing ~10x10^{-3} nmol m^{-2} s^{-1}. Average total monoterpene emissions from *C. fairchildiana* initially decreased from ~40x10^{-3} nmol m^{-2} s^{-1} to almost zero before increasing to ~20x10^{-3} nmol m^{-2} s^{-1} on the 12th day of drought and then decreasing to almost zero again on the 25th day of drought. A further increase in average emissions from *C. fairchildiana* was measured when emissions increased from almost zero, reaching an average maximum of ~53x10^{-3} nmol m^{-2} s^{-1} on the 41st day of drought. Afterward, emissions then decreased to ~17x10^{-3} nmol m^{-2} s^{-1}, which was measured on 59th day of drought.

Despite the second increase in *C. fairchildiana* emissions (**Fig. 5a**), during severe drought, corresponding with water potential becoming more negative (**Fig. 5b**), a large increase in emissions was not observed for *Piper* sp. (**Fig. 5a**), even though midday water potential also became more negative for *Piper* sp. (**Fig. 5b**). The early drought increase in *C. fairchildiana* emissions was smaller than the severe drought increase; however, for *Piper* sp. the opposite was true (**Fig. 5a**). The total monoterpene emissions of *C. fairchildiana* never increased substantially beyond the emissions measured during pre-drought, whereas for *Piper* sp. the emissions increased substantially, beyond pre-drought values. The average total monoterpene emission pattern measured for the *C. fairchildiana* negatively co-varied with the predawn (Ψ_{pd}) and midday (Ψ_{md}) plant water, whereas this did not happen for *Piper* sp. emissions. (**Fig. 5a-b**). The *C. fairchildiana* leaf relative water content reached maxima at the same time as the average relative humidity, which lagged behind the maxima Ψ_{md} by 10 days, however, changes in the relative leaf water content were relatively minor (**Fig. 5b-c**).

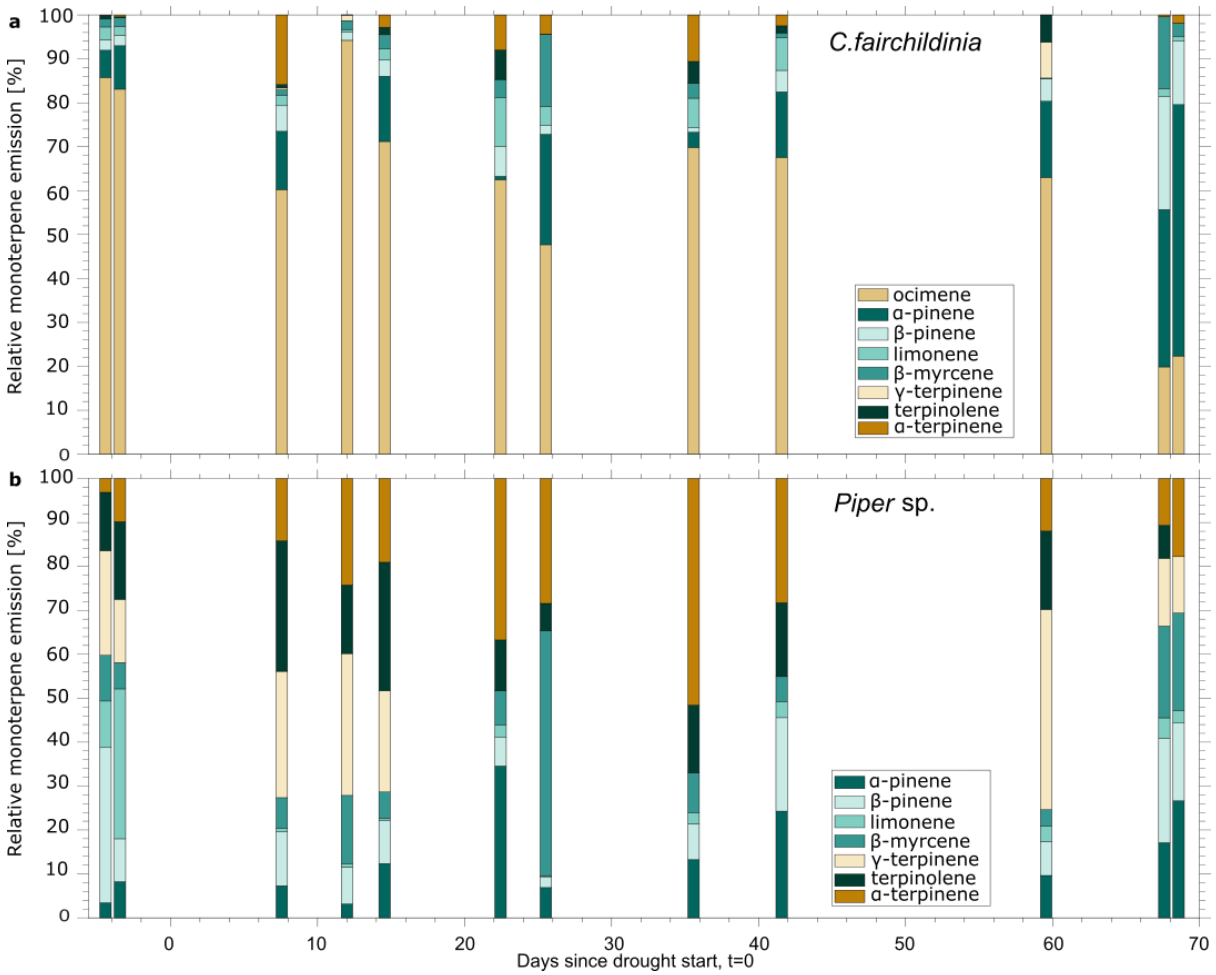

Figure 4. Average distribution of the monoterpene in the emissions calculated from the samples taken from branch cuvettes. **a**. *C. fairchildiana samples.* **b**. *Piper* sp. samples. Average values were obtained by calculating the mean percentages of monoterpenes from four branch cuvettes placed on four different trees for each species.

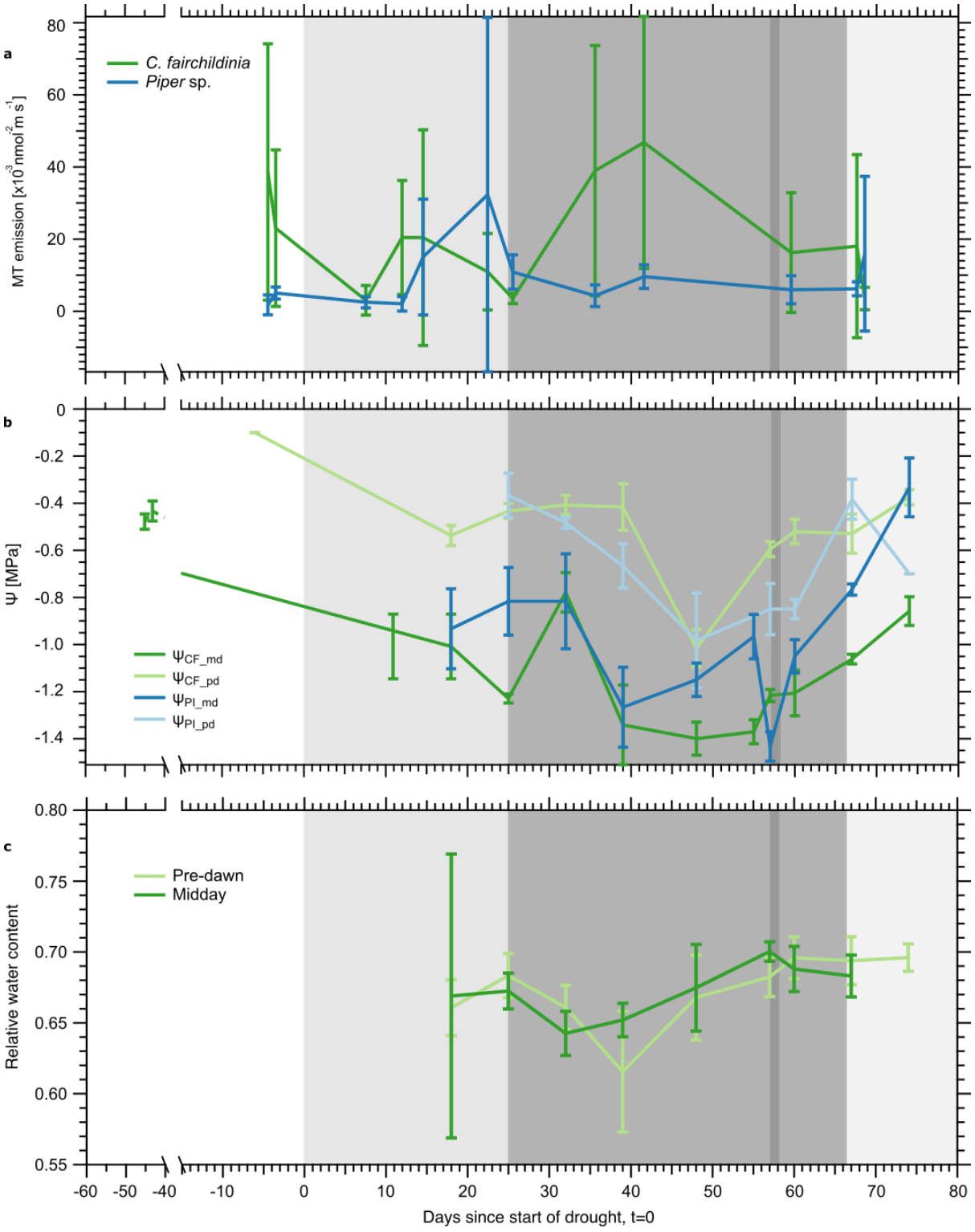

Figure 5. a. Mean total monoterpene (MT) emission rates and predawn and midday water potential for *C. fairchildiana* (CF) and *Piper* sp. (PI) leaves (n=4). **b**. Mean predawn Ψ_{pd} and midday Ψ_{md} water potential for *C. fairchildiana* (n=12) and *Piper* sp. leaves (n=4). **c**. Pre-dawn and midday relative water content (RWC) for the leaves of *C. fairchildiana*. All errors bars represent 1σ. Background shading is the same as explained in **Fig. 3**.

5.3.4. Species dependent change in enantiomeric composition

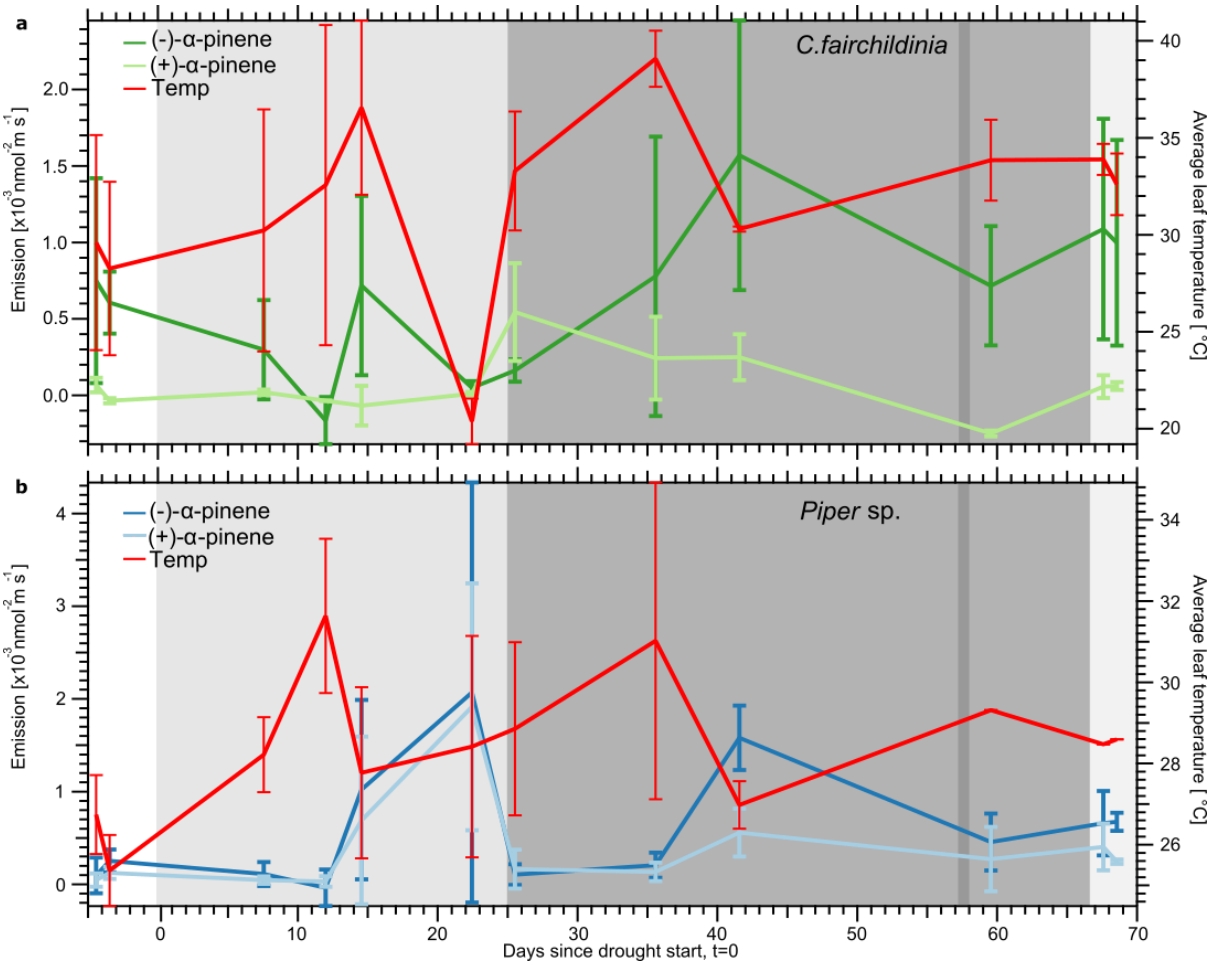

Figure 6. Average (-)-α-pinene and (+)-α-pinene emission rates, and average leaf temperature (Temp) for *C. fairchildiana* (**a**) *Piper* sp. (**b).** All error bars represent 1σ. Background shading is the same as explained in **Fig. 3**.

Throughout the measurement period, the average *C. fairchildiana* emission patterns of (-)-α-pinene and (+)-α-pinene behaved differently from each other (**Fig. 6a**). The average (-)-α-pinene emissions from *C. fairchildiana* initially decreased steadily from ~7x10^{-4} nmol m^{-2} s^{-1} to 0 nmol m^{-2} s^{-1} before increasing back to ~7x10^{-4} nmol m^{-2} s^{-1} on the 15th day of drought. Another increase in (-)-α-pinene emissions from *C. fairchildiana* was measured when emissions reached ~1.6x10^{-3} nmol m^{-2} s^{-1} on the 41st day of drought before decreasing to ~8x10^{-4} nmol m^{-2} s^{-1} and then increasing slightly with the rain rewet to ~1x10^{-3} nmol m^{-2} s^{-1}. Unexpectedly, the (+)-α-pinene emissions behaved differently to the (-)-α-pinene emissions. On average, *C. fairchildiana* emitted almost no amount of (+)-α-pinene from until the 25th day of drought when ~5x10^{-4} nmol m^{-2} s^{-1} of (+)-α-pinene was measured, which steadily decreased back down to zero thereafter. (-)-α-pinene dominated the emissions of α-pinene for the majority of the measurement period. However, after the 25th day of drought, (+)-α-pinene temporarily became the dominant enantiomer before a further increase in the emission of (-)-α-pinene beyond the emission of (+)-α-pinene in the severe drought phase. Both (-)-α-pinene and (+)-α-pinene emissions increased beyond the pre-drought emission rates, despite the total monoterpene emissions not increasing above pre-drought values for *C. fairchildiana*.

The emissions for (-)-α-pinene and (+)-α-pinene from *Piper* sp. showed similar patterns to each other (**Fig. 6b**), however (-)-α-Pinene was the dominant enantiomer emitted throughout the majority of the

measurement period. In contrast to the emissions from *C. fairchildiana*, the *Piper* sp. emissions of both α-pinene enantiomers increased more strongly during the early drought phase, instead of during the severe drought phase. Initially, *Piper* sp. on average emitted ~0 nmol m^{-2} s^{-1} of both α-pinene enantiomers, which then increased to a maximum measured average emission value of ~$2x10^{-3}$ nmol m^{-2} s^{-1}, emissions then decreased back down to 0 nmol m^{-2} s^{-1} before increasing to ~$1.5x10^{-3}$ nmol m^{-2} s^{-1} and ~$0.5x10^{-3}$ nmol m^{-2} s^{-1} for (-)-α-pinene and (+)-α-pinene, respectively. In agreement with *C. fairchildiana*, the emissions of both α-pinene enantiomers increased during the rain rewet phase, however, the increase during rain rewet was smaller for the *Piper* sp. than the *C. fairchildiana*. Furthermore, emissions of both α-pinene enantiomers negatively co-varied with leaf temperature throughout drought (**Fig. 6b**).

5.3.5. Ocimene emission as an indication of drought stress for *Clitoria fairchildiana* and chiral linalool emissions

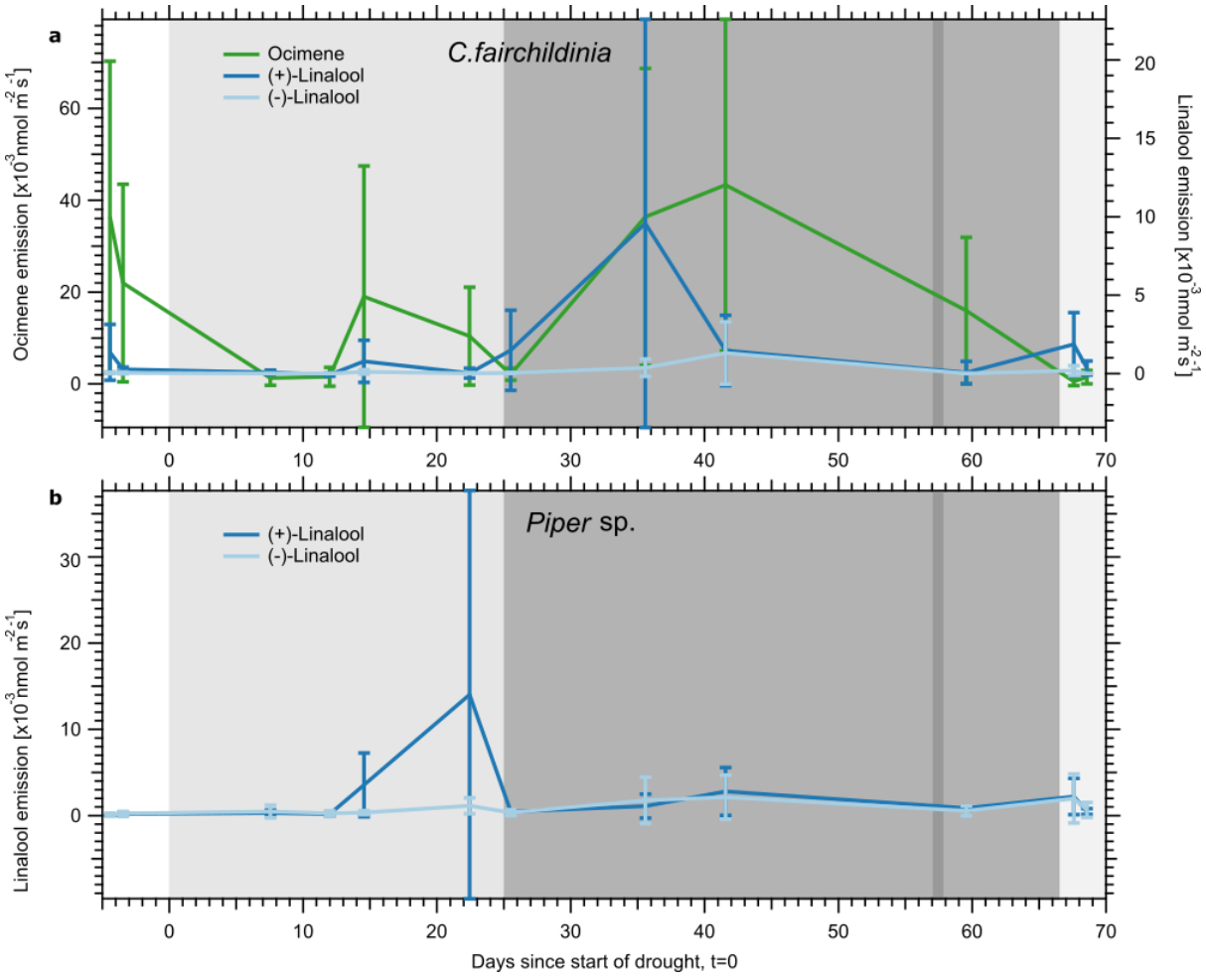

Figure 7. **a**. Average ocimene, (-)-linalool and (+)-linalool emission rates from *C. fairchildiana*. **b**. Average (-)-linalool and (+)-linalool emissions rates from *Piper* sp. All error bars represent 1σ. Background shading is the same as explained in **Fig. 3**.

On average, ocimene was the most dominant monoterpene emission measured from *C. fairchildiana* (**Fig. 4a**). However, the average emission rate through the drought did not increase substantially above

the pre-drought emission rate (**Fig. 7a**). For both *C. fairchildiana* and *Piper* sp. (+)-linalool dominated the linalool emissions over (-)-linalool (**Fig. 7a-b**), which was unexpected since (-)-α-pinene largely dominated over (+)-α-pinene (**Fig. 6a-b**). Further, the increase in *Piper* sp. (-)-linalool emissions (day 22) preceded the *C. fairchildiana* (-)-linalool emission (day 35). No significant increases were observed for (+)-linalool from either *C. fairchildiana* or *Piper* sp. The (-)-linalool emission from *C. fairchildiana* did not increase again until the rain rewet (day 67) but did not increase again for *Piper* sp. as the emission stayed low. For *C. fairchildiana*, it is likely that it reached a peak between day 25 and 35.

5.4. Discussion

In agreement with the *C. fairchildiana* measurements shown here, it has previously been reported that the monoterpene emissions from some individual plant species are dominated by ocimene (Jardine et al. 2017, Farré-Armengol et al. 2017). Although other studies have reported that the atmosphere in boreal and tropical rainforests is dominated by α-pinene or limonene (Zannoni et al. 2020, Yáñez-Serrano et al. 2018, Williams et al. 2007, Jardine et al. 2015). This discrepancy is likely because ocimene is more reactive than α-pinene and limonene (Atkinson and Arey 2003); thus, oxidative radicals in the amazon rainforest are removed by ocimene faster than α-pinene and limonene resulting in a lower atmospheric abundance of ocimene compared to these other compounds. Furthermore, it has previously been reported that ocimene is a biomarker for heat stress (Jardine et al. 2017). This study suggests that ocimene may also be a biomarker for drought stress for *C. fairchildiana* but not for *Piper* sp. Ocimene has been shown to be emitted *de novo* to the atmosphere of the B2-TRF (chapter 3), which means that it is strongly coupled with photosynthesis. Despite PAR, soil moisture and, therefore, photosynthesis steadily decreasing throughout the drought, ocimene emission did not follow the same trend. This may signal that there was an upregulation of *de novo* ocimene emission at specific times due to drought by using carbon stored elsewhere in the plant or ocimene was also stored in non-specific storage pools in the plant leaf. The observed increases in ocimene emission, and total monoterpene emissions generally, are of benefit to the plant, as drought is known to increase the presence of harmful reactive oxygen species, which ocimene can quickly react with which could prevent damage to internal plant tissue (Lee et al. 2012, Cruz de Carvalho 2008).

The different trends in monoterpene emissions from *C. fairchildiana* and *Piper* sp. show how different species of plants have different strategies for coping with drought (**Fig. 5a**). This experiment shows that it is not possible to simply conclude whether drought had a positive, negative, or zero effect on monoterpene emissions from both plant species, as previous laboratory drought experiments have concluded about other plant species. If the measurements had only been conducted between 11 and 14 days of drought (Radwan, Kleinwächter, and Selmar 2017, Ormeño et al. 2007), then it could be concluded that drought had a positive effect on the total monoterpene emission from *Piper* sp. but overall had a negative effect on the total monoterpene emission from the *C. fairchildiana*. When in truth, the monoterpene emissions from both plant species was dependent on whether they could access moisture in the soil at deeper depths. *C. fairchildiana* is a much bigger species of plant, a woody species that typically grow up 12 m tall, whereas the *Piper* sp. plants in this experiment were herbaceous plants with thin stems standing at approximately 3 m tall (Lorenzi and Flora 2002). Therefore, due to these differences in physiology *C. fairchildiana* has much deeper roots than *Piper* sp., which meant that it could access water from deeper depths than the *Piper* sp. This could explain why the emissions of monoterpenes from the *C. fairchildiana* were greater during the severe drought than the early drought, whereas, the opposite was true for *Piper* sp. since *Piper* sp. did not have access

to moisture at deep soil depths during the severe drought. Furthermore, the hypothesis that deeper roots (and therefore access to deeper levels of soil moisture) would mean that emissions from *C. fairchildiana* would be less affected by drought than *Piper* sp. was found to be true. Since monoterpene emissions from *C. fairchildiana* during early drought and severe drought only increased to within pre-drought emission values, whereas monoterpene emissions from *Piper* sp. increased by a factor ~10 above pre-drought emission values.

The emission of (-)-α-pinene and (+)-α-pinene from *Piper* sp. corresponded similarly with each other, suggesting that the two emissions were both likely to be from the same emission source i.e. *de novo* or storage emission. In contrast, the emission of (-)-α-pinene and (+)-α-pinene from the *C. fairchildiana* did not correspond with each other, which could be caused by different emission sources, one of them emitted *de novo* and one of them emitted from storage pools within the leaf. In chapter 4, it was shown that (+)-α-pinene in the atmosphere of the Biosphere 2 tropical rainforest did not become enriched in ^{13}C curing a $^{13}CO_2$ labelling experiment, providing evidence that the majority of the (+)-α-pinene in the atmosphere was emitted from storage pools. Measurements of monoterpenes in the atmosphere confirmed the peak abundance of (-)-α-pinene to shift from the morning to the afternoon, between pre-drought and severe drought. In doing so, (-)-α-pinene, which was primarily a *de novo* emission due to $^{13}CO_2$ enrichment, became more decoupled from photosynthesis and more aligned with peak temperature and other storage pool monoterpenes. This shift was explained as storage pools breaking down in severe drought and releasing more monoterpenes into the atmosphere, even those monoterpenes that were usually emitted *de novo*. If (+)-α-pinene is more abundant than (-)-α-pinene within the storage pools of C*. fairchildiana*, then the period when (+)-α-pinene becomes the most dominant enantiomer could be because the internal storage pools are breaking down or emptying, thereby releasing a greater amount of (+)-α-pinene than (-)-α-pinene out of the leaf and into the atmosphere. It is also important to consider that the measurements presented in this study were all taken around midday. Furthermore, it was shown in chapter 4 that light intensity (PAR) occurs in the morning around 11:00 whereas ambient temperature peaks in the afternoon around 14:00 and therefore the abundance of monoterpenes and their respective enantiomers could peak in the morning or afternoon. This difference in time was explained as being a characteristic of *de novo* emission or storage pool emission, respectively. Even though these measurements of plant emissions showed that (-)-α-pinene was more dominant than (+)-α-pinene, if measurements had instead been taken in the afternoon, it is likely that (-)-α-pinene would become less dominant and (+)-α-pinene would become more dominant with increasing temperature.

Linalool is produced within a leaf when a terpene synthase enzyme reacts with a substrate, usually geranyl or neryl diphosphate, yielding a carbocation intermediate, which can be further rearranged. The carbocation intermediate can become a linear or cyclic hydrocarbon by losing a proton or it can react with a water molecule and subsequently lose a proton (or react with a hydroxyl radical) to form a monoterpenol such as linalool (Degenhardt, Köllner, and Gershenzon 2009b). Since (+)-linalool peaks around the same time as the midday relative water content for *C. fairchildiana* between day 30 and 40 of drought, it could be that there is an increase in (+)-linalool emission due to the increased abundance of water molecules at that time. However, the relative water content peaks again at around day 60 of drought but (+)-linalool emissions remain low, which could be caused by a lack of substrate availability and is further corroborated by low monoterpene emissions that likely rely on the same substrate availability as linalool. A possible problem with this explanation is that the changes in relative water content are relatively small, varying by less than 10%, which is probably not large enough to vary the (+)-linalool emissions by such a large amount. Therefore, a second explanation could be that the emission of (+)-linalool signals a period when there is a high concentration of hydroxyl radicals (HO•), resulting from drought stress (Lee et al. 2012, Cruz de Carvalho 2008). Despite

the (-)-enantiomers dominating over the (+)-enantiomers for monoterpenes, the opposite was true for linalool. A reason for this could be that the synthesis of linalool relies upon the same enzymes and substrates as the synthesis of (+)-α-pinene and (+)-limonene and is a storage emission, as was shown for (+)-α-pinene and (+)-limonene by atmospheric labelling with $^{13}CO_2$ in chapter 4. Indeed, for *C. fairchildiana*, (+)-linalool emissions (**Fig. 7a**) start to increase when (+)-α-pinene emissions start to decrease (**Fig. 6a**), which suggests that drought-induced presence of hydroxyl radicals could be causing a shift from the production of (+)-α-pinene to the production of (+)-linalool. However, for *Piper* sp., (+)-linalool emissions (**Fig. 7b**) increase coincidentally with (+)-α-pinene (**Fig. 6b**), which suggests two likely possibilities: that the production of (+)-linalool and (+)-α-pinene does not rely on the same substrates and enzymes, or within *Piper* sp. there exists large storage pools of both compounds which have already been synthesized at an earlier date. To confirm which explanation is true, ^{13}C labelling experiments should be performed on *C. fairchildiana* and *Piper* sp., which resolve the enantiomers of the linalool emissions, to reveal which of the linalool emissions are emitted *de novo* or from storage pools. Measurements should also be taken at much shorter time intervals, which can reveal how the emissions of linalool enantiomers change throughout a daily cycle.

Since *Piper* sp. exhibited a strong short term increase in monoterpene emissions during early drought and *C. fairchildiana* exhibited strong long term increase in monoterpene emissions, if the monoterpene emissions from *Piper* sp. and *C. fairchildiana*, were to be combined the resulting pattern would resemble the same pattern for the total monoterpene abundance in the Biosphere 2 tropical rainforest atmosphere. This shows that both of these plant species combined likely had a large impact on the concentration of monoterpenes that were measured in the atmosphere. This is despite ocimene not being a major constituent of the atmospheric air, yet being a major emission from *C. fairchildiana*. The high ocimene emission from *C. fairchildiana* was unexpected since ocimene had been reported to be in very low abundance in the atmosphere and the known lack of air chemistry within the rainforest enclosure that could remove ocimene from the atmosphere. A possible explanation for the lack of atmospheric ocimene could be that there is a high abundance of ambient reactive oxygen species present in the Biosphere 2 tropical rainforest as a result of drought or otherwise which ocimene is rapidly reacting with. Additionally, monoterpenes are known to undergo biodegradation by soil microbes (Misra et al. 1996), thus another possible explanation might be that microbes preferentially remove ocimene from the atmosphere over other monoterpenes. However, since there is a large variety of plant species within the rainforest enclosure from which no emissions samples were taken, it could also be that ocimene is not emitted from the majority of the vegetation and emissions from *C. fairchildiana* actually represent a small contribution to the total atmospheric monoterpene concentration.

5.5. Conclusion

Monoterpene and linalool emissions from an understory plant species, *Piper* sp., and a canopy species, *C. fairchidiana*, were measured on selected days during a 9.5 week extended drought and rewetting experiment in an indoor managed tropical rainforest mesocosm to study the effect of drought on chiral VOC emissions. These results suggest a species-,monoterpene- and enantiomer-specific response to an extended severe drought and rewetting. *C. fairchildiana* monoterpene emissions increased most during severe drought, but *Piper* sp. monoterpene emissions increased most during early drought. Increases in monoterpene emissions from both plant species corresponded with the plant water potential for each species becoming more negative during early drought, however, this

was decreasing plant water potential only corresponded with *C. fairchildiana* during severe drought. It is hoped that the responses in emissions presented here can be further unravelled by comparing the emissions with stomatal conductance. These results explain how drought affects terpenoid emissions from two different tropical plant species, information which is not so available since drought experiments are more commonly performed on boreal and Mediterranean plant species. Information such as this is vital for the formulation of models, which can accurately predict how drought affects VOC emissions globally.

Chapter 6: Chiral analysis of a mechanically wounded pine tree using GC-ToF-MS and cavity-enhanced chiral polarimetry

This chapter has been adapted from a manuscript, which has been published in ChemRxiv and has been submitted for peer review. This chapter is not the original manuscript. I describe in my own words my personal contribution to a collaboration, which led to the original manuscript. Figures 2, 3 and 4 have been taken from the original manuscript with permission from the first author. I am the second author of the original manuscript. Only the CCP data displayed in figure 3 d-e was not collected by myself and was complementary to my work.

Original manuscript to which I refer in this chapter:

L. Bougas, J. Byron, D. Budker, J. Williams: Absolute optical chiral analysis using cavity-enhanced polarimetry. ChemRxiv. Cambridge: Cambridge Open Engage; 2021; this content is a preprint and has not been peer-reviewed.

Abstract. To track how mechanical wounding affects the emission profile of chiral volatile organic compounds (VOCs) of a pine tree, the abundance of chiral VOCs in an open pine tree enclosure was measured before and after the breaking of one of the pine tree branches. Measurements were performed off-line with sorbent cartridges in combination with gas chromatography-time of flight-mass spectrometry (GC-ToF-MS), and on-line with a brand new method known as cavity-enhanced polarimetry (CCP). The total concentration of measured VOCs increased in concertation by ~ 1 order of magnitude due to wounding, but the composition of emissions altered with an increase in the proportion of (-)-enantiomers in the short and long term resulting in a more negative chiral signal. The differences in the post-wounding dynamics between total concentration and chirality reveal how chiral measurements can be used to monitor the health status of vegetation. These measurements show how CCP can be used as a more convenient and efficient alternative for measuring chiral VOCs than GC-ToF-MS. Furthermore, a CCP was connected to a GC for the detection and measurement of chiral VOCs, for the first time. With this new technique, a chromatogram was obtained with separated peaks for (+)-α-pinene, camphene, (-)-α-phellandrene, and (+)-limonene. Furthermore, the polarimetric signal allows for the identification of two camphene enantiomers co-eluted from the GC column. The obtained chromatogram is shown in this chapter.

6.1. Introduction

Biogenic sources emit an estimated 760 Tg (C) of VOC every year into the Earth's atmosphere with the majority of emissions originating from terrestrial vegetation (Sindelarova et al. 2014). Once in the atmosphere biogenic VOCs (BVOCs) can undergo successive oxidation processes to form secondary organic aerosols, which alter the Earth's radiative budget (Zhang et al. 2018). BVOCs are known to be emitted from plants for three reasons: for reproduction, as products of processes related to plant growth, and as a defence mechanism (Peñuelas and Staudt 2010). Monoterpenes are a group of compounds ($C_{10}H_{16}$) that are among the most abundant BVOCs in the atmosphere (~11%) and are known to be emitted from vegetation to attract pollinators and as defence against biotic (e.g. pests and herbivores) and abiotic stress (light and temperature) (Loreto et al. 2014, Sindelarova et al. 2014, Holopainen and Gershenzon 2010). Many monoterpenes are chiral which means they exist in two mirror-image forms, also known as enantiomers, which can be found as trace gases in the atmosphere at mixing ratios at the sub-ppb level (Williams 2004, Zannoni et al. 2020).

Measuring the in situ emissions of chiral VOCs from plants and other biological organisms is possible by employing instrumentation, which can analyse the absolute chiral emissions in real-time. However, chirality is commonly ignored by many studies that measure and model VOCs since the sources of enantiomers are assumed to respond similarly to environmental stress based on the identical physical and chemical properties of enantiomers (e.g. boiling point, reaction rates with oxidative species, exact mass) (Sindelarova et al. 2014). Similarly, many studies which measure the BVOC emissions from individual plants tend to ignore enantiomers, despite chiral chemodiversity being critically important for plant-insect (Renwick, Hughes, and Krull 1976, Norin 1996, He et al. 2019) and plant-plant communication (Runyon, Mescher, and De Moraes 2006, Baldwin et al. 2006, Heil and Karban 2010). Recent studies have revealed surprising differences in enantiomeric ratios measured in the atmosphere at the local and regional scales. Studies sampling the emissions of plants from regions local to each other (i.e. within the same homogenous forest) identified compartment enantiospecific emissions in coniferous trees (Pureswaran, Gries, and Borden 2004, Sjödin et al. 2000, Staudt et al. 2019). Additionally, enantiospecific compositional changes of monoterpenes over the Amazon forest were observed to be dependent on altitude, time and season (Zannoni et al. 2020). Moreover, diurnal enantiospecific enhancements in BVOC emissions were observed in boreal forests (Song et al. 2011, Yassaa et al. 2012). A study investigating regional differences in trace gases in the atmosphere over a South American tropical rainforest and within a boreal forest revealed there to be a greater abundance of (-)-α-pinene than (+)-α-pinene over the tropical rainforest; but a greater abundance (+)-α-pinene then (-)-α-pinene within the boreal forest (Williams et al. 2007). These studies suggest that the current understanding of the emissions of enantiomers is not sufficient and more investigations need to be performed which separate enantiomers in order to gain further knowledge on how emissions are controlled and modelled (Sindelarova et al. 2014, Glasius and Goldstein 2016). Separately measuring enantiomers is also important considering that microbial degradation and plant metabolism are expected to be enantioselective, thereby affecting the abundance of enantiomers in the atmosphere (Fäldt et al. 2006) (Dudareva et al. 2006).

In this study, in situ measurements are presented which show the abundance of chiral monoterpenes emitted by a plant subjected to mechanical wounding. This study is the first to thoroughly investigate the mechanical stress response of chiral monoterpene emissions and helps explain chiral composition changes of monoterpenes in different global regions (Eerdekens et al. 2009, Yassaa and Williams 2005, Zannoni et al. 2020). The plant chosen for this experiment was, a *Pinus heldreichii*, which is a typical boreal plant species (**Fig. 1a**). The chiral dynamics of its branch emissions were measured before and

after mechanical wounding, i.e., a branch was cut and completely removed from the plant. To measure the abundance of emitted chiral monoterpenes offline chiral gas chromatography – time of flight – mass spectrometry (GC-ToF-MS) was used and for comparison, a brand new technique known as cavity-enhanced chiral polarimetry (CCP) was also used (**Fig. 1b**)

6.2. Methods and materials

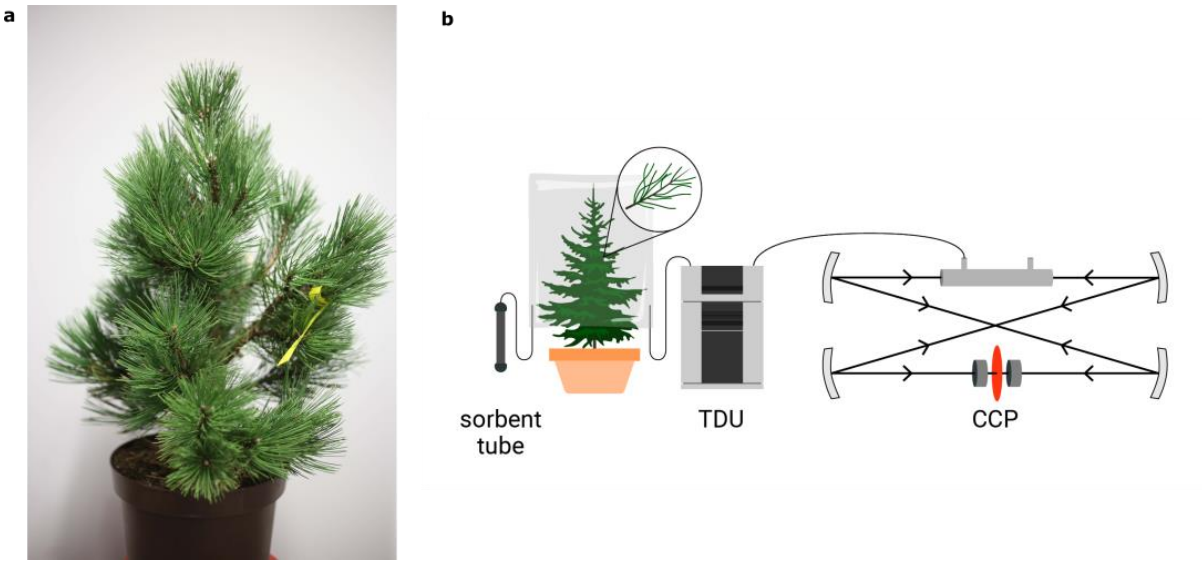

Figure 1. **a**. Photo of the pine tree (*Pinus heldreichii*) that was used for this experiment (photo L. Bougas). **b**. Schematic representation of the experiment. The air samples were collected on sorbent tubes and also collected using an online sampling and thermal desorption unit (TDU). Samples collected by the TDU were then sent to the cavity-enhanced polarimeter (CCP).

The 80 cm tall *Pinus heldreichii* plant was purchased from a local greenhouse (Blumenhaus Smedla, Mainz, Germany) (**Fig. 1a**). The plant's upper branches were enclosed in a 25 L Tedlar® sampling bag (ANALYT-MTC GmbH, Germany) that was secured around the tree stem to create an open-bottom sampling chamber (**Fig. 1b**). Leaving the bottom of the sampling bag open prevented the plant from suffocating whilst sampling by allowing air to move freely between the interior and exterior of the enclosed space. To avoid signal contamination from the soil compartment the sampling volume was located at a significant distance from the plant's soil (>10 cm). The plant chamber temperature was controlled and stabilised using a heating line that was wrapped around the sampling bag chamber (**Fig. 2b**)). Heat-induced damage to the branches and plant needles was prevented by ensuring that the heating line was not in contact with any part of the plant.

Air samples from the plant chamber were collected onto sorbent cartridges using a GilAir Plus Personal Air Sampling Pump (Sensidyne®, USA). Samples were drawn through a ¼-inch Teflon sampling line that was placed inside the sampling chamber, using a flow of 200 ml min^{-1}. The sorbent cartridges are made from inert coated stainless steel (SilcoNert 2000 (SilcoTek™, Germany)). The sorbent consists of 150 mg of Tenax® TA followed by 150 mg of Carbograph™ 5 TD (560 m^2 g^{-1}). The size of the Carbograph™ particles is in the range of 20- 40 mesh. The Carbograph™ 5 was supplied by L.A.R.A s.r.l. (Rome, Italy) and the Tenax® by Buchem BV (Apeldoorn, The Netherlands). Desorption of the cartridges was achieved using a TD100-xr automated thermal desorption unit (Markes International Ltd, U.K.). Four samples were collected before the branch was cut for approximately 10 mins each. Following the mechanical wounding of the plant, two or three consecutive samples were collected approximately every hour for 11 hours and two additional

samples were collected 24 hours after mechanical wounding for approximately 10 minutes each. For the resin data, two samples were directly sampled from the site of the exposed wound for approximately 5 minutes.

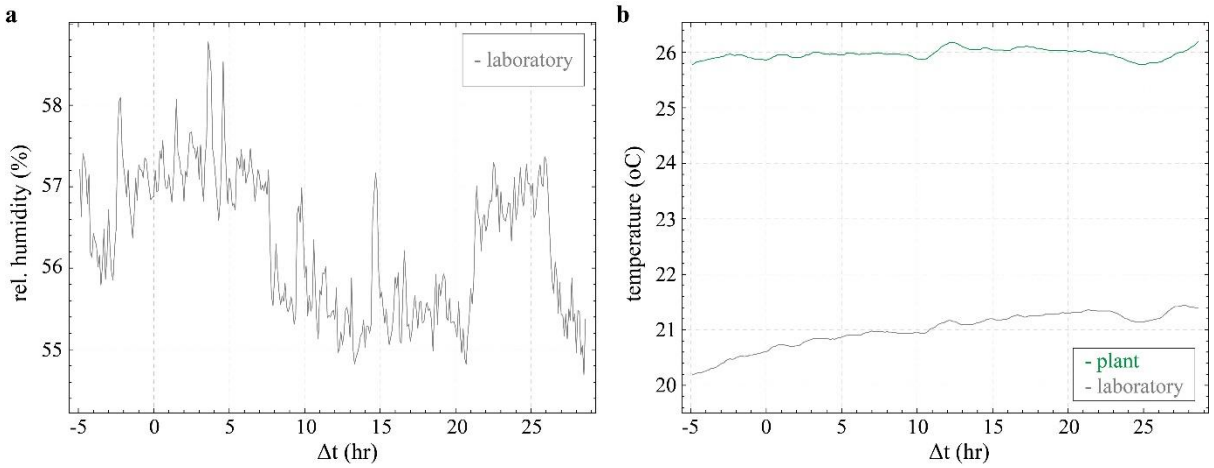

Figure 2. **a**. Relative humidity measurements of the laboratory's environment. **b**. Temperature measurements within and outside (i.e. laboratory temperature) the plant enclosure.

Collected samples were analysed using offline GC-ToF-MS. The cartridges are first dry-purged with 50 ml min^{-1} of helium 6.0 carrier gas for 5 minutes to remove water before being desorbed with a flow 50 ml min^{-1} at 250 °C for 10 minutes. After cartridge desorption, the sample is transferred to the cold focusing trap (Material emissions cold trap, Markes International, U.K.) at 30 °C. The trap is purged with helium 6.0 carrier gas at a flow of 50 ml min^{-1} for 1 minute and is then subsequently desorbed at 250 °C for 3 minutes. Specifically for the measurements of the pine plant emissions, cartridges that are sampled before the pine tree branch was broken are desorbed with a split ratio of 221:1, whereas cartridges that are sampled after the branch breaking were desorbed with a split ratio of 1005:1. The sample matrix was separated and detected using a GC-ToF-MS (GC 7890B, Agilent Technologies, U.S.A) (BenchToF-select, Markes International Ltd, U.K.). The separation of chiral compounds is achieved using a 30 m β-DEX™ 120 column (Sigma-Aldrich GmbH, Germany) with 0.25 mm internal diameter and a 0.25 μm film thickness. The column flow is chosen to be 1 ml min^{-1} and the temperature program was: 40 °C for 5 minutes then 40 °C to 150 °C at 4 °C min^{-1} until 220°C and then held again for 5 minutes. Identification of the target compounds was achieved by comparing the obtained mass spectra to the NIST database library and by spiking clean cartridges with the headspace from the relevant liquid standard. Each target compound was calibrated separately at each split ratio using a gas standard mixture (Apel Riemer Environmental Inc., 2019) and liquid standards of chiral molecules. The continuous online sampling was performed using a thermal desorption unit (TDU; TT24-7 x-r, Markes International). Approximately 1 l of ambient air from the chamber was sampled through the bag's valve. The desorbed sample was transferred through PEEK tubing (inner diameter 0.5 mm, Supelco Inc.) to the intracavity gas cell using helium 6.0 carrier gas for the CCP-based chirality measurements.

To fit the observed time-dependent behaviour of the observed concentrations of the most dominant VOCs (pre- and post-wounding), a non-linear, least-squares minimisation method was used, which was extracted from the GC-MS analysis, using the following model function:

$$C_i(t) = \frac{A}{2} \times \left(exp\left[\frac{1}{2} \cdot \left(\frac{\sigma}{\tau} \right)^2 - \frac{t - t_0}{\tau} \right] + c \right) \times erfc\left[\frac{1}{\sqrt{2}} \left(\frac{\sigma}{\tau} - \frac{t - t_0}{\sigma} \right) \right]$$

where C_i is the concentration of the *i*th chiral VOC (i=[1,7]) and t is the time (independent) variable. This model results from the convolution of a mono-exponential decaying function (characteristic decay constant τ) starting at $t = t_0$, $H(t-t_0) \times A\, exp\left(-\frac{t-t_0}{\tau}\right)$ ($H(t-t_0)$ is the Heaviside step function), with a normalized Gaussian function of standard deviation σ, which accounts for the sampling time. In addition, $erfc$ is the complementary error function, A is a proportionality constant and $c$an offset parameter accounting for the observed plateau.

The specific optical rotation $[\alpha]^{21^\circ}_{421\,nm}$ value (**Table 1**) for each of the dominant chiral monoterpenes observed in the plant emissions was used to calculate an effective expected specificoptical rotation signal from the GC-MS analysis using the following equation:

$$\varphi_{GCMS}(t)[\mathrm{deg}(gr/ml)^{-1}dm^{-1}] = \frac{1}{\sum_i C_i(t)} \sum_i [\alpha]_i \cdot l \cdot C_i(t)$$

where l is the length of the chiral medium. The results for $C_{total}(t) = \sum_i C_i(t)$ and $\varphi_{GCMS}(t)$ are presented in **Fig. 3d** and **Fig. 3e**, respectively. These results are in agreement with the CCP-based online chiroptical measurements.

Table 1. Chemical properties of chiral volatile organic compounds relevant to this work.

Compound name	Formula	Molar mass [gr/mol]	Boiling point [°C]	Vapour pressure @ 21°C [mbar]	$[\alpha]^{21^\circ}_{421nm}$ [deg. (gr/ml)$^{-1}$ dm^{-1}]
(+)-α-pinene	$C_{10}H_{16}$	136.24	156	4	123.2 ± 1.3
(+)-camphene			159	3	53.9 ± 1.2
(-)-β-pinene			166	3	16.2 ± 2.2
(R)-(+)-limonene			177	0.8-1.3	184.6 ± 1.8

6.3. Results

After the branch was cut, a sharp factor of ~ 10 increase in the concentration of the plant emissions was observed that started to stabilise at concentrations approaching pre-wounding values after a characteristic time of ~ 4 hours, in agreement with similar observations in the literature (**Fig. 3a-d)** (Niinemets et al. 2011). Mechanical wounding caused the composition of total monoterpene emissions to be more enriched in (-)-enantiomers as (-)-α-pinene became more dominant over (+)-α-pinene, and (-)-limonene further dominated the total monoterpene signal compared with the pre-wounding signal (**Fig. 3a-b**). In addition, before wounding (-)-β-pinene was more abundant than both camphene enantiomers, but upon wounding, both camphene enantiomers increased to concentrations greater than that of (-)-β-pinene which lasted for Δt ≈ 3 hours and 10 hours for (-)-camphene and (+)-camphene respectively (**Fig. 3c**). The chiroptical OR signal, φ, became increasingly negative to reach a maximal negative value at Δt ≈ 6 hours, prior to a long-term stabilization at a value of φ that was more negative than the one before wounding, close to value of φ for the independently measured resin (**Fig. 3e**).

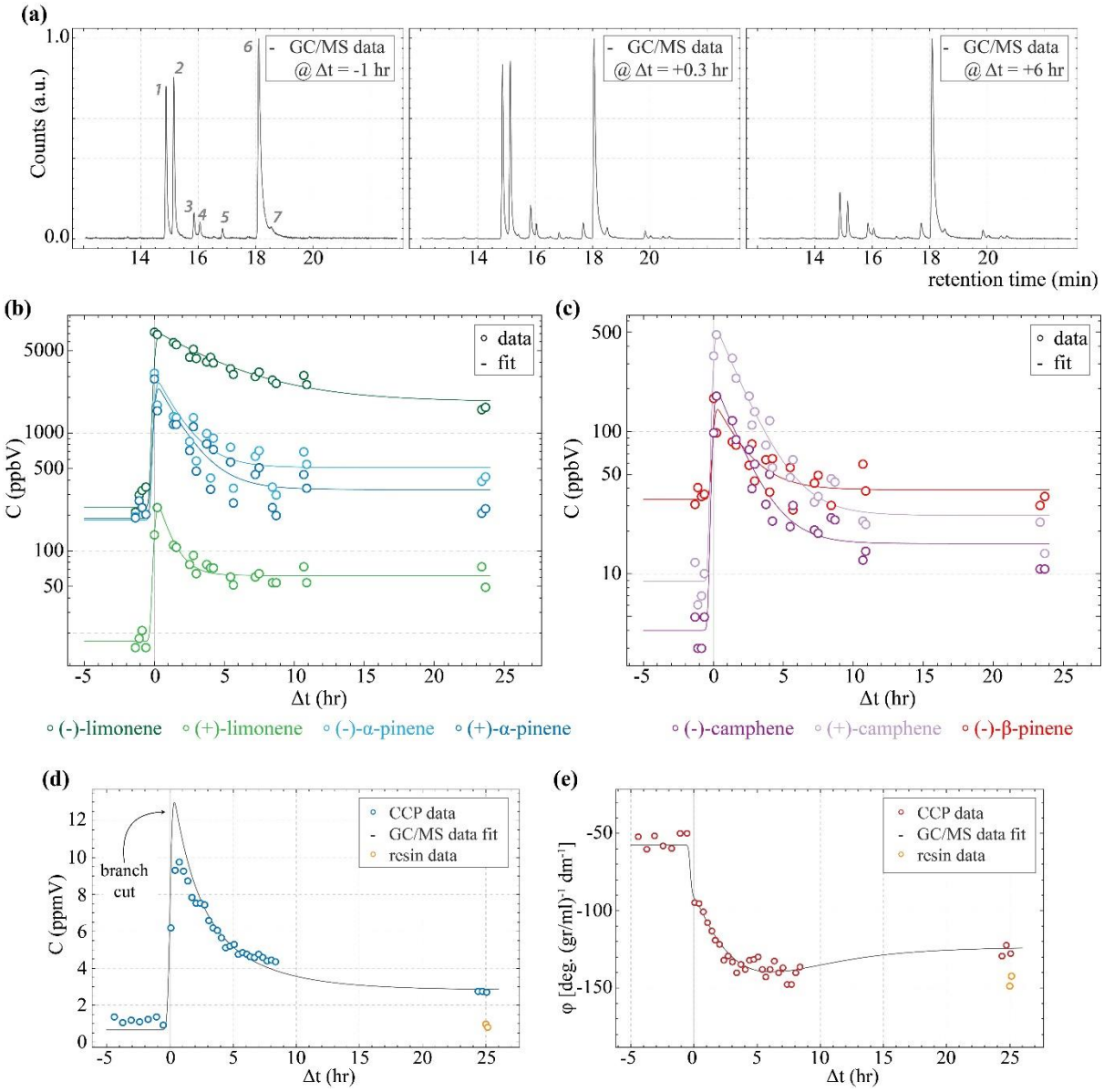

Figure 3. **a**. GC-MS chromatograms obtained for samples taken 1 hour before wounding, 0.3 hours after wounding and 6 hours after wounding. The spectra are normalized over the maximum signal measured, which was for (-)-limonene (peak 6), to visually aid the comparison between the relative signal changes among all eluted compounds. Labelled peaks: **1** (-)-α-pinene; **2** (+)-α-pinene; **3** (-)-camphene; **4** (+)-camphene; **5** (-)-β-pinene; **6** (-)-limonene; **7** (+)-limonene. **b-c**. Time dependent behaviour of the concentration of the dominant monoterpene VOCs in the plant emissions, pre-and post-wounding, obtained through an offline GC-MS analysis: (±)-α-pinene and (±)-limonene (**b**), and (±)-camphene and (-)-β-pinene (**c**). **d-e**. Total monoterpene concentration, C, and optical rotation, φ, measured with CCP and corroborated with GC-ToF-MS measurements. Measurement points of the secreted resin that covers the wounding site are in yellow.

6.4. Discussion

These results show how observing chiral emissions from a coniferous plant before and after being mechanically wounded allows for observations of the enantiospecific dynamics of different compounds stored within the plant, including the resin that is secreted to protect the wounding site. Measurements such as these are valuable for the real-time in situ identification of abiotic from biotic stress factors (Holopainen and Gershenzon 2010), and of the plants underlying enzymatically driven response mechanisms (Savatin et al. 2014). It has been shown that bark-boring beetles, which cause damage to boreal forests, can generate chiral signals similar to those of mechanical stress (i.e. strong increase in (+)-enantiomers) and recent observations of unusual enantiospecific changes of chiral BVOCs in the Amazon rainforest have been attributed to insect proliferation (Zannoni et al. 2020).

The distinct differences in the dynamics between φ and the overall VOC concentration signal following wounding directly reveals the presence of chirally specific differences in the dynamics of the emission of monoterpene isomers and their respective enantiomers (**Fig. 3d-e**). The observed dynamics of φ towards more negative values can be attributed to the increasing dominance of the emission of (-)-limonene over the other measured monoterpenes and the relative increase of (-)-α-pinene over (+)-α-pinene (**Fig. 3b**). The chiral signal of the resin secreted by the plant was also independently recorded to provide further insight into the observed chiral signals. Resin is secreted by the plant from specialised ducts and eventually hardens to form a protective seal over the site of the wound. The long-term φ value for the plant monoterpene emissions was close to the independently obtained φ value of the resin (**Fig. 3e**), indicating that in the long-term, mechanical wounding causes the total emission profile of the plant to be dominated by the chiral VOC composition of the resin.

The differences between the pre- and post-wounding emission profiles suggest differences in the underlying emission mechanisms for different monoterpene species. Coniferous plants are known to synthesize VOCs that are directly emitted from the leaf, termed *de novo* emission, and they are also known to store monoterpenes in specialised storage pools (Ghirardo et al. 2010). Therefore, before wounding it can be assumed that the emissions from this plant are a composition of *de novo* and storage emissions. Once wounded, storage pools become broken which leak emissions to form a greater component of the total monoterpene emissions, which weakens with time. Since the concentration of (-)-camphene and (+)-camphene increased above (-)-β-pinene only in the period directly following wounding (**Fig. 3c**), it is likely that (-)-β-pinene was more dominant in the *de novo* emissions than the storage emissions from this plant whereas the camphene enantiomers were more dominant in the storage emissions, more specifically in the emissions from the resin. However, this explanation assumes that in the period following wounding storage pool emissions, such as emissions from resin, dominated the signal over induced *de novo* emissions.

In this study, the offline chiral analysis of VOCs emitted by a biological organism under stress, in this case, a coniferous plant, was demonstrated using sorbent cartridges and GC-ToF-MS, and cavity-enhanced chiral polarimetry. In order for modern atmospheric organic chemistry to progress, all available sources of BVOC must be identified as well as the physical and chemical processes which determine their eventual fate, which will provide a greater understanding of how they impact the atmosphere and the climate 50. For this to be achieved, it is necessary to obtain accurate in-situ real-time measurements of the short and long-term dynamics of BVOCs. In particular, measurements of the dynamics of chiral compounds in relation to each other (**Fig. 3**) can serve as a unique signature for BVOC sources yet to be characterised. Sorbent cartridges are an extremely useful tool for capturing air samples from various sources and locations since they are easily transported and require little expertise to use in conjunction with a small sampling pump. However, the measurements

obtained from using sorbent cartridges are not obtained in real-time since air must be sampled onto the sorbent bed (typically 10-30 mins each) prior to the cartridge being transported to the location of the GC-ToF-MS and then subsequently desorbed and analysed (typically 1-2 hours each). Furthermore, following the data acquisition from the sorbent cartridge samples, extensive calibrations for each individual compound must be performed for accurate quantification (typically 1-2 days). Yet when absolute chiral analysis is performed in real-time, using cavity-enhanced chiral polarimetry, it becomes possible to non-invasively monitor the health status of plants and crops, instead of using invasive electrophysiological measurements. This study shows that cavity-enhanced chiral polarimetry is able to efficiently monitor the chiral monoterpene emissions from a plant suffering from mechanical wounding, in real-time. However, unlike GC-ToF-MS, cavity-enhanced polarimetry currently operates with a high limit of detection, which requires a large sample volume to be accumulated prior to analysis for the detection of compounds at the trace level. However, with refinements in the optical equipment and further instrumentation development, lower limits of detection are expected to be achieved.

In conclusion, these results highlight the potential for taking in-situ chiral VOC measurements in real-time for the detection of stress being applied to vegetation. Measurements of the monoterpene emissions from *Pinus heldreichii* revealed the chirality of its immediate atmosphere to become more negative once the plant had been mechanically wounded. Such results as these suggest that it is important to investigate how the chirality of emissions is affected by other biotic and abiotic stress factors (e.g. drought, heat stress, herbivory) for different plant species. If such chiral dynamics can be measured in real-time, chiral analysis can be used in the future as a convenient non-invasive method for measuring the health status of vegetation.

6.5. Combining GC and CCP

Chiral analysis in the gas phase is commonly performed using chiral chromatography or chemical reactions with chiral molecules in combination with mass spectrometry (Yu and Yao 2017). Measurements with a mass spectrometer are non-absolute, thus, extensive calibrations must be performed for accurate quantification and enantiomeric excess determination. Moreover, when employing gas chromatography, the elution order of enantiomers is dependent on the chosen column, column flow, and GC oven parameters and is not the same for all compounds, thereby increasing the difficulty to identify enantiomers. This work demonstrates how CCP-based absolute chiral analysis can overcome such limitations. Polarimetric-based chiral analysis uses the specific optical rotation (SOR) of a substance at a chosen wavelength to convert the acquired polarimetric signal to concentration.

Gas-chromatography (GC) was combined with CCP-based chiral detection, i.e., GC-CCP to demonstrate these advantages. **Fig. 4** shows the optical rotation (OR-) chromatogram, i.e., ϕ vs. retention time, of a mixture containing a group of monoterpenes in enantiopure or racemic form. GC-CCP makes it possible for eluted enantiomers to be identified through the sign of their chiroptical signal; whilst the refractometric measurements directly link to their relative concentrations within the mixture (particularly important when analysing a compound with unknown specific rotation). Additionally, since achiral substances do not possess a specific optical rotation, they do not appear in the polarimetric signal, but they do appear in the refractometric signal. Therefore, this approach allows for coeluting chiral/achiral substances to be distinguished from each other, in contrast to mass spectrometry, where coeluting chiral/achiral compounds are indistinguishable, which restricts accurate quantification and identification. Furthermore, if two enantiomers are coeluting in the refractometric signal, such as camphene (**Fig. 4**), the polarimetric signal is able to reveal the presence

of two coeluting enantiomers when the refractometric signal only detects a single peak for camphene. This new technique for measuring complex chiral/achiral mixtures has a light limit of detection (~ppm), requiring large sample accumulation times for the detection of trace-level compounds. Nevertheless, with further development and refinement, GC-CCP could be the future of chiral analysis.

GC-CCP analysis was performed using splitless injection (Agilent HP 6890A GC, Agilent Technologies, USA) of the mixture in ethanol (1µL of solution injected). The mixture contained 120µL (+)-α-pinene, 20µL (R)-(-)-α-phellandrene, 90µL (+)-limonene, and 100µL racemic camphene (all compounds purchased from Sigma Aldrich). Chiral compounds in the mixture were separated using a 120 m β-DEX™ 120 column (Sigma-Aldrich GmbH, Germany) with 0.25 mm internal diameter and a 0.25 µm film thickness (**Fig.4**). The column flow was 1.5 ml min^{-1} and the temperature program is shown in **Table 2**. More information about the CCP method is given elsewhere (Bougas 2021).

Table 2. GC oven program used for GC-CCP analysis.

Rate (°C min^{-1})	Temperature (°C)	Hold time (min)
	40	4
3.5	110	20
10	210	

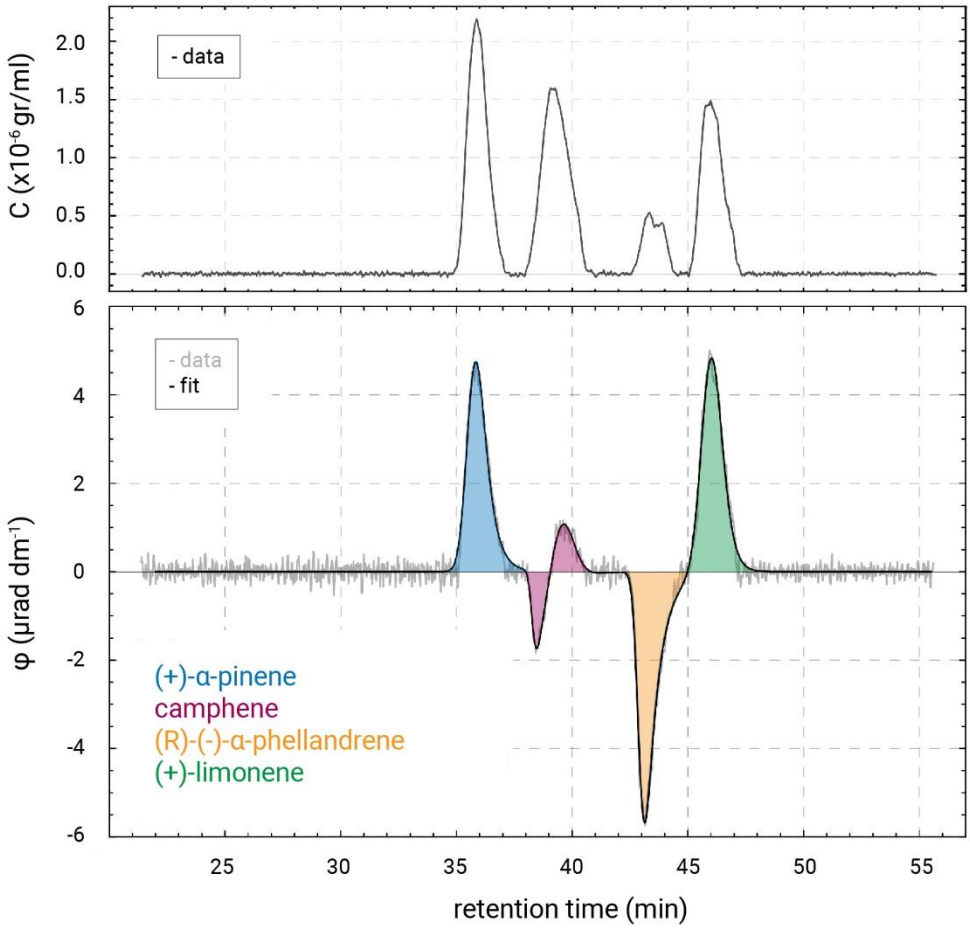

Figure 4. A chromatogram of a mixture of several chiral monoterpenes obtained using GC-CCP.

Chapter 7: Conclusions and future perspectives

7.1. Conclusions

In this doctoral project, gas chromatography – time of flight-mass spectrometry (GC-ToF-MS) and gas chromatography-quadrupole mass spectrometry (GC-QMS) were used to study the atmospheric concentrations and emission rates of chirally separated terpenoids in two different situations: (1) The monoterpene emissions from soil, and stem and branches of pine trees in a homogenous Mediterranean maritime forest were measured to look for differences in the chirality between different regions within the forest. (2) The atmosphere in an indoor managed tropical rainforest subjected to a 9.5-week drought and rewetting experiment was measured to see if drought had the same effect on the abundance of enantiomers and if enantiomers were emitted by the same pathways (i.e. *de novo* or storage pools) in the absence of atmospheric chemistry. Additionally, the chiral terpenoid emissions from a tropical upper canopy plant species and a tropical understory plant species were measured during the same 9.5-week drought experiment to see how drought affected the terpenoid emissions and if the enantiomer emission rates were affected in the same manner. Furthermore, a state-of-the-art cavity-enhanced chiral polarimeter was, for the first time, used to measure the concentration of chiral monoterpenes for two distinct applications: (1) The emissions from a pine tree before and after mechanical wounding to be able to detect a chiral stress response. (2) The individual headspaces from a range of perfumes and their commercially available clones. The measurements made with the polarimeter were validated with a gas chromatograph – time of flight – mass spectrometer, which is a commonly used method for measuring the abundance of chiral compounds.

Through this thesis, it was shown that the enantiomers of chiral monoterpenes should not be assumed to be emitted in the same way by vegetation to the atmosphere. The enantiomeric fraction of (-)-α-pinene emissions was shown to be different for emissions from the branches and stems of pine trees, and the surrounding soil in a homogenous forest. It was shown that the sources and sinks of volatile organic compounds (VOCs), such as soil and stems, that were formerly neglected, contributed significantly to the total ambient VOC flux, especially when ambient moisture levels were high. Chiral signatures of the emissions from the different forest compartments (branch, stem, and soil), were used to explore the possibility of using chirality as a marker for recognising shifts in the contributions from different VOC sources.

In a managed indoor tropical rainforest, subjected to a 9.5-week experimental drought and rewetting experiment, measuring the atmosphere showed the changes in the abundance of enantiomers of chiral monoterpenes is not equal. Firstly, it was shown that the ambient concentration of (-)-α-pinene increased more than the ambient concentration of (+)-α-pinene during the early stage of drought. $^{13}CO_2$ gas was introduced into the atmosphere of the tropical rainforest during the pre-drought and severe drought phases, which resulted in (-)-α-pinene, but not (+)-α-pinene becoming enriched in ^{13}C. This finding confirmed that (-)-α-pinene was mainly a *de novo* emission whereas (+)-α-pinene was solely emitted from storage pools. From pre-drought through to severe drought, the daily peak in atmospheric concentrations of (-)-α-pinene and (-)-β-pinene shifted from the morning to the afternoon; becoming aligned with the peaks in the compounds emitted from storage pools, (+)-α-pinene and (+)-limonene. As photosynthesis constantly peaked in the morning, this meant that the increases in (-)-α-pinene and (-)-β-pinene measured throughout the drought were primarily because of an increase in storage emissions rather than being an upregulation of *de novo* emissions. The increase in monoterpenes due to drought will potentially have a negative feedback effect on the climate due to the increase in formation of secondary organic aerosol and cloud formation.

The effect of drought on the emissions of chiral terpenoids from two individual plant species was investigated. It was found that the emissions of terpenoids from these plant species during drought were dependent on the humidity and access to moisture within the soil. For the upper canopy species, *C. fairchildiana*, it was found that the emissions of (-)-α-pinene and (+)-α-pinene respond differently to drought. In contrast, the emissions of (-)-α-pinene and (+)-α-pinene from the lower canopy species, *Piper* sp., responded in the same way to drought. Monoterpene emissions from both species were shown to be dependent on plant water potential. As the predawn and midday water potential decreased, the increase in the monoterpene emission lagged slightly behind. In past literature, it was reported that ocimene is a marker for heat stress in tropical plants (Jardine et al. 2017). In this study, the measurements made on the emissions from *C. fairchildiana* agreed with this finding, however, the measurements made from the *Piper* sp. plants disagreed. Since measurements on how drought affects the emissions from tropical plant species are scarce, these measurements help to further the understanding of how drought affects different ecosystems.

The first measurements highlighting the applications of cavity-enhanced polarimetry (CCP) for the detection of gaseous chiral compounds were conducted and validated using gas chromatography-time of flight-mass spectrometry (GC-ToF-MS). It was shown that measurements can be more conveniently and efficiently with CCP than with the GC-ToF-MS and without the need for extensive calibrations and method development. A pine tree was wounded by breaking one of its branches and the concentration of the ambient monoterpenes was measured before and after wounding which showed that the chiral composition of the ambient monoterpenes became more enriched in (-)-enantiomers. The results shown here reveal that real-time on-line chiral analysis can be used and a non-invasive method to monitor the health status of vegetation. However, more instrument development is needed to ensure that CCP can measure compounds at the trace level without the need for long sample collection times before analysis.

7.2. Chiral volatile organic compounds: Future perspectives for research

Despite measurements of chirality revealing that the assumptions about the sources of enantiomers are incorrect, separating enantiomers is still not standard practice in atmospheric chemistry. This is because the separation of enantiomers requires a specific separating column and extensive method development to ensure that there is no co-elution of enantiomers. The column that is widely used for separating enantiomers contains a cyclodextrin stationary phase. Despite achieving good chromatography of monoterpene peaks with a cyclodextrin stationary phase, the peaks of oxygenated compounds often lack sharpness and feature tailing. This means that measuring enantiomers with GC-ToF-MS requires sacrificing the ability to accurately measure other potentially interesting compounds. CCP may overcome this issue since it is possible to measure the overall chirality of a sample without the need for separating the enantiomers and hence, a cyclodextrin separating column. If CCP was to be used alongside GC-ToF-MS, future investigative studies could utilise GC-ToF-MS to measure all non-chiral substances and utilise CCP to measure the overall chirality in tandem.

Since cavity-enhanced polarimetry was able to detect changes in the chirality of the emissions of a mechanically stressed pine tree, it is hypothesized that when commercially grown plants, such as tomatoes, are subjected to a variety of biotic and abiotic stresses, the chiral changes in the plant emissions are distinguishable for each type of stress. Furthermore, it is hypothesized that ingested chiral substances (e.g. limonene) will be metabolised by the body and emitted through the breath. If proven correct, measurements of the chirality of breath could be used to calculate the speed of

metabolism, which may have future diagnostic uses in medicine. Cavity-enhanced polarimetry could be the optimal method for testing these hypotheses and if proven to be correct, cavity-enhanced polarimetry should be developed further and made commercially available. The disadvantage of using cavity-enhanced polarimetry for the detection of chiral VOCs is the high limit of detection. For cavity-enhanced polarimetry to be eventually realised as an eventual replacement for mass spectrometry, lower detection limits must be achieved.

There is still little understanding of how drought affects the flux of VOCs to the atmosphere for different ecosystems. This thesis showed that the abundance of monoterpenes emitted from vegetation, in a tropical rainforest, increases due to drought. However, past literature shows that the monoterpene emissions from a variety of plant species can increase, decrease, or be unaffected when subjected to drought. This is likely because most drought experiments are performed in laboratories rather than in the field. In a laboratory, plants will usually be potted and the plant will be subjected to individual stress factors, but in the field, plants are usually subjected to multiple stresses at once and have access to deeper levels of soil from where they can draw moisture. To better understand how vegetation will respond to drought and the impact that has the total VOC flux on the atmosphere, more drought experiments must be performed in the field or in laboratories where conditions can be better replicated that a plant would experience in its natural environment. Furthermore, more ^{13}C-labelling experiments are needed to unravel the mechanisms that cause monoterpenes and their respective enantiomers to be emitted from a leaf.

The projects reported in this thesis focused on the measurement of chiral monoterpenes, but sesquiterpenes (e.g. caryophyllene) and oxygenated monoterpenes (e.g. linalool) are entirely separate groups of compounds, some of which are also known to be chiral and of which very little is known about how the sources of their enantiomers differ. There are currently no published studies that have performed stress experiments on plants and reported enantiomerically resolved sesquiterpene emissions. This is because sesquiterpenes are chemically diverse, react rapidly with ozone, and have low volatility (Bourtsoukidis et al. 2018). Thus, samples must be taken as close as possible to the emission source and some calibration standards need to be synthesized in the laboratory, as they are not commercially available. However, by measuring the chirality of sesquiterpene emissions, more information will be revealed which can lead to a better understanding of insect-plant and biosphere-atmosphere interactions.

With an increase in studies reporting unexplainable differences in the abundance of enantiomers, it is becoming clear that the current understanding of how monoterpenes are emitted is not sufficient. To date, only a few studies have been conducted which have reported separate values for enantiomers emitted from forests. Further, before this doctoral project, no ^{13}C-labelling experiments had been conducted which reported separate values for enantiomers enriched in ^{13}C in the atmosphere. Therefore, it is necessary for atmospheric chiral VOC measurements to continue so that emission models can be improved and a better understanding of biosphere-atmosphere interactions can be achieved.

Appendices

Abbreviations and acronyms

AUC	Area under curve
B2WALD	Biosphere 2 water, atmosphere and life dynamics
B2-TRF	Biosphere 2 tropical rainforest
BVOC	Biogenic volatile organic compound
CCN	Cloud condensation nuclei
CCP	Cavity-enhanced chiral polarimetry
CF	*Clitoria fairchildiana*
CIS	Cold injection system
DMAPP	Dimethylallyl diphosphate
doy	Day of year
DRW	Deep water rewet
ED	Early drought
G3P	Glyceraldehyde 3-phosphate
GC-CCP	Gas chromatography-cavity-enhanced chiral polarimetry
GC-MS	Gas chromatography-mass spectrometry
GC-ToF-MS	Gas chromatography – time of flight – mass spectrometry
GPP	Geranyl Diphosphate
IPP	Isopentanyl diphosphate
IRMS	Isotope ratio mass spectrometer
LOD	Limit of detection
MEP	2-C-methyl-D-erythitol 4-phosphate
MFC	Mass flow controller
MPIC	Max Planck institute for chemistry
MR	Mixing ratio
MST	Mountain time zone
MT	Monoterpene
MVA	Mevalonate
NEE	Net ecosystem exchange
NIST	National institute of standards and technology
PAR	Photosynthetically active radiation
PD	Pre-drought
PFA	Perfluoroalkoxy alkane
PI	*Piper* sp.
ppb	Parts per billion
ppm	Parts per million
pptv	Parts per trillion (volume)
PPFD	Photosynthetic Photon Flux Density
PTFE	Polytetrafluoroethylene
PTR	Proton transfer reaction-mass spectrometry
RH	Relative humidity
ROS	Reactive oxygen species
RRW	Rain rewet
SD	Severe drought
SM	Soil moisture
SOA	Secondary organic aerosol
sp.	Species
TD	Thermal desorber
TDU	Thermal desorption unit

UV	Ultraviolet
vmr	Volume mixing ratio
VOC	Volatile organic compound
WP	Water potential

Bibliography

Aaltonen, H., J. Aalto, P. Kolari, M. Pihlatie, J. Pumpanen, M. Kulmala, E. Nikinmaa, T. Vesala, and J. Bäck. 2013. "Continuous VOC flux measurements on boreal forest floor." *Plant and Soil* 369 (1):241-256. doi: 10.1007/s11104-012-1553-4.

Abbott, Tristan H., and Timothy W. Cronin. 2021. "Aerosol invigoration of atmospheric convection through increases in humidity." *Science* 371 (6524):83-85. doi: 10.1126/science.abc5181.

Amin, Hardik S, Rachel S Russo, Barkley Sive, E Richard Hoebeke, Craig Dodson, Ian B McCubbin, A Gannet Hallar, and Kara E Huff Hartz. 2013. "Monoterpene emissions from bark beetle infested Engelmann spruce trees." *Atmospheric Environment* 72:130-133.

Asensio, Dolores, Josep Peñuelas, Iolanda Filella, and Joan Llusià. 2007. "On-line screening of soil VOCs exchange responses to moisture, temperature and root presence." *Plant and Soil* 291 (1):249-261. doi: 10.1007/s11104-006-9190-4.

Atkinson, Roger, and Janet Arey. 2003. "Atmospheric Degradation of Volatile Organic Compounds." *Chemical Reviews* 103 (12):4605-4638. doi: 10.1021/cr0206420.

Aydin, Y. M., B. Yaman, H. Koca, O. Dasdemir, M. Kara, H. Altiok, Y. Dumanoglu, A. Bayram, D. Tolunay, M. Odabasi, and T. Elbir. 2014. "Biogenic volatile organic compound (BVOC) emissions from forested areas in Turkey: determination of specific emission rates for thirty-one tree species." *Sci Total Environ* 490:239-53. doi: 10.1016/j.scitotenv.2014.04.132.

Baldwin, I. T., R. Halitschke, A. Paschold, C. C. von Dahl, and C. A. Preston. 2006. "Volatile signaling in plant-plant interactions: "talking trees" in the genomics era." *Science* 311 (5762):812-5. doi: 10.1126/science.1118446.

Bamberger, I., L. Hörtnagl, T. M. Ruuskanen, R. Schnitzhofer, M. Müller, M. Graus, T. Karl, G. Wohlfahrt, and A. Hansel. 2011. "Deposition Fluxes of Terpenes over Grassland." *J Geophys Res Atmos* 116 (D14). doi: 10.1029/2010jd015457.

Bartram, Stefan, Andreas Jux, Gerd Gleixner, and Wilhelm Boland. 2006. "Dynamic pathway allocation in early terpenoid biosynthesis of stress-induced lima bean leaves." *Phytochemistry* 67 (15):1661-1672. doi: https://doi.org/10.1016/j.phytochem.2006.02.004.

Bastings, Jjaj, H. M. van Eijk, S. W. Olde Damink, and S. S. Rensen. 2019. "d-amino Acids in Health and Disease: A Focus on Cancer." *Nutrients* 11 (9). doi: 10.3390/nu11092205.

Bertin, N., and M. Staudt. 1996. "Effect of water stress on monoterpene emissions from young potted holm oak (Quercus ilex L.) trees." *Oecologia* 107 (4):456-462. doi: 10.1007/BF00333935.

Bigg, EK. 2004. "Gas emissions from soil and leaf litter as a source of new particle formation." *Atmospheric research* 70 (1):33-42.

Blanch, J.-S., L. Sampedro, J. Llusià, X. Moreira, R. Zas, and J. Peñuelas. 2012. "Effects of phosphorus availability and genetic variation of leaf terpene content and emission rate in Pinus pinaster seedlings susceptible and resistant to the pine weevil, Hylobius abietis." *Plant Biology* 14 (s1):66-72. doi: https://doi.org/10.1111/j.1438-8677.2011.00492.x.

Blanch, J. S., J. Peñuelas, and J. Llusià. 2007. "Sensitivity of terpene emissions to drought and fertilization in terpene-storing Pinus halepensis and non-storing Quercus ilex." *Physiol Plant* 131 (2):211-25. doi: 10.1111/j.1399-3054.2007.00944.x.

Bonan, Gordon B. 2008. "Forests and Climate Change: Forcings, Feedbacks, and the Climate Benefits of Forests." *Science* 320 (5882):1444. doi: 10.1126/science.1155121.

Bougas, L., Byron, J., Budker, D., Williams, J. . 2021. Absolute optical chiral analysis using cavity-enhanced polarimetry. Cambridge: Cambridge Open Engage: ChemRxiv. This content is a preprint and has not been peer-reviewed.

Bourtsoukidis, E., T. Behrendt, A. M. Yañez-Serrano, H. Hellén, E. Diamantopoulos, E. Catão, K. Ashworth, A. Pozzer, C. A. Quesada, D. L. Martins, M. Sá, A. Araujo, J. Brito, P. Artaxo, J. Kesselmeier, J. Lelieveld, and J. Williams. 2018. "Strong sesquiterpene emissions from Amazonian soils." *Nature Communications* 9 (1):2226. doi: 10.1038/s41467-018-04658-y.

Brilli, Federico, Paolo Ciccioli, Massimiliano Frattoni, Marco Prestininzi, Antonio Franco Spanedda, and Francesco Loreto. 2009. "Constitutive and herbivore-induced monoterpenes emitted by Populus × euroamericana leaves are key volatiles that orient Chrysomela populi beetles." *Plant, Cell & Environment* 32 (5):542-552. doi: https://doi.org/10.1111/j.1365-3040.2009.01948.x.

Brodersen, Craig R., Adam B. Roddy, Jay W. Wason, and Andrew J. McElrone. 2019. "Functional Status of Xylem Through Time." *Annual Review of Plant Biology* 70 (1):407-433. doi: 10.1146/annurev-arplant-050718-100455.

Churkina, Galina, Friderike Kuik, Boris Bonn, Axel Lauer, Rüdiger Grote, Karolina Tomiak, and Tim M. Butler. 2017. "Effect of VOC Emissions from Vegetation on Air Quality in Berlin during a Heatwave." *Environmental Science & Technology* 51 (11):6120-6130. doi: 10.1021/acs.est.6b06514.

Copolovici, Lucian O., and Ülo Niinemets. 2005. "Temperature dependencies of Henry's law constants and octanol/water partition coefficients for key plant volatile monoterpenoids." *Chemosphere* 61 (10):1390-1400. doi: https://doi.org/10.1016/j.chemosphere.2005.05.003.

Copolovici, Lucian, Andreea Pag, Astrid Kännaste, Adina Bodescu, Daniel Tomescu, Dana Copolovici, Maria-Loredana Soran, and Ülo Niinemets. 2017. "Disproportionate photosynthetic decline and inverse relationship between constitutive and induced volatile emissions upon feeding of Quercus robur leaves by large larvae of gypsy moth (Lymantria dispar)." *Environmental and Experimental Botany* 138:184-192. doi: https://doi.org/10.1016/j.envexpbot.2017.03.014.

Croteau, Rodney. 1987. "Biosynthesis and catabolism of monoterpenoids." *Chemical Reviews* 87 (5):929-954. doi: 10.1021/cr00081a004.

Cruz de Carvalho, Maria Helena. 2008. "Drought stress and reactive oxygen species: Production, scavenging and signaling." *Plant signaling & behavior* 3 (3):156-165. doi: 10.4161/psb.3.3.5536.

Degenhardt, J., T. G. Köllner, and J. Gershenzon. 2009a. "Monoterpene and sesquiterpene synthases and the origin of terpene skeletal diversity in plants." *Phytochemistry* 70 (15-16):1621-37. doi: 10.1016/j.phytochem.2009.07.030.

Degenhardt, Jörg, Tobias G. Köllner, and Jonathan Gershenzon. 2009b. "Monoterpene and sesquiterpene synthases and the origin of terpene skeletal diversity in plants." *Phytochemistry* 70 (15):1621-1637. doi: https://doi.org/10.1016/j.phytochem.2009.07.030.

Dement, William A., Bennett J. Tyson, and Harold A. Mooney. 1975. "Mechanism of monoterpene volatilization in Salvia mellifera." *Phytochemistry* 14 (12):2555-2557. doi: https://doi.org/10.1016/0031-9422(75)85223-X.

Dudareva, Natalia, Florence Negre, Dinesh A. Nagegowda, and Irina Orlova. 2006. "Plant Volatiles: Recent Advances and Future Perspectives." *Critical Reviews in Plant Sciences* 25 (5):417-440. doi: 10.1080/07352680600899973.

Eerdekens, G., N. Yassaa, V. Sinha, P. P. Aalto, H. Aufmhoff, F. Arnold, V. Fiedler, M. Kulmala, and J. Williams. 2009. "VOC measurements within a boreal forest during spring 2005: on the occurrence of elevated monoterpene concentrations during night time intense particle concentration events." *Atmos. Chem. Phys.* 9 (21):8331-8350. doi: 10.5194/acp-9-8331-2009.

Eller, Allyson SD, Peter Harley, and Russell K Monson. 2013. "Potential contribution of exposed resin to ecosystem emissions of monoterpenes." *Atmospheric Environment* 77:440-444.

Engelhart, G. J., A. Asa-Awuku, A. Nenes, and S. N. Pandis. 2008. "CCN activity and droplet growth kinetics of fresh and aged monoterpene secondary organic aerosol." *Atmos. Chem. Phys.* 8 (14):3937-3949. doi: 10.5194/acp-8-3937-2008.

Erbilgin, Nadir, and Kenneth F. Raffa. 2000. "Opposing Effects of Host Monoterpenes on Responses by Two Sympatric Species of Bark Beetles to Their Aggregation Pheromones." *Journal of Chemical Ecology* 26 (11):2527-2548. doi: 10.1023/A:1005532612117.

Faiola, C. L., A. Buchholz, E. Kari, P. Yli-Pirilä, J. K. Holopainen, M. Kivimäenpää, P. Miettinen, D. R. Worsnop, K. E. J. Lehtinen, A. B. Guenther, and A. Virtanen. 2018. "Terpene Composition

Complexity Controls Secondary Organic Aerosol Yields from Scots Pine Volatile Emissions." *Scientific Reports* 8 (1):3053. doi: 10.1038/s41598-018-21045-1.

Faiola, C. L., B. T. Jobson, and T. M. VanReken. 2015. "Impacts of simulated herbivory on volatile organic compound emission profiles from coniferous plants." *Biogeosciences* 12 (2):527-547. doi: 10.5194/bg-12-527-2015.

Faiola, C., and D. Taipale. 2020. "Impact of insect herbivory on plant stress volatile emissions from trees: A synthesis of quantitative measurements and recommendations for future research." *Atmospheric Environment: X* 5:100060. doi: https://doi.org/10.1016/j.aeaoa.2019.100060.

Faiola, Celia L., Graham S. VanderSchelden, Miao Wen, Farah C. Elloy, Douglas R. Cobos, Richard J. Watts, B. Thomas Jobson, and Timothy M. VanReken. 2014. "SOA Formation Potential of Emissions from Soil and Leaf Litter." *Environmental Science & Technology* 48 (2):938-946. doi: 10.1021/es4040045.

Fäldt, J., H. Solheim, B. Långström, and A. K. Borg-Karlson. 2006. "Influence of fungal infection and wounding on contents and enantiomeric compositions of monoterpenes in phloem of Pinus sylvestris." *J Chem Ecol* 32 (8):1779-95. doi: 10.1007/s10886-006-9109-9.

Fankhauser-Noti, Anja, and Koni Grob. 2007. "Blank problems in trace analysis of diethylhexyl and dibutyl phthalate: Investigation of the sources, tips and tricks." *Analytica Chimica Acta* 582 (2):353-360. doi: https://doi.org/10.1016/j.aca.2006.09.012.

Farré-Armengol, Gerard, Iolanda Filella, Joan Llusià, and Josep Peñuelas. 2017. "β-Ocimene, a Key Floral and Foliar Volatile Involved in Multiple Interactions between Plants and Other Organisms." *Molecules* 22 (7):1148.

Finn, Matt. 1996. "The mangrove mesocosm of Biosphere 2: Design, establishment and preliminary results." *Ecological Engineering* 6 (1):21-56. doi: https://doi.org/10.1016/0925-8574(95)00050-X.

Ghimire, Rajendra P, Minna Kivimäenpää, Anne Kasurinen, Elina Häikiö, Toini Holopainen, and Jarmo K Holopainen. 2017. "Herbivore-induced BVOC emissions of Scots pine under warming, elevated ozone and increased nitrogen availability in an open-field exposure." *Agricultural and Forest Meteorology* 242:21-32.

Ghirardo, Andrea, Kristine Koch, Risto Taipale, Ina Zimmer, Jörg-Peter Schnitzler, and Janne Rinne. 2010. "Determination of de novo and pool emissions of terpenes from four common boreal/alpine trees by 13CO2 labelling and PTR-MS analysis." *Plant, Cell & Environment* 33 (5):781-792. doi: https://doi.org/10.1111/j.1365-3040.2009.02104.x.

Gill, Sarvajeet Singh, and Narendra Tuteja. 2010. "Reactive oxygen species and antioxidant machinery in abiotic stress tolerance in crop plants." *Plant Physiology and Biochemistry* 48 (12):909-930. doi: https://doi.org/10.1016/j.plaphy.2010.08.016.

Glasius, Marianne, and Allen H. Goldstein. 2016. "Recent Discoveries and Future Challenges in Atmospheric Organic Chemistry." *Environmental Science & Technology* 50 (6):2754-2764. doi: 10.1021/acs.est.5b05105.

Goldstein, A. H., and I. E. Galbally. 2007. "Known and unknown organic constituents in the Earth' s atmosphere." *Environ Sci Technol* 41 (5):1514-21. doi: 10.1021/es072476p.

Gray, Christopher M, Russell K Monson, and Noah Fierer. 2010. "Emissions of volatile organic compounds during the decomposition of plant litter." *Journal of Geophysical Research: Biogeosciences* 115 (G3).

Gray, Christopher M, Russell K Monson, and Noah Fierer. 2014. "Biotic and abiotic controls on biogenic volatile organic compound fluxes from a subalpine forest floor." *Journal of Geophysical Research: Biogeosciences* 119 (4):547-556.

Greenberg, J. P., D. Asensio, A. Turnipseed, A. B. Guenther, T. Karl, and D. Gochis. 2012. "Contribution of leaf and needle litter to whole ecosystem BVOC fluxes." *Atmospheric Environment* 59:302-311. doi: https://doi.org/10.1016/j.atmosenv.2012.04.038.

Griffin, Robert J., David R. Cocker Iii, Richard C. Flagan, and John H. Seinfeld. 1999. "Organic aerosol formation from the oxidation of biogenic hydrocarbons." *Journal of Geophysical Research: Atmospheres* 104 (D3):3555-3567. doi: https://doi.org/10.1029/1998JD100049.

Grote, Rüdiger, Monica Sharma, Andrea Ghirardo, and Jörg-Peter Schnitzler. 2019. "A New Modeling Approach for Estimating Abiotic and Biotic Stress-Induced de novo Emissions of Biogenic Volatile Organic Compounds From Plants." *Frontiers in Forests and Global Change* 2 (26). doi: 10.3389/ffgc.2019.00026.

Guenther, AB, Xiaoyan Jiang, CL Heald, T Sakulyanontvittaya, Tiffany Duhl, LK Emmons, and X Wang. 2012. "The Model of Emissions of Gases and Aerosols from Nature version 2.1 (MEGAN2. 1): an extended and updated framework for modeling biogenic emissions."

Guenther, Alex. 1997. "SEASONAL AND SPATIAL VARIATIONS IN NATURAL VOLATILE ORGANIC COMPOUND EMISSIONS." *Ecological Applications* 7 (1):34-45. doi: 10.1890/1051-0761(1997)007[0034:sasvin]2.0.co;2.

Guenther, Alex B., Patrick R. Zimmerman, Peter C. Harley, Russell K. Monson, and Ray Fall. 1993. "Isoprene and monoterpene emission rate variability: Model evaluations and sensitivity analyses." *Journal of Geophysical Research: Atmospheres* 98 (D7):12609-12617. doi: https://doi.org/10.1029/93JD00527.

Guenther, Alex, C. Nicholas Hewitt, David Erickson, Ray Fall, Chris Geron, Tom Graedel, Peter Harley, Lee Klinger, Manuel Lerdau, W. A. McKay, Tom Pierce, Bob Scholes, Rainer Steinbrecher, Raja Tallamraju, John Taylor, and Pat Zimmerman. 1995. "A global model of natural volatile organic compound emissions." *Journal of Geophysical Research: Atmospheres* 100 (D5):8873-8892. doi: 10.1029/94JD02950.

Haberstroh, S., J. Kreuzwieser, R. Lobo-do-Vale, M. C. Caldeira, M. Dubbert, and C. Werner. 2018. "Terpenoid Emissions of Two Mediterranean Woody Species in Response to Drought Stress." *Front Plant Sci* 9:1071. doi: 10.3389/fpls.2018.01071.

Hallquist, M., J. C. Wenger, U. Baltensperger, Y. Rudich, D. Simpson, M. Claeys, J. Dommen, N. M. Donahue, C. George, A. H. Goldstein, J. F. Hamilton, H. Herrmann, T. Hoffmann, Y. Iinuma, M. Jang, M. E. Jenkin, J. L. Jimenez, A. Kiendler-Scharr, W. Maenhaut, G. McFiggans, Th F. Mentel, A. Monod, A. S. H. Prévôt, J. H. Seinfeld, J. D. Surratt, R. Szmigielski, and J. Wildt. 2009. "The formation, properties and impact of secondary organic aerosol: current and emerging issues." *Atmos. Chem. Phys.* 9 (14):5155-5236. doi: 10.5194/acp-9-5155-2009.

Hansen, U., and G. Seufert. 1999. "Terpenoid emission from citrus sinensis (L.) OSBECK under drought stress." *Physics and Chemistry of the Earth, Part B: Hydrology, Oceans and Atmosphere* 24 (6):681-687. doi: https://doi.org/10.1016/S1464-1909(99)00065-9.

Hari, Vittal, Oldrich Rakovec, Yannis Markonis, Martin Hanel, and Rohini Kumar. 2020. "Increased future occurrences of the exceptional 2018–2019 Central European drought under global warming." *Scientific Reports* 10 (1):12207. doi: 10.1038/s41598-020-68872-9.

Hayward, S, RJ Muncey, AE James, Crispin J Halsall, and C Nicholas Hewitt. 2001. "Monoterpene emissions from soil in a Sitka spruce forest." *Atmospheric Environment* 35 (24):4081-4087.

He, Jun, Richard A. Fandino, Rayko Halitschke, Katrin Luck, Tobias G. Köllner, Mark H. Murdock, Rishav Ray, Klaus Gase, Markus Knaden, Ian T. Baldwin, and Meredith C. Schuman. 2019. "An unbiased approach elucidates variation in (S)-(+)-linalool, a context-specific mediator of a tri-trophic interaction in wild tobacco." *Proceedings of the National Academy of Sciences* 116 (29):14651-14660. doi: 10.1073/pnas.1818585116.

Heil, M., and R. Karban. 2010. "Explaining evolution of plant communication by airborne signals." *Trends Ecol Evol* 25 (3):137-44. doi: 10.1016/j.tree.2009.09.010.

Helmig, Detlev, Jim Greenberg, Alex Guenther, Pat Zimmerman, and Chris Geron. 1998. "Volatile organic compounds and isoprene oxidation products at a temperate deciduous forest site." *Journal of Geophysical Research: Atmospheres* 103 (D17):22397-22414.

Hoesly, R. M., S. J. Smith, L. Feng, Z. Klimont, G. Janssens-Maenhout, T. Pitkanen, J. J. Seibert, L. Vu, R. J. Andres, R. M. Bolt, T. C. Bond, L. Dawidowski, N. Kholod, J. I. Kurokawa, M. Li, L. Liu, Z. Lu,

M. C. P. Moura, P. R. O'Rourke, and Q. Zhang. 2018. "Historical (1750–2014) anthropogenic emissions of reactive gases and aerosols from the Community Emissions Data System (CEDS)." *Geosci. Model Dev.* 11 (1):369-408. doi: 10.5194/gmd-11-369-2018.

Holopainen, J. K., and J. Gershenzon. 2010. "Multiple stress factors and the emission of plant VOCs." *Trends Plant Sci* 15 (3):176-84. doi: 10.1016/j.tplants.2010.01.006.

Huang, Honglin, Farhan Ullah, Dao-Xiu Zhou, Ming Yi, and Yu Zhao. 2019. "Mechanisms of ROS Regulation of Plant Development and Stress Responses." *Frontiers in Plant Science* 10 (800). doi: 10.3389/fpls.2019.00800.

Hutyra, Lucy R., J. William Munger, Scott R. Saleska, Elaine Gottlieb, Bruce C. Daube, Allison L. Dunn, Daniel F. Amaral, Plinio B. de Camargo, and Steven C. Wofsy. 2007. "Seasonal controls on the exchange of carbon and water in an Amazonian rain forest." *Journal of Geophysical Research: Biogeosciences* 112 (G3). doi: https://doi.org/10.1029/2006JG000365.

IPCC. 2014. Climate Change 2014: Synthesis Report. Contribution of Working Groups I, II and III to the fifth Assessment Report of the Intergovernmental Panel on Climate Change. edited by R.K. Pachauri and L.A. Meyer (eds.). IPCC, Geneva, Switzerland.

Isidorov, V. A., M. Smolewska, A. Purzyńska-Pugacewicz, and Z. Tyszkiewicz. 2010. "Chemical composition of volatile and extractive compounds of pine and spruce leaf litter in the initial stages of decomposition." *Biogeosciences* 7 (9):2785-2794. doi: 10.5194/bg-7-2785-2010.

Janson, Robert W. 1993. "Monoterpene emissions from Scots pine and Norwegian spruce." *Journal of geophysical research: atmospheres* 98 (D2):2839-2850.

Jardine, Angela B, Kolby J Jardine, José D Fuentes, Scot T Martin, G Martins, F Durgante, V Carneiro, Niro Higuchi, Antônio Ocimar Manzi, and Jeffrey Quintin Chambers. 2015. "Highly reactive light-dependent monoterpenes in the Amazon." *Geophysical Research Letters* 42 (5):1576-1583.

Jardine, K. J., A. B. Jardine, J. A. Holm, D. L. Lombardozzi, R. I. Negron-Juarez, S. T. Martin, H. R. Beller, B. O. Gimenez, N. Higuchi, and J. Q. Chambers. 2017. "Monoterpene 'thermometer' of tropical forest-atmosphere response to climate warming." *Plant Cell Environ* 40 (3):441-452. doi: 10.1111/pce.12879.

Jokinen, Tuija, Torsten Berndt, Risto Makkonen, Veli-Matti Kerminen, Heikki Junninen, Pauli Paasonen, Frank Stratmann, Hartmut Herrmann, Alex B. Guenther, Douglas R. Worsnop, Markku Kulmala, Mikael Ehn, and Mikko Sipilä. 2015. "Production of extremely low volatile organic compounds from biogenic emissions: Measured yields and atmospheric implications." *Proceedings of the National Academy of Sciences* 112 (23):7123-7128. doi: 10.1073/pnas.1423977112.

Kainulainen, P., J. Oksanen, V. Palomäki, J. K. Holopainen, and T. Holopainen. 1992. "Effect of drought and waterlogging stress on needle monoterpenes of Picea abies." *Canadian Journal of Botany* 70 (8):1613-1616. doi: 10.1139/b92-203.

Kammer, J., E. Perraudin, P. M. Flaud, E. Lamaud, J. M. Bonnefond, and E. Villenave. 2018. "Observation of nighttime new particle formation over the French Landes forest." *Sci Total Environ* 621:1084-1092. doi: 10.1016/j.scitotenv.2017.10.118.

Karl, T., A. Guenther, R. J. Yokelson, J. Greenberg, M. Potosnak, D. R. Blake, and P. Artaxo. 2007. "The tropical forest and fire emissions experiment: Emission, chemistry, and transport of biogenic volatile organic compounds in the lower atmosphere over Amazonia." *Journal of Geophysical Research-Atmospheres* 112 (D18):17. doi: 10.1029/2007jd008539.

Kautz, Markus, Arjan J. H. Meddens, Ronald J. Hall, and Almut Arneth. 2017. "Biotic disturbances in Northern Hemisphere forests – a synthesis of recent data, uncertainties and implications for forest monitoring and modelling." *Global Ecology and Biogeography* 26 (5):533-552. doi: https://doi.org/10.1111/geb.12558.

Kesselmeier, J., U. Kuhn, S. Rottenberger, T. Biesenthal, A. Wolf, G. Schebeske, M. O. Andreae, P. Ciccioli, E. Brancaleoni, M. Frattoni, S. T. Oliva, M. L. Botelho, C. M. A. Silva, and T. M. Tavares. 2002. "Concentrations and species composition of atmospheric volatile organic compounds

(VOCs) as observed during the wet and dry season in Rondônia (Amazonia)." *Journal of Geophysical Research: Atmospheres* 107 (D20):LBA 20-1-LBA 20-13. doi: https://doi.org/10.1029/2000JD000267.

Kesselmeier, J., and M. Staudt. 1999. "Biogenic Volatile Organic Compounds (VOC): An Overview on Emission, Physiology and Ecology." *Journal of Atmospheric Chemistry* 33 (1):23-88. doi: 10.1023/A:1006127516791.

Khanal, Bishnu P., and Moritz Knoche. 2017. "Mechanical properties of cuticles and their primary determinants." *Journal of Experimental Botany* 68 (19):5351-5367. doi: 10.1093/jxb/erx265.

Kleist, E., T. F. Mentel, S. Andres, A. Bohne, A. Folkers, A. Kiendler-Scharr, Y. Rudich, M. Springer, R. Tillmann, and J. Wildt. 2012. "Irreversible impacts of heat on the emissions of monoterpenes, sesquiterpenes, phenolic BVOC and green leaf volatiles from several tree species." *Biogeosciences* 9 (12):5111-5123. doi: 10.5194/bg-9-5111-2012.

Klenø, J. G., P. Wolkoff, P. A. Clausen, C. K. Wilkins, and T. Pedersen. 2002. "Degradation of the adsorbent Tenax TA by nitrogen oxides, ozone, hydrogen peroxide, OH radical, and limonene oxidation products." *Environ Sci Technol* 36 (19):4121-6. doi: 10.1021/es025680f.

Kozlowski, T. T. 1997. "Responses of woody plants to flooding and salinity." *Tree Physiology* 17 (7):490-490. doi: 10.1093/treephys/17.7.490.

Kreuzwieser, J, E Papadopoulou, and H Rennenberg. 2004. "Interaction of flooding with carbon metabolism of forest trees." *Plant Biology* 6 (3):299-306.

Kuhn, U., S. Rottenberger, T. Biesenthal, A. Wolf, G. Schebeske, P. Ciccioli, E. Brancaleoni, M. Frattoni, T. M. Tavares, and J. Kesselmeier. 2004. "Seasonal differences in isoprene and light-dependent monoterpene emission by Amazonian tree species." *GLOBAL CHANGE BIOLOGY* 10 (5):663-682. doi: 10.1111/j.1529-8817.2003.00771.x.

Kurz, W. A., C. C. Dymond, G. Stinson, G. J. Rampley, E. T. Neilson, A. L. Carroll, T. Ebata, and L. Safranyik. 2008. "Mountain pine beetle and forest carbon feedback to climate change." *Nature* 452 (7190):987-990. doi: 10.1038/nature06777.

Lamb, Brian, Hal Westberg, Gene Allwine, and Tim Quarles. 1985. "Biogenic hydrocarbon emissions from deciduous and coniferous trees in the United States." *Journal of Geophysical Research: Atmospheres* 90 (D1):2380-2390.

Lambers, Hans, and Rafael S. Oliveira. 2019. "Plant Water Relations." In *Plant Physiological Ecology*, 187-263. Cham: Springer International Publishing.

Laothawornkitkul, Jullada, Jane E. Taylor, Nigel D. Paul, and C. Nicholas Hewitt. 2009. "Biogenic volatile organic compounds in the Earth system." *New Phytologist* 183 (1):27-51. doi: 10.1111/j.1469-8137.2009.02859.x.

Lavoir, A. V., M. Staudt, J. P. Schnitzler, D. Landais, F. Massol, A. Rocheteau, R. Rodriguez, I. Zimmer, and S. Rambal. 2009. "Drought reduced monoterpene emissions from the evergreen Mediterranean oak Quercus ilex: results from a throughfall displacement experiment." *Biogeosciences* 6 (7):1167-1180. doi: 10.5194/bg-6-1167-2009.

Lee, Anita, Allen H. Goldstein, Melita D. Keywood, Song Gao, Varuntida Varutbangkul, Roya Bahreini, Nga L. Ng, Richard C. Flagan, and John H. Seinfeld. 2006. "Gas-phase products and secondary aerosol yields from the ozonolysis of ten different terpenes." *Journal of Geophysical Research: Atmospheres* 111 (D7). doi: https://doi.org/10.1029/2005JD006437.

Lee, Anita, Allen H. Goldstein, Jesse H. Kroll, Nga L. Ng, Varuntida Varutbangkul, Richard C. Flagan, and John H. Seinfeld. 2006. "Gas-phase products and secondary aerosol yields from the photooxidation of 16 different terpenes." *Journal of Geophysical Research: Atmospheres* 111 (D17). doi: https://doi.org/10.1029/2006JD007050.

Lee, Sangmin, Pil Joon Seo, Hyo-Jun Lee, and Chung-Mo Park. 2012. "A NAC transcription factor NTL4 promotes reactive oxygen species production during drought-induced leaf senescence in Arabidopsis." *The Plant Journal* 70 (5):831-844. doi: https://doi.org/10.1111/j.1365-313X.2012.04932.x.

Lee, Shan-Hu, Janek Uin, Alex B. Guenther, Joost A. de Gouw, Fangqun Yu, Alex B. Nadykto, Jason Herb, Nga L. Ng, Abigail Koss, William H. Brune, Karsten Baumann, Vijay P. Kanawade, Frank N. Keutsch, Athanasios Nenes, Kevin Olsen, Allen Goldstein, and Qi Ouyang. 2016. "Isoprene suppression of new particle formation: Potential mechanisms and implications." *Journal of Geophysical Research: Atmospheres* 121 (24):14,621-14,635. doi: https://doi.org/10.1002/2016JD024844.

Lehner, Bernhard, Petra Döll, Joseph Alcamo, Thomas Henrichs, and Frank Kaspar. 2006. "Estimating the Impact of Global Change on Flood and Drought Risks in Europe: A Continental, Integrated Analysis." *Climatic Change* 75 (3):273-299. doi: 10.1007/s10584-006-6338-4.

Lelieveld, J., T. M. Butler, J. N. Crowley, T. J. Dillon, H. Fischer, L. Ganzeveld, H. Harder, M. G. Lawrence, M. Martinez, D. Taraborrelli, and J. Williams. 2008. "Atmospheric oxidation capacity sustained by a tropical forest." *Nature* 452 (7188):737-740. doi: 10.1038/nature06870.

Lichtenthaler, Hartmut K., Michel Rohmer, and Jörg Schwender. 1997. "Two independent biochemical pathways for isopentenyl diphosphate and isoprenoid biosynthesis in higher plants." *Physiologia Plantarum* 101 (3):643-652. doi: 10.1111/j.1399-3054.1997.tb01049.x.

Llusià, J, and J Peñuelas. 1998. "Changes in terpene content and emission in potted Mediterranean woody plants under severe drought." *Canadian Journal of Botany* 76 (8):1366-1373. doi: 10.1139/b98-141.

Loewenstein, N. J., and S. G. Pallardy. 1998. "Drought tolerance, xylem sap abscisic acid and stomatal conductance during soil drying: a comparison of young plants of four temperate deciduous angiosperms." *Tree Physiol* 18 (7):421-430. doi: 10.1093/treephys/18.7.421.

Lorenzi, H., and Instituto Plantarum de Estudos da Flora. 2002. *Brazilian Trees: A Guide to the Identification and Cultivation of Brazilian Native Trees*: Instituto Plantarum de Estudos da Flora.

Loreto, Francesco, Marcel Dicke, JÖRg-Peter Schnitzler, and Ted C. J. Turlings. 2014. "Plant volatiles and the environment." *Plant, Cell & Environment* 37 (8):1905-1908. doi: https://doi.org/10.1111/pce.12369.

Loreto, Francesco, and Silvano Fares. 2007. "Is Ozone Flux Inside Leaves Only a Damage Indicator? Clues from Volatile Isoprenoid Studies." *Plant Physiology* 143 (3):1096-1100. doi: 10.1104/pp.106.091892.

Loreto, Francesco, and Jörg-Peter Schnitzler. 2010. "Abiotic stresses and induced BVOCs." *Trends in Plant Science* 15 (3):154-166. doi: https://doi.org/10.1016/j.tplants.2009.12.006.

Lough, W.J., and I.W. Wainer. 2002. *Chirality in Natural and Applied Science*: Blackwell Science.

Lüpke, M., M. Leuchner, R. Steinbrecher, and A. Menzel. 2017. "Quantification of monoterpene emission sources of a conifer species in response to experimental drought." *AoB Plants* 9 (5):plx045. doi: 10.1093/aobpla/plx045.

Martin, D. M., J. Fäldt, and J. Bohlmann. 2004. "Functional characterization of nine Norway Spruce TPS genes and evolution of gymnosperm terpene synthases of the TPS-d subfamily." *Plant Physiol* 135 (4):1908-27. doi: 10.1104/pp.104.042028.

McFiggans, Gordon, Thomas F. Mentel, Jürgen Wildt, Iida Pullinen, Sungah Kang, Einhard Kleist, Sebastian Schmitt, Monika Springer, Ralf Tillmann, Cheng Wu, Defeng Zhao, Mattias Hallquist, Cameron Faxon, Michael Le Breton, Åsa M. Hallquist, David Simpson, Robert Bergström, Michael E. Jenkin, Mikael Ehn, Joel A. Thornton, M. Rami Alfarra, Thomas J. Bannan, Carl J. Percival, Michael Priestley, David Topping, and Astrid Kiendler-Scharr. 2019. "Secondary organic aerosol reduced by mixture of atmospheric vapours." *Nature* 565 (7741):587-593. doi: 10.1038/s41586-018-0871-y.

Melcher, Gerhard. 1974. "Stereospecificity of the genetic code." *Journal of Molecular Evolution* 3 (2):121-140. doi: 10.1007/BF01796558.

Messina, Palmira, Juliette Lathière, Katerina Sindelarova, Nicolas Vuichard, Claire Granier, Josefine Ghattas, Anne Cozic, and Didier A. Hauglustaine. 2016. "Global biogenic volatile organic

compound emissions in the ORCHIDEE and MEGAN models and sensitivity to key parameters." *Atmospheric Chemistry and Physics* 16 (22):14169-14202. doi: 10.5194/acp-16-14169-2016.

Michel, Alexa, Anne-Katrin Prescher, and Kai Schwärzel. 2020. *Forest Condition in Europe: 2019 Technical Report of ICP Forests. Report under the UNECE Convention on Long-Range Transboundary Air Pollution (Air Convention)*.

Misra, G., S. G. Pavlostathis, E. M. Perdue, and R. Araujo. 1996. "Aerobic biodegradation of selected monoterpenes." *Applied Microbiology and Biotechnology* 45 (6):831-838. doi: 10.1007/s002530050770.

Mochizuki, Tomoki, Akira Tani, Yoshiyuki Takahashi, Nobuko Saigusa, and Masahito Ueyama. 2014. "Long-term measurement of terpenoid flux above a Larix kaempferi forest using a relaxed eddy accumulation method." *Atmospheric Environment* 83:53-61.

Monson, Russell K., Rüdiger Grote, Ülo Niinemets, and Jörg-Peter Schnitzler. 2012. "Modeling the isoprene emission rate from leaves." *New Phytologist* 195 (3):541-559. doi: https://doi.org/10.1111/j.1469-8137.2012.04204.x.

Monson, Russell K., Sarathi M. Weraduwage, Maaria Rosenkranz, Jörg-Peter Schnitzler, and Thomas D. Sharkey. 2021. "Leaf isoprene emission as a trait that mediates the growth-defense tradeoff in the face of climate stress." *Oecologia*. doi: 10.1007/s00442-020-04813-7.

Myneni, R. B., C. D. Keeling, C. J. Tucker, G. Asrar, and R. R. Nemani. 1997. "Increased plant growth in the northern high latitudes from 1981 to 1991." *Nature* 386 (6626):698-702. doi: 10.1038/386698a0.

Niinemets, Ü, U. Kuhn, P. C. Harley, M. Staudt, A. Arneth, A. Cescatti, P. Ciccioli, L. Copolovici, C. Geron, A. Guenther, J. Kesselmeier, M. T. Lerdau, R. K. Monson, and J. Peñuelas. 2011. "Estimations of isoprenoid emission capacity from enclosure studies: measurements, data processing, quality and standardized measurement protocols." *Biogeosciences* 8 (8):2209-2246. doi: 10.5194/bg-8-2209-2011.

Niinemets, Ü., J. D. Tenhunen, P. C. Harley, and R. Steinbrecher. 1999. "A model of isoprene emission based on energetic requirements for isoprene synthesis and leaf photosynthetic properties for Liquidambar and Quercus." *Plant, Cell & Environment* 22 (11):1319-1335. doi: https://doi.org/10.1046/j.1365-3040.1999.00505.x.

Niinemets, Ülo, Francesco Loreto, and Markus Reichstein. 2004. "Physiological and physicochemical controls on foliar volatile organic compound emissions." *Trends in Plant Science* 9 (4):180-186. doi: https://doi.org/10.1016/j.tplants.2004.02.006.

Niinemets, Ülo, and Markus Reichstein. 2002. "A model analysis of the effects of nonspecific monoterpenoid storage in leaf tissues on emission kinetics and composition in Mediterranean sclerophyllous Quercus species." *Global Biogeochemical Cycles* 16 (4):57-1-57-26. doi: 10.1029/2002gb001927.

Noe, Steffen M., Paolo Ciccioli, Enzo Brancaleoni, Francesco Loreto, and Ülo Niinemets. 2006. "Emissions of monoterpenes linalool and ocimene respond differently to environmental changes due to differences in physico-chemical characteristics." *Atmospheric Environment* 40 (25):4649-4662. doi: https://doi.org/10.1016/j.atmosenv.2006.04.049.

Nogués, Isabel, Mauro Medori, and Carlo Calfapietra. 2015. "Limitations of monoterpene emissions and their antioxidant role in Cistus sp. under mild and severe treatments of drought and warming." *Environmental and Experimental Botany* 119 (Complete):76-86. doi: 10.1016/j.envexpbot.2015.06.001.

Norin, T. 1996. "Chiral chemodiversity and its role for biological activity. Some observations from studies on insect/insect and insect/plant relationships." *Pure and Applied Chemistry* 68 (11):2043-2049. doi: doi:10.1351/pac199668112043.

Ormeño, E., J. P. Mévy, B. Vila, A. Bousquet-Mélou, S. Greff, G. Bonin, and C. Fernandez. 2007. "Water deficit stress induces different monoterpene and sesquiterpene emission changes in Mediterranean species. Relationship between terpene emissions and plant water potential." *Chemosphere* 67 (2):276-84. doi: 10.1016/j.chemosphere.2006.10.029.

Pan, Yude, Richard A. Birdsey, Jingyun Fang, Richard Houghton, Pekka E. Kauppi, Werner A. Kurz, Oliver L. Phillips, Anatoly Shvidenko, Simon L. Lewis, Josep G. Canadell, Philippe Ciais, Robert B. Jackson, Stephen W. Pacala, A. David McGuire, Shilong Piao, Aapo Rautiainen, Stephen Sitch, and Daniel Hayes. 2011. "A Large and Persistent Carbon Sink in the World's Forests." *Science* 333 (6045):988. doi: 10.1126/science.1201609.

Pasteur, L. 1848. *C. R. Acad. Sci. Paris* 26:535–538.

Pazouki, Leila, and Ülo Niinemets. 2016. "Multi-Substrate Terpene Synthases: Their Occurrence and Physiological Significance." *Frontiers in Plant Science* 7 (1019). doi: 10.3389/fpls.2016.01019.

Pegoraro, Emiliano, Leif Abrell, Joost Van Haren, Greg Barron-Gafford, Katherine Ann Grieve, Yadvinder Malhi, Ramesh Murthy, and Guanghui Lin. 2005. "The effect of elevated atmospheric CO2 and drought on sources and sinks of isoprene in a temperate and tropical rainforest mesocosm." *Global Change Biology* 11 (8):1234-1246. doi: https://doi.org/10.1111/j.1365-2486.2005.00986.x.

Pegoraro, Emiliano, ANA REY, LEIF ABRELL, JOOST VAN HAREN, and GUANGHUI LIN. 2006. "Drought effect on isoprene production and consumption in Biosphere 2 tropical rainforest." *Global Change Biology* 12 (3):456-469. doi: https://doi.org/10.1111/j.1365-2486.2006.01112.x.

Peñuelas, Josep, and Joan Llusià. 2003. "BVOCs: plant defense against climate warming?" *Trends in Plant Science* 8 (3):105-109. doi: https://doi.org/10.1016/S1360-1385(03)00008-6.

Peñuelas, Josep, and Sergi Munné-Bosch. 2005. "Isoprenoids: an evolutionary pool for photoprotection." *Trends in plant science* 10 (4):166-169.

Peñuelas, Josep, and Michael Staudt. 2010. "BVOCs and global change." *Trends in plant science* 15 (3):133-144.

Perkins-Kirkpatrick, S. E., and P. B. Gibson. 2017. "Changes in regional heatwave characteristics as a function of increasing global temperature." *Scientific Reports* 7 (1):12256. doi: 10.1038/s41598-017-12520-2.

Perkins, S. E., L. V. Alexander, and J. R. Nairn. 2012. "Increasing frequency, intensity and duration of observed global heatwaves and warm spells." *Geophysical Research Letters* 39 (20). doi: https://doi.org/10.1029/2012GL053361.

Pétron, G., P. Harley, J. Greenberg, and A. Guenther. 2001. "Seasonal temperature variations influence isoprene emission." *Geophysical Research Letters* 28 (9):1707-1710. doi: https://doi.org/10.1029/2000GL011583.

Pfannerstill, Eva Y., Anke C. Nölscher, Ana M. Yáñez-Serrano, Efstratios Bourtsoukidis, Stephan Keßel, Ruud H. H. Janssen, Anywhere Tsokankunku, Stefan Wolff, Matthias Sörgel, Marta O. Sá, Alessandro Araújo, David Walter, Jošt Lavrič, Cléo Q. Dias-Júnior, Jürgen Kesselmeier, and Jonathan Williams. 2018. "Total OH Reactivity Changes Over the Amazon Rainforest During an El Niño Event." *Frontiers in Forests and Global Change* 1 (12). doi: 10.3389/ffgc.2018.00012.

Phillips, Michael A., Thomas J. Savage, and Rodney Croteau. 1999. "Monoterpene Synthases of Loblolly Pine (Pinus taeda) Produce Pinene Isomers and Enantiomers." *Archives of Biochemistry and Biophysics* 372 (1):197-204. doi: https://doi.org/10.1006/abbi.1999.1467.

Porté, Annabel, Alexandre Bosc, Isabelle Champion, and Denis Loustau. 2000. "Estimating the foliage area of Maritime pine (Pinus pinaster Aït.) branches and crowns with application to modelling the foliage area distribution in the crown." *Annals of Forest Science* 57 (1):73-86.

Puentes-Cala, E., M. Liebeke, S. Markert, and J. Harder. 2018. "Anaerobic Degradation of Bicyclic Monoterpenes in Castellaniella defragrans." *Metabolites* 8 (1). doi: 10.3390/metabo8010012.

Pureswaran, Deepa S, Regine Gries, and John H Borden. 2004. "Quantitative variation in monoterpenes in four species of conifers." *Biochemical systematics and ecology* 32 (12):1109-1136.

Radwan, A., M. Kleinwächter, and D. Selmar. 2017. "Impact of drought stress on specialised metabolism: Biosynthesis and the expression of monoterpene synthases in sage (Salvia officinalis)." *Phytochemistry* 141:20-26. doi: 10.1016/j.phytochem.2017.05.005.

Rascher, U., E. G. Bobich, G. H. Lin, A. Walter, T. Morris, M. Naumann, C. J. Nichol, D. Pierce, K. Bil, V. Kudeyarov, and J. A. Berry. 2004. "Functional diversity of photosynthesis during drought in a model tropical rainforest – the contributions of leaf area, photosynthetic electron transport and stomatal conductance to reduction in net ecosystem carbon exchange." *Plant, Cell & Environment* 27 (10):1239-1256. doi: https://doi.org/10.1111/j.1365-3040.2004.01231.x.

Rayment, M. B., and P. G. Jarvis. 1997. "An improved open chamber system for measuring soil CO2 effluxes in the field." *Journal of Geophysical Research: Atmospheres* 102 (D24):28779-28784. doi: https://doi.org/10.1029/97JD01103.

Reddemann, J., and R. Schopf. 1996. "Zur Bedeutung von Monoterpenen bei der Aggregation des Buchdruckers Ips typographus (Coleoptera: Scolytidae: Ipinae)." *Entomologia Generalis* 21:69-80.

Reichstein, Markus, Michael Bahn, Philippe Ciais, Dorothea Frank, Miguel D. Mahecha, Sonia I. Seneviratne, Jakob Zscheischler, Christian Beer, Nina Buchmann, David C. Frank, Dario Papale, Anja Rammig, Pete Smith, Kirsten Thonicke, Marijn van der Velde, Sara Vicca, Ariane Walz, and Martin Wattenbach. 2013. "Climate extremes and the carbon cycle." *Nature* 500 (7462):287-295. doi: 10.1038/nature12350.

Renwick, J. A., P. R. Hughes, and I. S. Krull. 1976. "Selective production of cis- and trans-verbenol from (-)-and (+)-alpha by a bark beetle." *Science* 191 (4223):199-201. doi: 10.1126/science.1246609.

Restrepo-Coupe, Natalia, Humberto R. da Rocha, Lucy R. Hutyra, Alessandro C. da Araujo, Laura S. Borma, Bradley Christoffersen, Osvaldo M. R. Cabral, Plinio B. de Camargo, Fernando L. Cardoso, Antonio C. Lola da Costa, David R. Fitzjarrald, Michael L. Goulden, Bart Kruijt, Jair M. F. Maia, Yadvinder S. Malhi, Antonio O. Manzi, Scott D. Miller, Antonio D. Nobre, Celso von Randow, Leonardo D. Abreu Sá, Ricardo K. Sakai, Julio Tota, Steven C. Wofsy, Fabricio B. Zanchi, and Scott R. Saleska. 2013. "What drives the seasonality of photosynthesis across the Amazon basin? A cross-site analysis of eddy flux tower measurements from the Brasil flux network." *Agricultural and Forest Meteorology* 182-183:128-144. doi: https://doi.org/10.1016/j.agrformet.2013.04.031.

Ricci, M. P., D. A. Merritt, K. H. Freeman, and J. M. Hayes. 1994. "Acquisition and processing of data for isotope-ratio-monitoring mass spectrometry." *Org Geochem* 21 (6-7):561-71. doi: 10.1016/0146-6380(94)90002-7.

Rissanen, K., T. Hölttä, A. Vanhatalo, J. Aalto, E. Nikinmaa, H. Rita, and J. Bäck. 2016. "Diurnal patterns in Scots pine stem oleoresin pressure in a boreal forest." *Plant, Cell & Environment* 39 (3):527-538. doi: https://doi.org/10.1111/pce.12637.

Rowen, E., and I. Kaplan. 2016. "Eco-evolutionary factors drive induced plant volatiles: a meta-analysis." *New Phytol* 210 (1):284-94. doi: 10.1111/nph.13804.

Runyon, J. B., M. C. Mescher, and C. M. De Moraes. 2006. "Volatile chemical cues guide host location and host selection by parasitic plants." *Science* 313 (5795):1964-7. doi: 10.1126/science.1131371.

Sander, Ricardo. 2015. "Compilation of Henry's law constants (Version 4.0) for water as solvent." *Atmospheric Chemistry and Physics* 15:4399-4981. doi: 10.5194/acp-15-4399-2015.

Savatin, D. V., G. Gramegna, V. Modesti, and F. Cervone. 2014. "Wounding in the plant tissue: the defense of a dangerous passage." *Front Plant Sci* 5:470. doi: 10.3389/fpls.2014.00470.

Schade, Gunnar W, Allen H Goldstein, and Mark S Lamanna. 1999. "Are monoterpene emissions influenced by humidity?" *Geophysical Research Letters* 26 (14):2187-2190.

Seco, R., T. Karl, A. Guenther, K. P. Hosman, S. G. Pallardy, L. Gu, C. Geron, P. Harley, and S. Kim. 2015. "Ecosystem-scale volatile organic compound fluxes during an extreme drought in a broadleaf temperate forest of the Missouri Ozarks (central USA)." *Glob Chang Biol* 21 (10):3657-74. doi: 10.1111/gcb.12980.

Seinfeld, J.H., and S.N. Pandis. 2012. *Atmospheric Chemistry and Physics: From Air Pollution to Climate Change*: Wiley.

Sharkey, T. D., and S. S. Yeh. 2001. "Isoprene emission from plants." *Annual Review of Plant Physiology and Plant Molecular Biology* 52:407-436. doi: 10.1146/annurev.arplant.52.1.407.

Sharkey, Thomas D., Amy E. Wiberley, and Autumn R. Donohue. 2007. "Isoprene Emission from Plants: Why and How." *Annals of Botany* 101 (1):5-18. doi: 10.1093/aob/mcm240.

Simon, V, B Clement, M-L Riba, and L Torres. 1994. "The Landes experiment: Monoterpenes emitted from the maritime pine." *Journal of Geophysical Research: Atmospheres* 99 (D8):16501-16510.

Sindelarova, K., C. Granier, I. Bouarar, A. Guenther, S. Tilmes, T. Stavrakou, J. F. Müller, U. Kuhn, P. Stefani, and W. Knorr. 2014. "Global data set of biogenic VOC emissions calculated by the MEGAN model over the last 30 years." *Atmos. Chem. Phys.* 14 (17):9317-9341. doi: 10.5194/acp-14-9317-2014.

Sjödin, Kristina, Monika Persson, Jenny Fäldt, Inger Ekberg, and Anna-Karin Borg-Karlson. 2000. "Occurrence and Correlations of Monoterpene Hydrocarbon Enantiomers in Pinus sylvestris and Picea abies." *Journal of Chemical Ecology* 26 (7):1701-1720. doi: 10.1023/A:1005547131427.

Song, W., M. Staudt, I. Bourgeois, and J. Williams. 2014. "Laboratory and field measurements of enantiomeric monoterpene emissions as a function of chemotype, light and temperature." *Biogeosciences* 11 (5):1435-1447. doi: 10.5194/bg-11-1435-2014.

Song, Wei, Jonathan Williams, Noureddine Yassaa, Monica Martinez, José Antonio Adame Carnero, Pablo J. Hidalgo, Heiko Bozem, and Jos Lelieveld. 2011. "Winter and summer characterization of biogenic enantiomeric monoterpenes and anthropogenic BTEX compounds at a Mediterranean Stone Pine forest site." *Journal of Atmospheric Chemistry* 68 (3):233-250. doi: 10.1007/s10874-012-9219-4.

Spielmann, Felix M., Stephan Langebner, Andrea Ghirardo, Armin Hansel, Jörg-Peter Schnitzler, and Georg Wohlfahrt. 2017. "Isoprene and α-pinene deposition to grassland mesocosms." *Plant and Soil* 410 (1):313-322. doi: 10.1007/s11104-016-3009-8.

Staudt, M., I. Bourgeois, R. Al Halabi, W. Song, and J. Williams. 2017. "New insights into the parametrization of temperature and light responses of mono - and sesquiterpene emissions from Aleppo pine and rosemary." *Atmospheric Environment* 152:212-221. doi: https://doi.org/10.1016/j.atmosenv.2016.12.033.

Staudt, M., J. Byron, K. Piquemal, and J. Williams. 2019. "Compartment specific chiral pinene emissions identified in a Maritime pine forest." *Sci Total Environ* 654:1158-1166. doi: 10.1016/j.scitotenv.2018.11.146.

Staudt, M., and G. Seufert. 1995. "Light-dependent emission of monoterpenes by holm oak (Quercus ilex L.)." *Naturwissenschaften* 82 (2):89-92. doi: 10.1007/BF01140148.

Staudt, Michael, Serge Rambal, Richard Joffre, and Jürgen Kesselmeier. 2002. "Impact of drought on seasonal monoterpene emissions from Quercus ilex in southern France." *Journal of Geophysical Research: Atmospheres* 107 (D21):ACH 15-1-ACH 15-9.

Teuber, M., I. Zimmer, J. Kreuzwieser, P. Ache, A. Polle, H. Rennenberg, and J.-P. Schnitzler. 2008. "VOC emissions of Grey poplar leaves as affected by salt stress and different N sources." *Plant Biology* 10 (1):86-96. doi: https://doi.org/10.1111/j.1438-8677.2007.00015.x.

Tiiva, Päivi, Jing Tang, Anders Michelsen, and Riikka Rinnan. 2017. "Monoterpene emissions in response to long-term night-time warming, elevated CO2 and extended summer drought in a temperate heath ecosystem." *Science of The Total Environment* 580:1056-1067. doi: https://doi.org/10.1016/j.scitotenv.2016.12.060.

Tognetti, Roberto, Marco Michelozzi, Marco Lauteri, Enrico Brugnoli, and Raffaello Giannini. 2000. "Geographic variation in growth, carbon isotope discrimination, and monoterpene composition in Pinus pinaster Ait. provenances." *Canadian Journal of Forest Research* 30 (11):1682-1690. doi: 10.1139/x00-096.

Turtola, Satu, Anne-Marja Manninen, Risto Rikala, and Pirjo Kainulainen. 2003. "Drought stress alters the concentration of wood terpenoids in Scots pine and Norway spruce seedlings." *Journal of chemical ecology* 29 (9):1981-1995.

Ulbricht, Tilo L. V. 1981. "Reflections on the origin of optical asymmetry on earth." *Origins of life* 11 (1):55-70. doi: 10.1007/BF00927998.

Urban, J., M. Ingwers, M. A. McGuire, and R. O. Teskey. 2017. "Stomatal conductance increases with rising temperature." *Plant Signal Behav* 12 (8):e1356534. doi: 10.1080/15592324.2017.1356534.

Vanhatalo, A., T. Chan, J. Aalto, J. F. Korhonen, P. Kolari, T. Hölttä, E. Nikinmaa, and J. Bäck. 2015. "Tree water relations can trigger monoterpene emissions from Scots pine stems during spring recovery." *Biogeosciences* 12 (18):5353-5363. doi: 10.5194/bg-12-5353-2015.

Varaprath, Sudarsanan, Debra H. Stutts, and Gary E. Kozerski. 2006. "A Primer on the Analytical Aspects of Silicones at Trace Levels-Challenges and Artifacts – A Review." *Silicon Chemistry* 3 (1):79-102. doi: 10.1007/s11201-006-9005-8.

Vickers, Claudia E., Malcolm Possell, Cristian I. Cojocariu, Violeta B. Velikova, Jullada Laothawornkitkul, Annette Ryan, Philip M. Mullineaux, and C. Nicholas Hewitt. 2009. "Isoprene synthesis protects transgenic tobacco plants from oxidative stress." *Plant, Cell & Environment* 32 (5):520-531. doi: https://doi.org/10.1111/j.1365-3040.2009.01946.x.

Warneke, Carsten, Thomas Karl, Helmut Judmaier, Armin Hansel, Alfons Jordan, Werner Lindinger, and Paul J. Crutzen. 1999. "Acetone, methanol, and other partially oxidized volatile organic emissions from dead plant matter by abiological processes: Significance for atmospheric HOx chemistry." *Global Biogeochemical Cycles* 13 (1):9-17. doi: https://doi.org/10.1029/98GB02428.

Werkhoff, Peter, and Wilfried Bretschneider. 1987. "Dynamic headspace gas chromatography: concentration of volatile components after thermal desorption by intermediate cryofocusing in a cold trap: I. Principle and applications." *Journal of Chromatography A* 405:87-98. doi: https://doi.org/10.1016/S0021-9673(01)81750-7.

Werner, Christiane, Lukas Fasbender, Katarzyna M. Romek, Ana Maria Yáñez-Serrano, and Jürgen Kreuzwieser. 2020. "Heat Waves Change Plant Carbon Allocation Among Primary and Secondary Metabolism Altering CO2 Assimilation, Respiration, and VOC Emissions." *Frontiers in Plant Science* 11 (1242). doi: 10.3389/fpls.2020.01242.

Wibe, Atle, Anna-Karin Borg-Karlson, Monika Persson, Torbjörn Norin, and Hanna Mustaparta. 1998. "Enantiomeric Composition of Monoterpene Hydrocarbons in Some Conifers and Receptor Neuron Discrimination of α-Pinene and Limonene Enantiomers in the Pine Weevil, Hylobius abietis." *Journal of Chemical Ecology* 24 (2):273-287. doi: 10.1023/A:1022580308414.

Wiberley, Amy E., Autumn R. Donohue, Mary E. Meier, Maiken M. Westphal, and Thomas D. Sharkey. 2008. "Regulation of isoprene emission in Populus trichocarpa leaves subjected to changing growth temperature." *Plant, Cell & Environment* 31 (2):258-267. doi: https://doi.org/10.1111/j.1365-3040.2007.01758.x.

Wigneron, Jean-Pierre, Lei Fan, Philippe Ciais, Ana Bastos, Martin Brandt, Jérome Chave, Sassan Saatchi, Alessandro Baccini, and Rasmus Fensholt. 2020. "Tropical forests did not recover from the strong 2015–2016 El Niño event." *Science Advances* 6 (6):eaay4603. doi: 10.1126/sciadv.aay4603.

Williams, J, N Yassaa, S Bartenbach, and J Lelieveld. 2007. "Mirror image hydrocarbons from Tropical and Boreal forests." *Atmospheric Chemistry and Physics* 7 (3):973-980.

Williams, J., J. Crowley, H. Fischer, H. Harder, M. Martinez, T. Petäjä, J. Rinne, J. Bäck, M. Boy, M. Dal Maso, J. Hakala, M. Kajos, P. Keronen, P. Rantala, J. Aalto, H. Aaltonen, J. Paatero, T. Vesala, H. Hakola, J. Levula, T. Pohja, F. Herrmann, J. Auld, E. Mesarchaki, W. Song, N. Yassaa, A. Nölscher, A. M. Johnson, T. Custer, V. Sinha, J. Thieser, N. Pouvesle, D. Taraborrelli, M. J. Tang, H. Bozem, Z. Hosaynali-Beygi, R. Axinte, R. Oswald, A. Novelli, D. Kubistin, K. Hens, U. Javed, K. Trawny, C. Breitenberger, P. J. Hidalgo, C. J. Ebben, F. M. Geiger, A. L. Corrigan, L. M. Russell,

H. G. Ouwersloot, J. Vilà-Guerau de Arellano, L. Ganzeveld, A. Vogel, M. Beck, A. Bayerle, C. J. Kampf, M. Bertelmann, F. Köllner, T. Hoffmann, J. Valverde, D. González, M. L. Riekkola, M. Kulmala, and J. Lelieveld. 2011. "The summertime Boreal forest field measurement intensive (HUMPPA-COPEC-2010): an overview of meteorological and chemical influences." *Atmos. Chem. Phys.* 11 (20):10599-10618. doi: 10.5194/acp-11-10599-2011.

Williams, Jonathan. 2004. "Organic trace gases in the atmosphere: an overview." *Environmental Chemistry* 1 (3):125-136.

Wolfrom, M. L., R. U. Lemieux, and S. M. Olin. 1949. "CONFIGURATIONAL CORRELATION OF L-(LEVO)-GLYCERALDEHYDE WITH NATURAL (DEXTRO)-ALANINE BY A DIRECT CHEMICAL METHOD." *Journal of the American Chemical Society* 71 (8):2870-2873. doi: 10.1021/ja01176a085.

Woolfenden, E. 2010. "Sorbent-based sampling methods for volatile and semi-volatile organic compounds in air. Part 2. Sorbent selection and other aspects of optimizing air monitoring methods." *J Chromatogr A* 1217 (16):2685-94. doi: 10.1016/j.chroma.2010.01.015.

Woolfenden, Elizabeth. 1997. "Monitoring VOCs in Air Using Sorbent Tubes Followed by Thermal Desorption-Capillary GC Analysis: Summary of Data and Practical Guidelines." *Journal of the Air & Waste Management Association* 47 (1):20-36. doi: 10.1080/10473289.1997.10464411.

Yáñez-Serrano, A. M., A. C. Nölscher, E. Bourtsoukidis, E. Gomes Alves, L. Ganzeveld, B. Bonn, S. Wolff, M. Sa, M. Yamasoe, J. Williams, M. O. Andreae, and J. Kesselmeier. 2018. "Monoterpene chemical speciation in a tropical rainforest:variation with season, height, and time of dayat the Amazon Tall Tower Observatory (ATTO)." *Atmos. Chem. Phys.* 18 (5):3403-3418. doi: 10.5194/acp-18-3403-2018.

Yáñez-Serrano, Ana Maria, Lucas Mahlau, Lukas Fasbender, Joseph Byron, Jonathan Williams, Jürgen Kreuzwieser, and Christiane Werner. 2019. "Heat stress increases the use of cytosolic pyruvate for isoprene biosynthesis." *Journal of Experimental Botany* 70 (20):5827-5838. doi: 10.1093/jxb/erz353.

Yassaa, N., E. Brancaleoni, M. Frattoni, and P. Ciccioli. 2001. "Trace level determination of enantiomeric monoterpenes in terrestrial plant emission and in the atmosphere using a beta-cyclodextrin capillary column coupled with thermal desorption and mass spectrometry." *J Chromatogr A* 915 (1-2):185-97. doi: 10.1016/s0021-9673(01)00587-8.

Yassaa, N., W. Song, J. Lelieveld, A. Vanhatalo, J. Bäck, and J. Williams. 2012. "Diel cycles of isoprenoids in the emissions of Norway spruce, four Scots pine chemotypes, and in Boreal forest ambient air during HUMPPA-COPEC-2010." *Atmos. Chem. Phys.* 12 (15):7215-7229. doi: 10.5194/acp-12-7215-2012.

Yassaa, N., and Jonathan Williams. 2005. "Analysis of enantiomeric and non-enantiomeric monoterpenes in plant emissions using portable dynamic air sampling/solid-phase microextraction (PDAS-SPME) and chiral gas chromatography/mass spectrometry." *Atmospheric Environment* 39:4875-4884.

Ye, Jiayan, Yifan Jiang, Linda-Liisa Veromann-Jürgenson, and Ülo Niinemets. 2019. "Petiole gall aphid (Pemphigus spyrothecae) infestation of Populus × petrovskiana leaves alters foliage photosynthetic characteristics and leads to enhanced emissions of both constitutive and stress-induced volatiles." *Trees* 33 (1):37-51. doi: 10.1007/s00468-018-1756-2.

Yu, X., and Z. P. Yao. 2017. "Chiral recognition and determination of enantiomeric excess by mass spectrometry: A review." *Anal Chim Acta* 968:1-20. doi: 10.1016/j.aca.2017.03.021.

Zannoni, Nora, Denis Leppla, Pedro Ivo Lembo Silveira de Assis, Thorsten Hoffmann, Marta Sá, Alessandro Araújo, and Jonathan Williams. 2020. "Surprising chiral composition changes over the Amazon rainforest with height, time and season." *Communications Earth & Environment* 1 (1):4. doi: 10.1038/s43247-020-0007-9.

Zhang, Haofei, Lindsay D. Yee, Ben H. Lee, Michael P. Curtis, David R. Worton, Gabriel Isaacman-VanWertz, John H. Offenberg, Michael Lewandowski, Tadeusz E. Kleindienst, Melinda R. Beaver, Amara L. Holder, William A. Lonneman, Kenneth S. Docherty, Mohammed Jaoui, Havala O. T. Pye, Weiwei Hu, Douglas A. Day, Pedro Campuzano-Jost, Jose L. Jimenez, Hongyu

Guo, Rodney J. Weber, Joost de Gouw, Abigail R. Koss, Eric S. Edgerton, William Brune, Claudia Mohr, Felipe D. Lopez-Hilfiker, Anna Lutz, Nathan M. Kreisberg, Steve R. Spielman, Susanne V. Hering, Kevin R. Wilson, Joel A. Thornton, and Allen H. Goldstein. 2018. "Monoterpenes are the largest source of summertime organic aerosol in the southeastern United States." *Proceedings of the National Academy of Sciences* 115 (9):2038. doi: 10.1073/pnas.1717513115.